SESSION 2B

Structural design – Structural engineering

Chairmen:
K. Kovari, Switzerland, and T. Franzén, Sweden

Leere Seite

Blank page

Page vide

The Øresund Tunnel - "Design and Build" in Practice

Chris Marshall
Project Manager
Symonds Travers Morgan
East Grinstead, UK

Chris Marshall obtained a
BSc in civil engineering
from the University of
Bristol (UK) and is a
Chartered Engineer. He has
17 years experience in the
design of civil engineering
structures including the
Conwy Tunnel (UK) and the
Lee Tunnel (Ireland). He is
currently project manager
for design of the Øresund
Tunnel

Eric Paillas
Engineering Manager
Øresund Tunnel Contractors I/S
Copenhagen, Denmark

Eric Paillas obtained a
degree in engineering from
the Ecole Nationale des
Ponts et Chaussées
(France) and an MSc from
MIT (USA). He has
worked for DUMEZ-GTM
for over 12 years on major
civil projects including the
Second Severn Bridge
(UK) where he was
Construction Manager,
before joining ØTC.

Summary

This paper describes some aspects of the design and construction of the Øresund Tunnel. The
aim of the paper is to illustrate how the partnership between designer and contractor, made
possible by the 'design and build' form of contract, has contributed to the project, with benefits
for all parties involved. Particular issues discussed include tender preparation, early age stresses,
joints, reinforcement, marine operations and the tunnel foundation. The paper concludes with
some comments on the benefits of design and build and some suggestions for how to use this
form of procurement to best effect in the future.

1.   Introduction

The Øresund Tunnel is a 3.5km long road/rail immersed tunnel, forming part of the Øresund Link
between Copenhagen in Denmark and Malmö in Sweden. It is being constructed on behalf of the
Øresundskonsortiet (a client company set up and owned jointly by the Danish and Swedish
governments) by Øresund Tunnel Contractors (ØTC), a joint venture comprising NCC AB of
Sweden, John Laing Construction Ltd of the UK, Dumez-GTM SA of France, Boskalis
Westminster Dredging BV of The Netherlands and E Pihl & Son A/S of Denmark. Design of the
tunnel is being performed on behalf of ØTC by UK consultant Symonds Travers Morgan (STM).

2.   Contractor's Contract Philosophy

ØTC appointed a designer early, some six months ahead of invitation to tender and before the
joint venture itself had been fully established. Thus from first concepts, the designer and
contractor were able to develop design ideas and construction methods in a fully integrated way.
The aim through the pre-tender and tender phases was to develop winning designs and methods
which neither party could have developed alone.

3.   Preparation of Tender

The tender documents issued by ØSK contained detailed specifications for many aspects of the works. The key opportunity for the tendering contractor to create an advantage lay in the construction method for the tunnel. Due to its exceptional size and length, methods which are usually uneconomic for immersed tunnel construction became viable. The chosen solution, which involves many innovative features, was developed jointly by contractor and designer during the tender phase. The method, which is described in more detail in another paper, involves casting each 22m long tunnel segment in a single concrete pour in a purpose built factory. Completed segments are stressed together in groups of eight and jacked about 300m into a dock before being floated. Figure 1 shows the tunnel casting facility.

1	REINFORCEMENT PREFABRICATION BUILDING	5	SLIDING GATE
2	BUFFER ZONE	6	SHALLOW BASIN/SKIDDING BEAMS AREA
3	BATCHING PLANT	7	DEEP BASIN
4	CASTING BED	8	FLOATING GATE
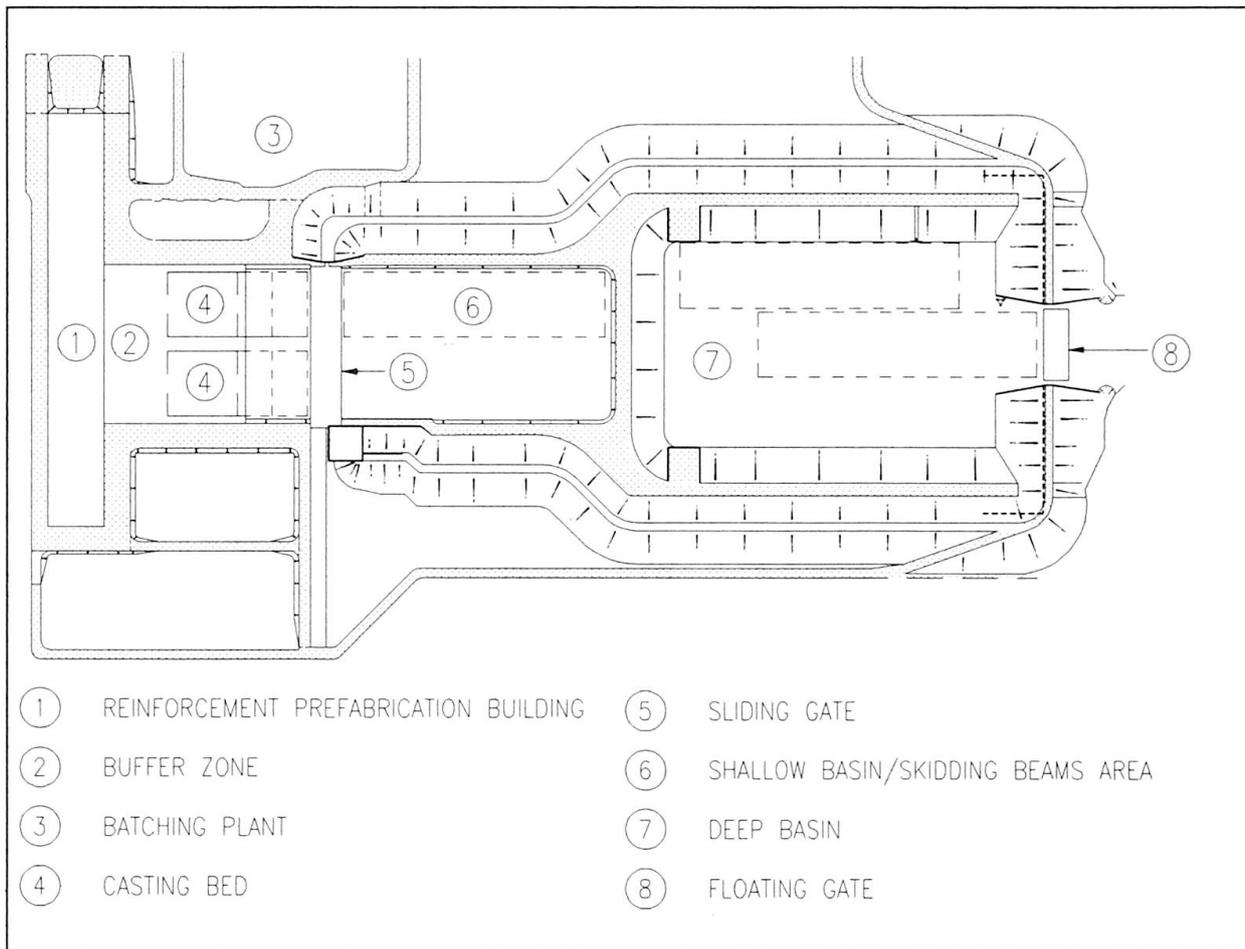
Figure 1   Tunnel Element Casting Yard

In developing this method, the key permanent works design consideration was the early-age stresses arising in the tunnel cross section from the combined effects of curing temperatures, self-weight stresses and foundation distortions, particularly during jacking. Extensive analysis was performed at tender stage, both to prove the method in principle, and to determine the optimum pour sequence, stripping times, jacking method, temporary foundations and bearing system. All of these considerations involved close contractor/designer co-operation without which the very real pressure to revert to a more traditional construction method would have been irresistible.

Figure 2   Typical Tunnel Element

4.   Early Age Stresses

Early age stresses in concrete immersed tunnels, particularly those associated with thermal effects, can cause through-section cracking in the tunnel exterior, resulting in leakage. Traditional construction, in which the tunnel cross secti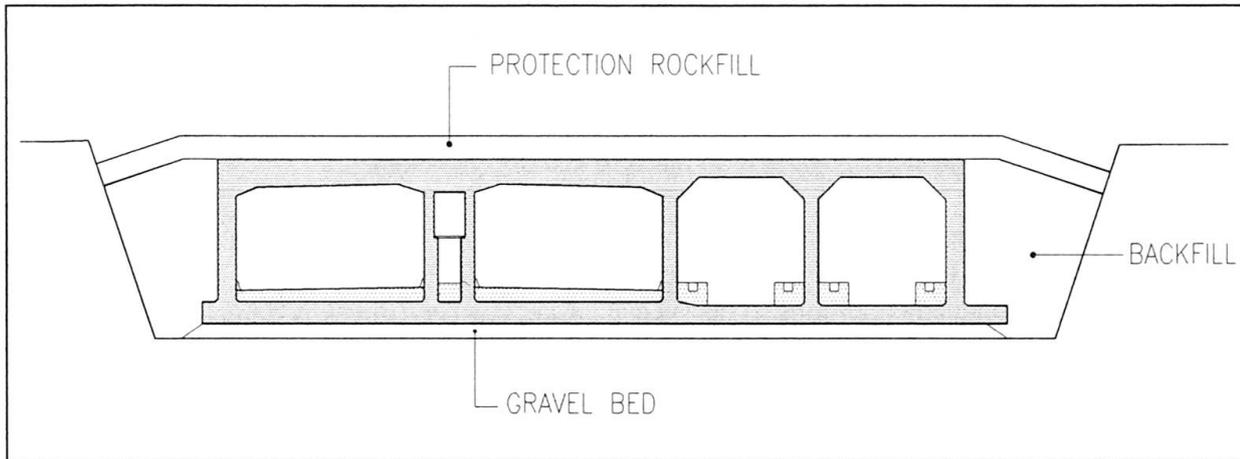on is cast in three stages, exacerbates this problem, since restraint afforded by the base concrete restrains the later-cast wall concrete, resulting in severe tension stresses in the walls. These are normally moderated by cooling the concrete using cast in water pipes.

The Øresund Tunnel has largely avoided this problem by casting each tunnel segment in a single pour, and cooling pipes are not therefore used. However, early-age stresses have been an important consideration throughout, since the chosen construction method superimposes self-weight and differential foundation movement stresses on the structure at early ages, at which time the thermal effects are still significant.

Thus to safeguard the permanent works, the design of the temporary works has been carefully customised. Particular aspects influenced in this way include tunnel foundations, temporary bearings, pour sequence, ambient temperature control in the factory, selective thermal insulation of the concrete and the timing of all aspects of the pour, strip and jack sequence.

5.   Joints

5.1   Immersion Joints

In conventional designs, the final alignment of the immersed tunnel relies on accuracy of immersion joint construction. Strict tolerances are specified and these are met through a two stage process by welding a plate to each steel end frame after casting the element and grouting behind the end frame. There is no recognised way of correcting the alignment after immersion.

It was soon realised on this project that given the unusual length of the tunnel, and number of elements, the conventional solution was too uncertain to rely upon to meet the correct horizontal alignment. A positive means of aligning the tunnel elements had to be found. To this effect, a

realignment system has been developed, where three 500 tonne jacks are incorporated in each external wall. The system is activated after dewatering the joint chamber between the two bulkheads and the tunnel element is realigned from its natural position (dictated by the tolerances of the joint) to the correct final position. The jacks are then locked and are only removed after permanent ballast and enough backfill are in place to stabilise the element.

A special soft-nosed Gina gasket has been developed for the project in order to allow both for primary watertightness at first contact when dewatering the joint chamber and for permanent watertightness in realigned conditions. This special gasket has been developed in close co-operation with Trelleborg-Bakker of The Netherlands.

The logical consequence of the above has been to make possible a relaxation of the tolerances on the joint end frame, which led to simplified joint detailing with an L profile replacing the conventional H profile, and no secondary welded plate. This simpler detail is one of the key factors favouring better quality and durability through ease of construction (simpler concreting and less welding). Figure 3 compares the final joint design with the original.

Key dimensional data relating to the immersion joint are as follows:

- Casting tolerances: ± 5mm
- Horizontal positioning tolerance: ± 25mm
- Realignment capacity: 25mm at joint (gives 180mm at secondary end of element)
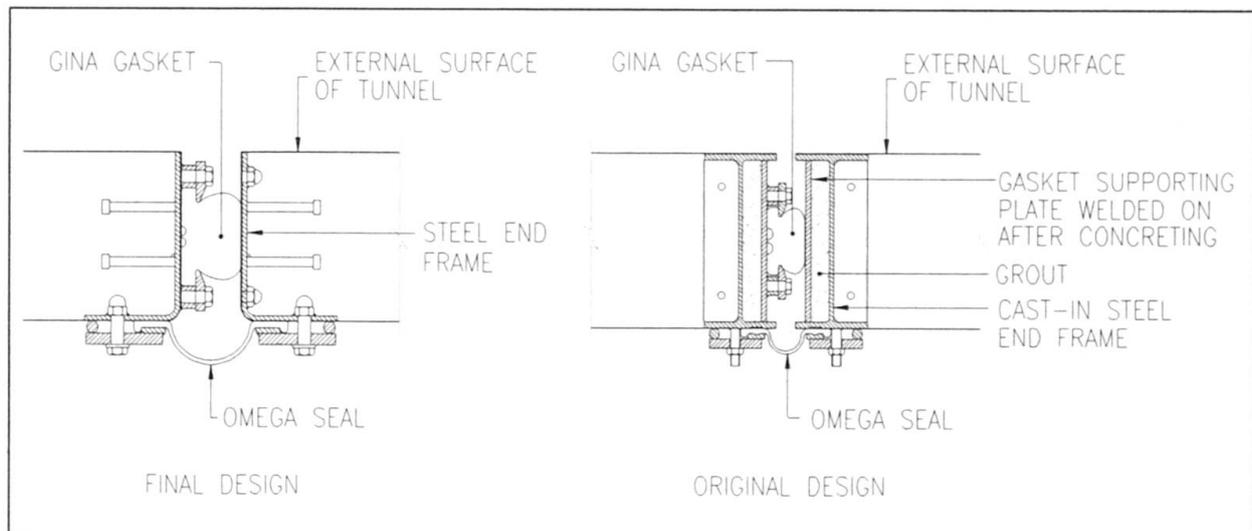
Figure 3   Immersion Joint - Comparison of Original Design with Final Design

5.2   Tunnel Segment Joints

The contract requirement for tunnel segment joints specifies a continuous half-joint around the tunnel perimeter sealed with a groutable waterstop. Whilst this is a common detail, the half-joint itself is difficult to concrete, and the resulting joint provides vertical shear resistance in the slab members and horizontal shear resistance in the walls - the opposite of where the natural shear strength of the structure is to be found.

An alternative joint design, developed jointly by contractor and designer, was proposed. The alternative replaces the half-joint with a plain joint, and introduces discrete shear keys in the walls

(plus one in the base to resist horizontal shear). This solution, accepted by the owner, places shear forces in appropriate structural elements and simplifies construction, with consequential benefits for the quality and durability of the structure.

6.   Tunnel Reinforcement

6.1   Aims of the Design

The weight of reinforcement in the immersed tunnel is approximately 40,000 tonnes, making it one of the contractor's largest single costs on the project. The challenge for the design and construct team was to develop a tunnel reinforcement scheme which met all the following aims:

- contract compliance;
- sound design, particularly from the point of view of durability;
- buildability, taking into account the unusual construction method;
- minimum quantity of steel.

6.2   Key Design Features

To achieve these aims, a major preliminary design/planning exercise was undertaken between the designer and contractor. This involved establishing the order of magnitude of steel required in key parts of the cross section, then developing bar arrangements which fitted all the stated aims. An extensive preliminary effort was justified in this case given the degree of repetition afforded by the 160 tunnel segments. Key features of the resulting design included the following:

- All reinforcement is set out on a standard 150mm/300mm grid to facilitate the use of prefabricated jigs in the casting yard.
- Sophisticated handling equipment in the casting yard permits extensive use of longer bars (up to 21m in length) thus minimising the need for laps.
- The basic transverse reinforcement arrangement consists of a complete frame of 25mm diameter bars at 300mm centres. Where local bending stresses cannot be resisted by this quantity of steel, additional bars are introduced in between the frames, and subsequently by bundling, but none of these additional bars is lapped. This is illustrated in Figure 4.
- Small box-outs and recesses are detailed independently from the main reinforcement, the latter being detailed as if there were no recesses and subsequently cut to suit on site.
- The use of shear reinforcement is kept to a minimum, but cannot be avoided altogether. Where it is required, *shear assemblies* are adopted. This technique achieves adequate shear resistance, but avoids the need for shear reinforcement to pass around the main bending reinforcement, thus greatly simplifying fabrication.

6.3   Reinforcement Handling

In the context of a line factory prefabrication process, the reinforcement fabrication is kept off the construction critical path (which goes through the casting process); complete reinforcement cages for each segment are assembled upstream in the rebar shed, then moved to a buffer area before finally entering the casting area. Each reinforcement cage is made of separately prefabricated subassemblies which provides further flexibility in the process (Figure 5).
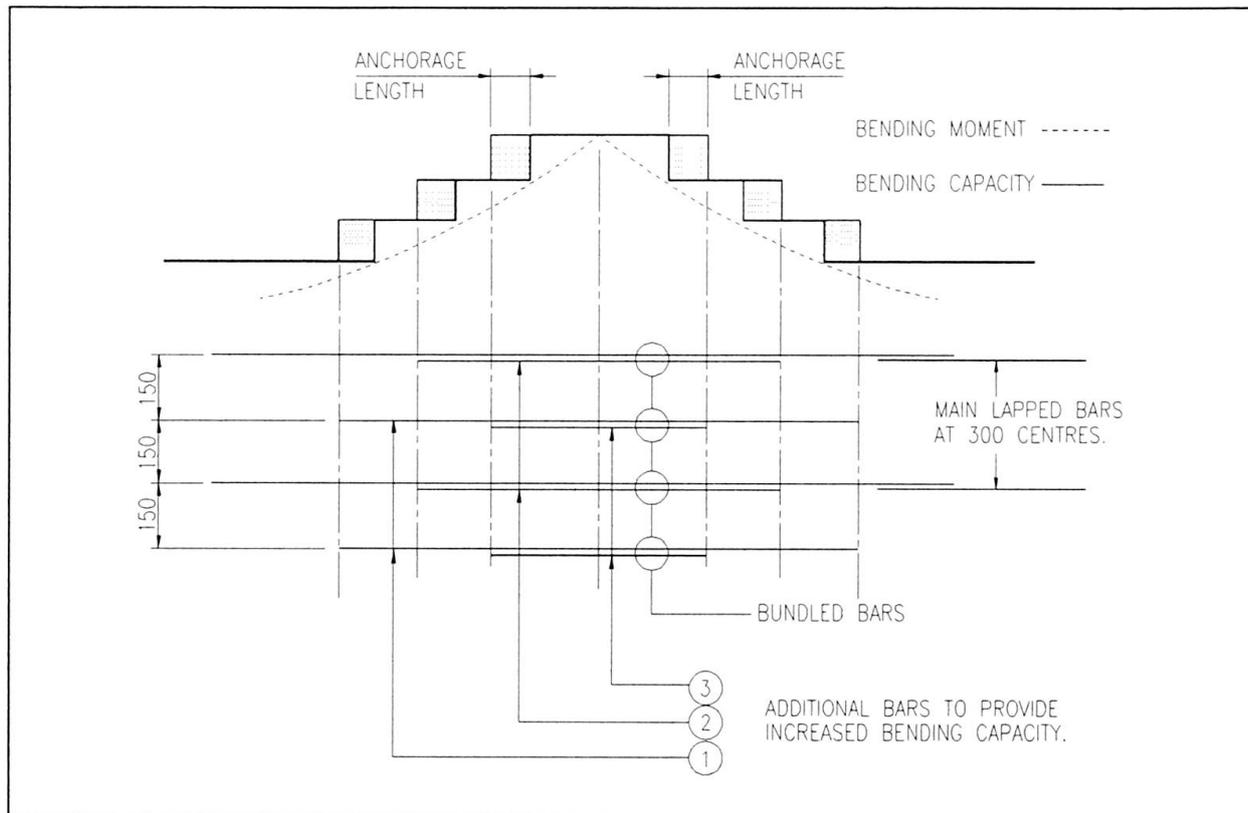
Figure 4   *Reinforcement in Areas of High Stress*

The subassemblies have been chosen by designer and contractor to suit both the constraints imposed by design and the lifting and handling capacities available in the shed. They comprise the base slab (assembled directly on the transfer rails to the buffer area), the six walls, and various panels for the top slab. The completed cage must be self-supporting, since it is assembled remote from the casting cells. This is achieved by the incorporation of fixing frames comprising steel angle trusses inside the cage; these provide the necessary stiffening.

The cage is moved from the final assembly zone to the buffer area on rail-mounted trolleys pulled by winches and from the buffer area to the casting cell on inflatable rails on needle bearings. Trial tests of the equipment and the experience on the first segments have enabled the contractor to fine tune the system to ensure that the cage arrives in the casting area in the correct position and with minimal distortion.

As well as removing the reinforcement from the critical path, this method also simplifies many other activities such as the incorporation of embedded items in the cage, since they can be performed with the cage completely unencumbered by shuttering.

From a design point of view, the reinforcement solution minimises steel tonnage without in any way compromising the quality of the finished product. This is achieved partly by the detailing measures described above, and partly by very careful attention to accurate curtailment of reinforcement, with each element of the tunnel being the subject of a separate design.
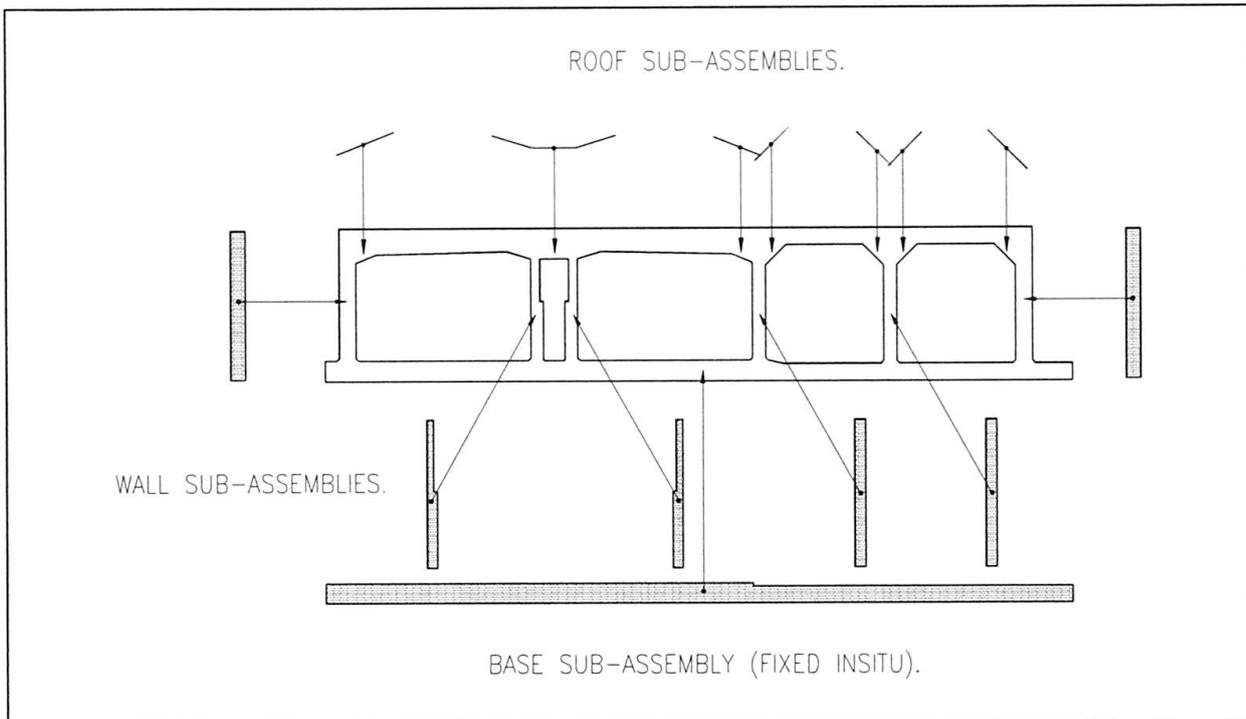
Figure 5   Reinforcement Sub-assemblies

7.   Marine Works

7.1   Marine Engineering Philosophy

The marine engineering for an immersed tunnel is dominated by the construction considerations of how to transport, manoeuvre and place a tunnel element. For economical as well as practical reasons, the different construction stages should have little or no impact on the permanent works design other than the necessary temporary works provisions (i.e. temporary prestress cables to hold the segments together during transportation and immersion, and marine works outfittings).

A "weather window" philosophy has been adopted for all marine works activities whereby a suitable hydrological and climatological window for the various marine operations is defined. The requisite window for an operation depends on the type and expected duration of the works. Forecasts of hydrological and climatological conditions are used to determine a duration which is suitable for performing the operation and which can be forecast with sufficient confidence.

The operational factors which have been considered are water depth, wave condition, wind, current, water level, salinity, ice, visibility, temperature and passing shipping. The operational limits are a function of tunnel element design assumptions, equipment and materials used and the nature of the marine works in question. Where appropriate, a distinction is made between survival (ultimate) design conditions and operational conditions. In practice, decisions are taken on suitable operational windows based on 24, 48 and 72 hour weather forecasts. Should such forecasts prove unreliable, and conditions deteriorate during an operation, a decision is taken either to continue, to go to survival positions, or to return to a safe harbour.

The main permanent works design considerations relating to marine works are tunnel foundation (see section 8), temporary prestress, vertical balance of tunnel elements during float-up, transport and immersion, effect of marine outfitting on the structure, and design of tunnel rock protection.

7.2   Temporary Prestress

The design of temporary prestressing is a hybrid between temporary and permanent works, since its purpose is to safeguard the permanent works during element transport and immersion, yet its life is temporary, since the tendons are cut once the element is on its foundation. The prestress is designed to accommodate two distinct loading conditions, each of which is separately evaluated for normal operational conditions and for survival conditions:

- loads arising due to sea conditions during transport;
- loads arising from placing the element in the tunnel trench.

Due to the form of foundation the latter case is never critical, and the tendons are designed to ensure that the segment joints remain closed during transport and immersion. The main loadings come from waves, partly direct and partly transmitted through the immersion pontoons. Loading due to waves was derived by the contractor, based on physical model tests performed by the Danish Hydraulic Institute and hydrodynamic modelling performed by SIMTECH of The Netherlands, a specialist marine engineering consultancy. The final structural design, in terms of quantity of prestress, anchorage design and disposition of tendons within the structure was the responsibility of the designer. A particular issue here was finding sufficient space in the slabs for the tendons, whilst successfully avoiding other obstacles, notably bulkhead fixings and ventilation fan niches.

For the purposes of tendon design, 'survival' condition bending moments were determined about both horizontal and vertical axes from the following parameters: significant wave heights 1.25m in 10m of water and 1.60m in 15m of water; wave period 4.5 seconds. The expected ultimate limit state failure mode of the structure under such loading is a shear failure at one of the segment joints. Failure is induced by combined shear and tension in the shear key, the latter induced by friction as the joint begins to open. For design purposes therefore, 'failure' was defined as the point at which the compression stress due to prestress at any point in one of the shear keys drops to zero (i.e. the point at which longitudinal tension can be induced in the key).

7.3   Vertical Balance of Tunnel Elements

An immersed tunnel has to be designed to be buoyant for transportation purposes, and stable against uplift once immersed. The change from one condition to another is typically achieved first by the introduction of temporary water ballast and subsequently by its replacement by permanent concrete ballast. For the Øresund Tunnel, an additional complicating factor was introduced by the asymmetry of the tunnel section, which is significantly heavier on the motorway side of the box than on the railway side (a symmetrical arrangement of bores was not possible due to constraints on road and rail approach alignments on the Danish coast).

For transport of the elements, uniform freeboard is achieved by construction of part of the permanent concrete ballast in the element casting yard. This is sufficient to balance the element, but leaves little margin for error in freeboard calculations, since the tunnel is close to minimum freeboard once sufficient ballast is added to make it float level (Figure 6).
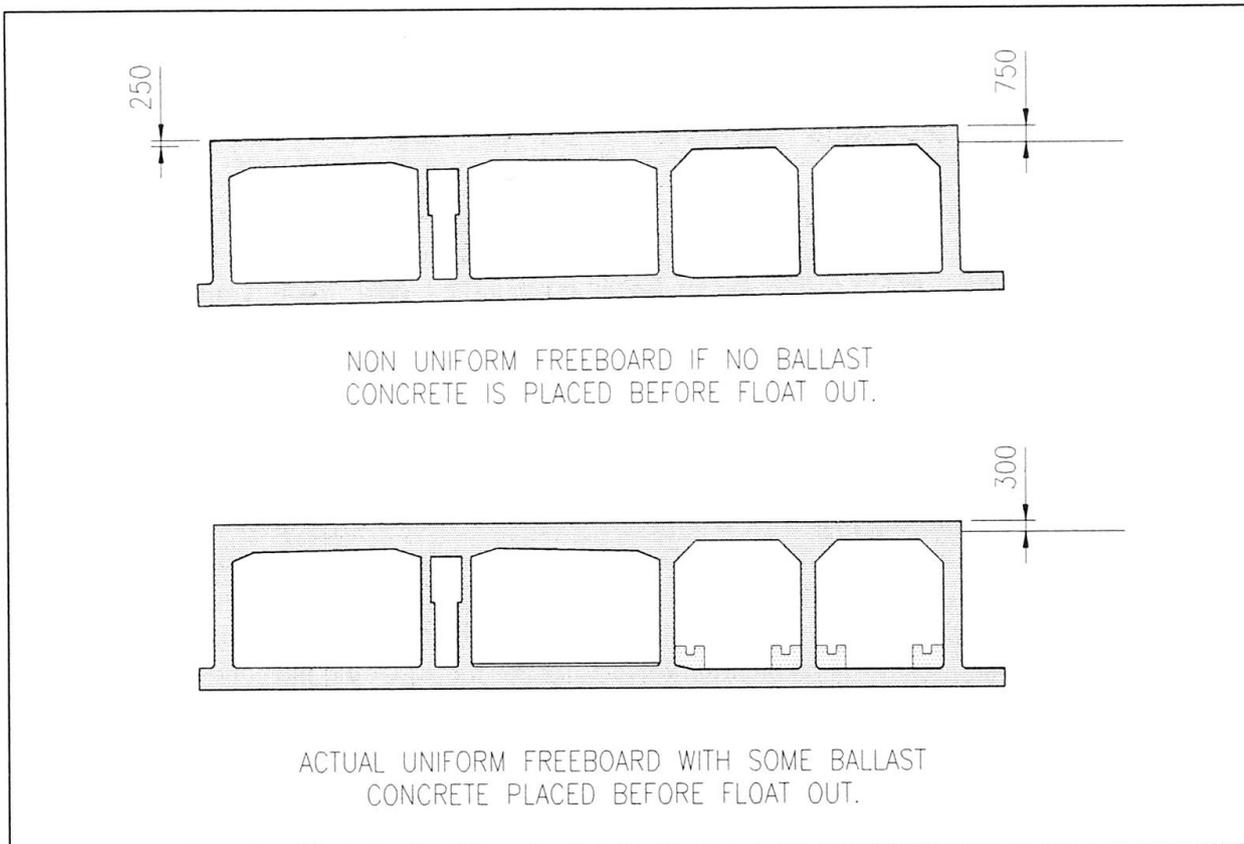
250

750

NON UNIFORM FREEBOARD IF NO BALLAST
CONCRETE IS PLACED BEFORE FLOAT OUT.

300

ACTUAL UNIFORM FREEBOARD WITH SOME BALLAST
CONCRETE PLACED BEFORE FLOAT OUT.

Figure 6   Tunnel Element Freeboard

In the permanent condition, the majority of the remaining ballast has to be added in the motorway bores, as little space exists in the railway; this results in a tunnel with uneven ground bearing pressures. Whilst this is theoretically acceptable, the designer deemed it desirable for the long term integrity of the works that bearing pressures be approximately uniform under the cross section. This was achieved by extending the base outside the external walls asymmetrically, with a 0.8m toe on the motorway side, and a 2.25m toe on the railway side.

7.4   Marine Outfitting

For purposes of transport and immersion, each tunnel element has to be fitted out with an access snorkel, survey towers and towing bollards. All of these are temporary works items, but all have to be attached to the tunnel structure, in many cases with large anchorage and fixing devices. Design of the temporary items themselves is performed by the contractor, fixings to the permanent works by the designer. This requires care at the interface, since it is a critically important point of design principle that in the event of unforeseen loading, for example due to storm conditions, the first point of failure should be in the temporary works item, without any damage to the permanent structure; thus it is essential not to over-design the temporary items, but instead to ensure that the weak link is outside the permanent structure.

7.5   Tunnel Rock Protection

The tunnel is protected from sunken ships, anchors, propeller-induced scour and current-induced scour by a layer of crushed rock placed on the tunnel roof. Two sizes of rock are used, a nominal 500mm rock in and adjacent to the main Drogden shipping channel, where the critical design

consideration for rock size is propeller scour, and a nominal 300mm rock closer to shore, where current and anchor considerations are critical in determining rock size. The layer thickness throughout is 1200mm, which arises from the falling anchor load case.

Rock placement is performed using a grab which is brought as close to the tunnel roof as possible before opening. By specifying a closely controlled placement method, it has been possible to eliminate the need for any additional protection layer between the tunnel structure and the rock protection.

8. Tunnel Foundation

8.1 Choice of Foundation Type

At tender stage, options for foundation construction were studied in some detail. A screeded gravel bed, of the type traditionally used for steel immersed tunnels, was rejected since the typically achieved tolerances of such construction (±50mm or more) would introduce unacceptable stresses into the relatively wide, flexible concrete box proposed for Øresund. At tender stage, therefore, a conventional concrete tunnel solution - temporary jacks combined with pumped pancakes of sand - was proposed.

Early in the contract, ØTC developed an alternative foundation proposal for consideration. This consists of a gravel bed, placed in such a manner that no subsequent screeding of the gravel is necessary. Based on experience gained by one of the ØTC joint venture partners on another project, it was forecast that such a bed could be placed to an accuracy of ±25mm. A detailed study was performed to compare the two options, and the gravel bed was in due course adopted. The most important benefits afforded by this change were:

- programme considerations (the gravel bed is off the critical path for the marine works as it is laid *before* immersing the tunnel element);
- elimination of the temporary supports (which are subject to a risk of overload during ship passage over a tunnel element);
- elimination of the risk of siltation beneath a placed element;
- elimination of a complex system of large cast-in pipes (with their associated leakage risk) for the sand flow system;
- no requirement to make good openings in the structure arising from the sand flow system and jacks, thus improving structural integrity.

In opting for the gravel bed, a number of important technical issues had to be addressed. The most important among these were:

- gravel placing methodology and ØTC's ability to design and deliver the placing equipment;
- choice of gravel materials and bed geometry;
- bed level accuracy - both placing accuracy and accuracy with which the finished bed levels could be measured;
- stresses in the tunnel structure due to imperfections in bed level; this was not just a question of absolute level tolerances, but crucially of the *distribution* of high and low parts of the bed.

8.2   Foundation Placing Methodology

The basic principle for placing the bed is to feed gravel down a pipe directly into position on the trench floor. The lower end of the pipe is equipped with a screeding plate which moves slowly across the trench, leaving the top of the gravel at the correct level *as it is placed*. The process is continuous, and there is no secondary screeding operation.

The feeder pipe equipment is mounted on a multi-purpose pontoon, fixed temporarily in position by spuds. The equipment is arranged such that each pass of the feeder pipe tracks in a straight line across the full width of the tunnel trench. During each pass, gravel supply is controlled such that the feeder pipe is never empty.
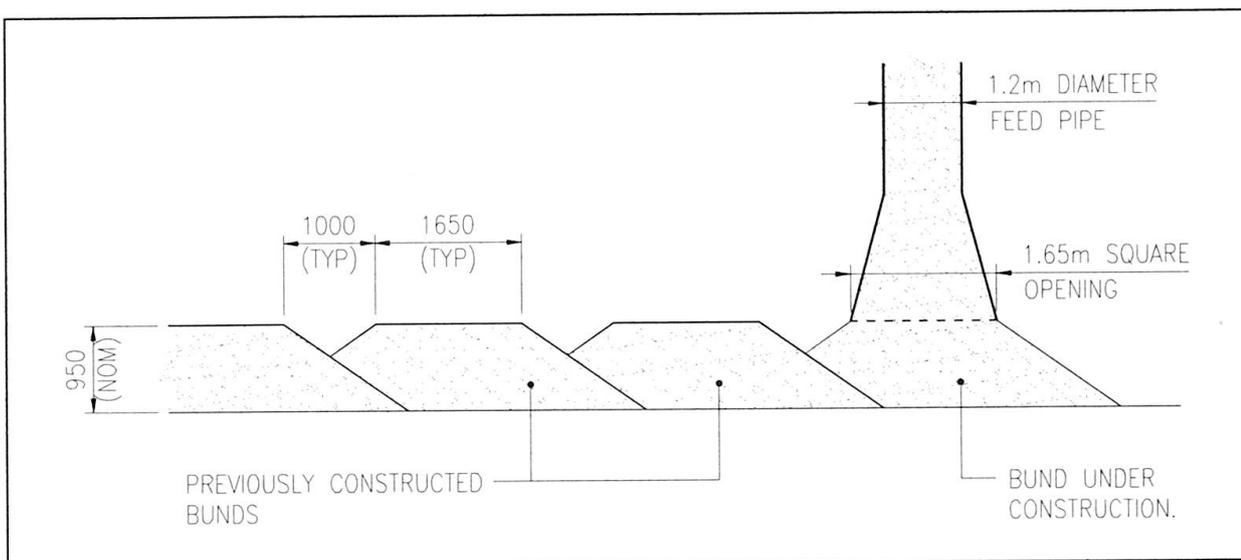

Figure 7   *Gravel Bed - Placing Technique and Bund Geometry*

8.3   Material Specification and Bed Geometry

Each pass of the feeder pipe places a line of gravel approximately 1.65m wide. During development of the method, it was recognised that a risk existed that the feeder pipe would disturb already placed gravel as it placed the adjacent line. It was therefore decided that each pass of the pipe should create a bund of gravel, separated at the bed surface from adjacent bunds. The final chosen geometry, illustrated in Figure 7, also has the merit of creating a drainage path for water as the tunnel element makes contact with the bed. The individual bunds thus produced were analysed to determine long term stability. This resulted in an angle of internal friction of 40 degrees being specified for the bed material.

8.4   Accuracy of Construction and Survey

It was recognised at the outset that the gravel bed proposal would not be viable unless accurate bed levels could be achieved. The system finally specified is capable of delivering an overall level accuracy of ±25mm from the design line throughout. This is achieved by a laser levelling system linked by computer to hydraulic cylinders on the feeder pipe. The system is sufficiently responsive to maintain the pipe level against wave-induced movements of the pontoon.

During development of the proposal, it was recognised that *demonstrating* that the gravel had been placed accurately to level was going to be no easier than constructing the bed accurately in the first place. Levels of the finished bed are measured (independently of bed construction) by means of a row of echo-sounders mounted on the feeder pipe. The design can accommodate inaccuracies in the levelling system (allowing for errors in the echo sounders, in the position of the fall pipe and in the laser measurements), of up to ±23mm; performance on site is confidently expected to better this figure.

8.5   Effect of Bed Levels on Tunnel Stresses

Due to the sensitivity of the tunnel box to even quite small distortions, the accuracy of the gravel bed levels is an important permanent works design matter. To define an acceptable bed level is not simply a matter of specifying the ±25mm tolerance; much smaller deviations can be unacceptable if they follow a regular pattern (for example a consistent pattern of +10mm under the middle of the tunnel base and -10mm under both edges would be unacceptable, even though well within the overall tolerance). To address this, it has been specified that variations in bed level must be distributed in a random pattern.

A study has been performed to determine what precisely is meant by 'random' in this context, and a numerical test has been developed which can be applied to any actual bed level data set to test for the needed degree of randomness. Beds which pass this test will be accepted for tunnel immersion directly, whilst any that fail the numerical test will trigger a check analysis of the element in question for the as-built bed. This will either result in the bed being accepted as-built, or recommendations for remedial action being put forward. Possible remedial works include local removal of high spots without reinstatement, or more extensive removal of out-of-tolerance construction followed by reinstatement.

9.   Conclusions

A "design and build" type of contract is recommended for major projects as it provides substantial benefits for both the designer/contractor team and for the owner. The designer and contractor can combine their efforts and make maximum use of their potential and experience in optimising the design and the construction methods in an integrated fashion. Consequently, the owner is assured of good value financially, and is able to minimise his involvement throughout the design and construction phase.

In order to make "design and build" successful, the contract needs to allow the fullest possible flexibility to the designer/contractor by depending on performance specifications, and keeping firm, specific requirements to a minimum.

For the Øresund Tunnel in particular, "design and build" has created the opportunity for tunnel design to be optimised to a degree impossible under more traditional forms of procurement, and has permitted the development of an exciting and innovative construction method customised to the challenges and opportunities of this particular project.

Design of Reinforcement to Control Cracking Due to Imposed Strains

Agnes Nagy
PhD
Dept. of Struct. Engineering
Lund University, Sweden

Agnes Nagy, born 1963, received her civil engineering degree 1986, the degree of licentiate of engineering 1994 and the PhD degree 1997.
During the period 1990-1997 she published 4 articles in Materials and Structures and in ASCE Journal of Material in Civil Engineering.

Summary

The amount of reinforcement to control cracking of concrete structures is investigated. The effect of non-uniform cooling and shrinkage is studied with regard to the external and internal restraint acting on the structure. By means of a simple model several different cooling processes and restraint degrees are simulated for different wall sections. The results of the computation give the force actually arising in the structure during the cooling or shrinkage process and the range of softening and cracking in the concrete section. The aim is to investigate the parameters having major impact on the magnitude of this force and consequently influence the design of minimum reinforcement. The investigation concludes some simple guidelines regarding the design of minimum reinforced concrete structures in practical cases.

1. Introduction

Most existent concrete structures are provided with a significant amount of reinforcement to control cracking due to imposed strains. The amount of reinforcement necessary for crack control depends on three factors: the magnitude and distribution of imposed strains in the section, the degree of restraint of the structure and the deformation capacity of the concrete. Especially the first two factors are difficult to estimate and in practical design it is usually assumed on the safe side that the imposed strains are large and that the restraint is almost complete without further analysis. The consequence of such an overestimation in massive structures is a large amount of reinforcement, which makes the casting process difficult and counteracts durability performance.

Present design rules require that the capacity of the minimum reinforcement at yield should be higher than the force necessary to create a new crack [1]. In this way the reinforcement redistributes the stresses after the appearance of the first crack so that several narrower cracks arise instead of a few wide-opened [2].

In this paper investigations are made regarding walls with restraint exposed to different cooling processes. Rapid as well as slow temperature changes on the surface, the influence of wind and daily temperature cycles for summer and winter are considered. The spatial distribution of imposed strain developed from sudden cooling is roughly equivalent with the imposed strain from drying shrinkage [3], i.e. the results and conclusions regarding sudden cooling can also be applied for drying shrinkage.

2. Constitutive Model

In this paper a medium-thick wall, characterized by the geometry shown in Fig.1, is used as a reference structure. The external restraint acting on the wall is modeled with a set of springs characterized by the spring coefficient k (N/m^2) related to the spring force P_z (N/m).Cooling is modeled as a linear thermal diffusion process, one dimensional and symmetric with respect to the mid plane of the wall. The wall is assumed to be in a state of generalized plane strain in the y and z directions.
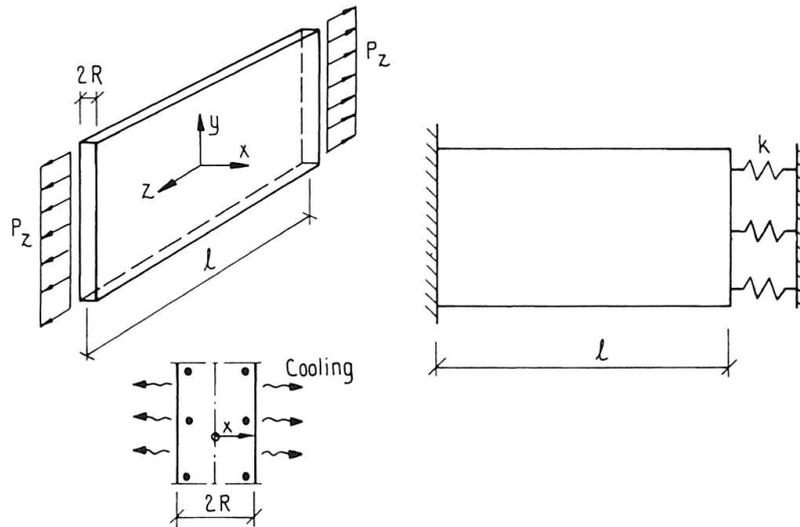

Fig.1 Geometry of the medium-thick wall.

The overall equilibrium in the z direction gives

$$\int_0^R \sigma_z dx + \sigma_{zs} \cdot A_s = \frac{P_z}{2} \qquad (1)$$

where σ_z is the stress in the concrete, σ_{zs} is the stress in the steel, A_s is the reinforcement area/unit length at each surface of the wall and P_z is restraint force/unit length. The assumed stress-strain relation for the concrete in tension is shown in Fig.2. The steel is assumed to be linearly elastic during the whole cooling process.

The restraint force P_z during the cooling process and its maximum value P_{zmax} may be computed under these assumptions. This value may be compared with the maximum possible force in the section, P_z^{lim} - the nominal tensile capacity, corresponding to the case when the tensile strength of the concrete is reached simultaneously over the whole section. The following relation is valid for P_z^{lim}:

$$\frac{P_z^{lim}}{2} = Rf_{ct} + E_s A_s \varepsilon_{sT\,tot} \qquad (2)$$

where f_{ct} is the tensile strength of the concrete, E_s is the Young's modulus of the steel and ε_{sTtot} is the total imposed thermal strain in the steel. In reality the actual force P_{zmax} is usually less than P_z^{lim} due to successive softening and cracking over the section. For further details regarding the principles of this analysis, see [4].
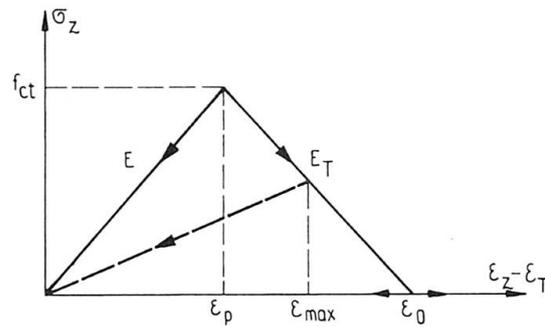
Fig.2 Assumed bilinear stress-strain relation for concrete in tension.

3. Characterization of Imposed Strains

Computations of the temperature fields in a wall with thickness 2R=0.4 m has been made by Hacon-T [5], a program for simulation of temperature in concrete. The initial uniform temperature of the concrete is taken to 20 °C. The following data were used for the concrete: coefficient of heat transfer λ= 2.1 W/m·K, heat capacity c=1000 J/kg·K and density ρ=2350 kg/m^3. Fig.3a shows the results for the case when the ambient temperature suddenly drops to zero. The computations were made for three different values of the surface heat transfer coefficient h corresponding to three values of wind velocity. Fig.3b corresponds to slow cooling, with a rate of decrease in ambient temperature equal to 0.27 °C /h. It is seen that the temperature distribution in the wall is fairly uniform in most cases, except for the extreme situation in Fig.3a with h=1000 W/m^2·K. This value corresponds to a case with practically no surface resistance, which may occur in practice if the surface is directly exposed to wind with very high velocity or due to shrinkage process.

a) sudden cooling from 20°C
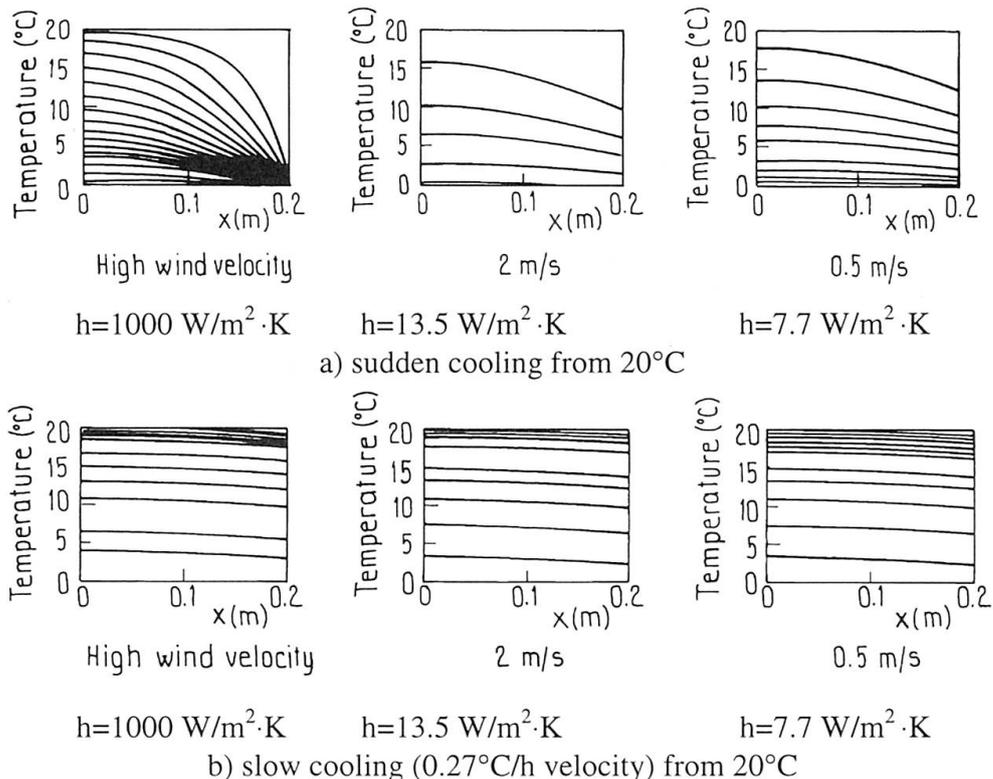

b) slow cooling (0.27°C/h velocity) from 20°C

Fig.3 Temperature distribution in concrete wall for different cooling processes.

Investigation of the effect of daily temperature cycles in summer and winter has been made. Simulation of the temperature fields in a wall with thickness R=0.6 m is made for a daily variation of ambient temperature between 12.9 °C and 21.2 °C during summer.

The initial uniform temperature in the wall is set to 17 °C during summer and the value of h was chosen to 7.7 W/m^2°C corresponding to a very low wind velocity. Fig.4 illustrates the range of temperature variation in the wall when exposed to a daily summer cycle. It is seen that the daily temperature cycle has almost no influence in the middle of the wall and causes only a few degrees change near the surface. During winter the temperature changes are even smaller.

The investigation leads to the conclusion that imposed thermal strain in general may occur both with an almost uniform distribution and with a highly non-uniform distribution over the cross section. For the purpose of discussion, it seems rational to idealize the thermal action as two types of processes, one where the imposed strain is *uniform* over the cross section, corresponding to most of the cooling processes in practice such as temperature change from summer to winter. The other one is with highly *non-uniform* distribution of the imposed strains corresponding to a shrinkage process characterized by a step change at the surface or a cooling process with high wind velocity.
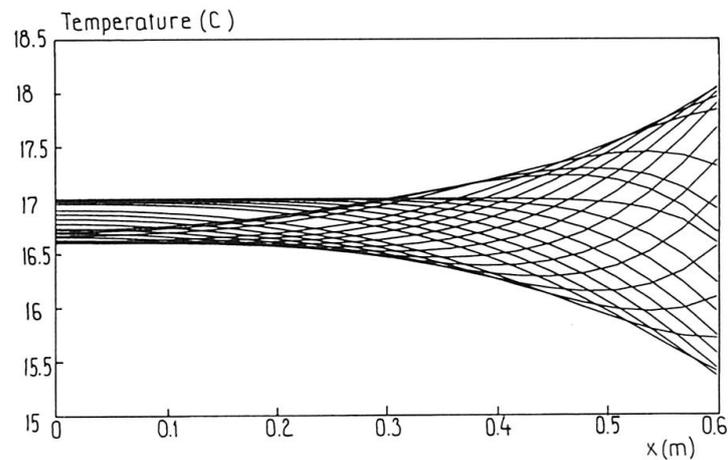

Fig.4 24 hours temperature cycle during summer in a wall with 2R=1.2 m.

4. Influence of Internal and External Restraint

The simulations presented in this section are based on cooling processes of the type shown in Fig.3a for sudden cooling, with five different values of the temperature drop ranging from 10°C to 35°C. The calculations are made for two different values of the spring coefficient k: one with $k\ell/2ER=225$, i.e. very strong external restraint representing a wall with practically full restraint, and the other with $k\ell/2ER=1$ representing a wall with a restraint stiffness equal to the axial stiffness of the wall itself. Two different concrete sections have been investigated: one with 2R=0.4 m and a thicker one with 2R=1.2 m. The temperature field in the wall is computed both with a high heat transfer coefficient (h=1000 W/m^{2}K, c.f. the left Fig.3a) and with a comparatively low heat transfer coefficient (h=7.7 W/m^{2}K, c.f. the right Fig.3a). The most important characteristics of the concrete used in the parametric investigation are: E=20 GPa, ε_p=0.000145. The amount of reinforcement is A_s=0.0004 m^2/m corresponding to ϕ 10 c 200 at each surface of the wall and with E_s=200 GPa. (ρ=0.002, $\alpha\rho$=0.02, where $\rho=A_s/A_c$ and $\alpha=E_s/E$). The value of the ratio E_T/E is taken to -1.55. The computed ratio P_{zmax}/P_z^{lim} is given as a function of the parameter $\varepsilon_{Ttot}/\varepsilon_p$, the ratio between the total induced thermal strain ε_{Ttot} (at the

end of the process) and the strain capacity ε_p at tension failure. P_{zmax} is the maximum restraint force obtained during the process and P_z^{lim} is the upper limit of the force according to Eq. (2).

In Fig.6 results from computations for sudden cooling or strong internal restraint are shown. For the case with strong external restraint when the imposed thermal strain ε_{Ttot} is higher than the ultimate tensile strain ε_o a through crack is developed. With the chosen value of E_T/E, this occurs for values of the ratio $\varepsilon_{Ttot}/\varepsilon_p$ higher than 1.65, c.f. For cases with weak external restraint a through crack is developed for values of $\varepsilon_{Ttot}/\varepsilon_p$ higher than 2.5.
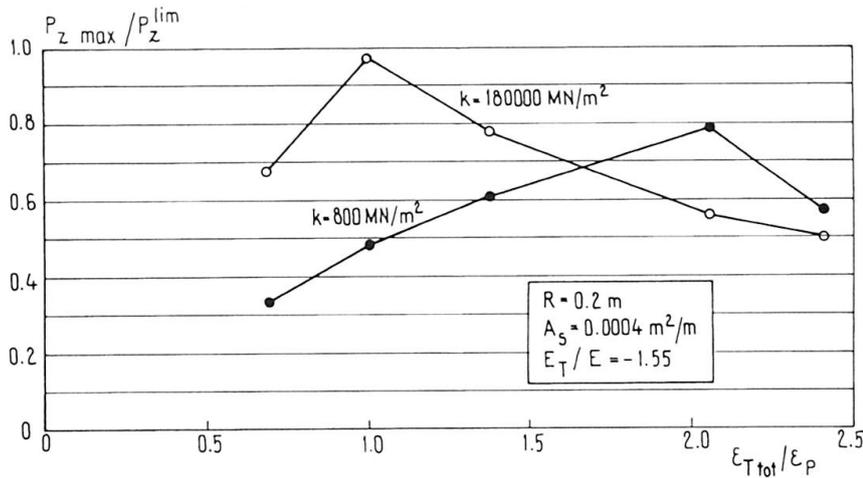

Fig.6 Force in restrained wall subjected to sudden cooling.
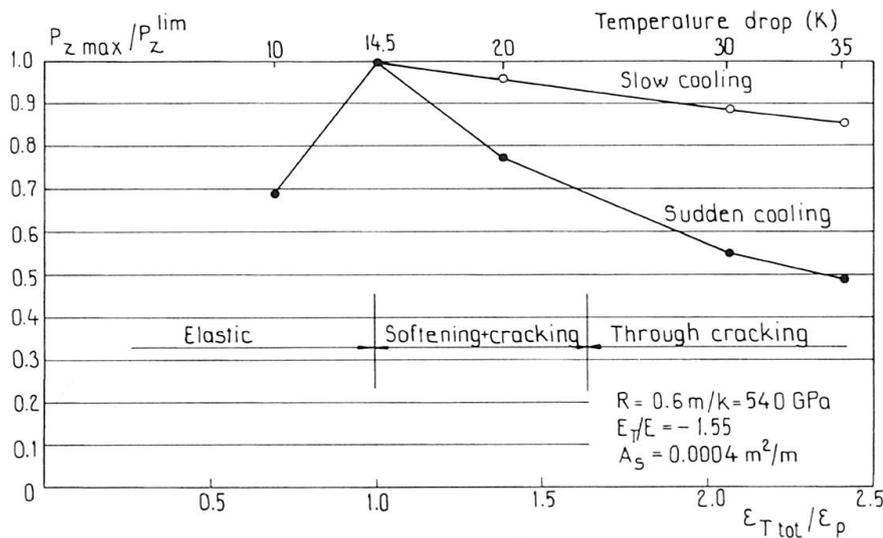

Fig.7 Force in restrained wall for strong external restraint with rapid and slow cooling.

The reinforcement is fully needed only after a through crack has developed. The design of the reinforcement should be based on the maximum restraint force P_{zmax} developed in processes where a through crack occurs. Fig.6 shows that both for strong external restraint and weak external restraint the force actually arising when a through crack develops is only about 0.5-0.7 of the maximum possible force P_z^{lim} leading to a considerable reduction of the amount of reinforcement. The reason for this is the successive growth of softening and cracking through the section created by the non-uniform distribution of imposed strain in this case.

In Fig.7 similar results are displayed for a slower cooling process with a heat transfer coefficient h=7.7 W/m^2K. A comparison is made with the case with rapid cooling with a surface heat transfer coefficient h=1000 W/m^2K. The slow cooling process gives higher values of the actual force for high values of $\varepsilon_{Ttot}/\varepsilon_p$, since the diminished temperature gradient during slow cooling leads to a more uniform stress state in the section. Consequently, the tensile stresses are primarily governed by the external restraint acting on the wall. Similar results for weak external restraint also show that the ratio P_{zmax}/P_z^{lim} is higher for slow than for rapid cooling for large values of $\varepsilon_{Ttot}/\varepsilon_p$.

5. Conclusions

The minimum reinforcement needed to control cracking due to imposed strain in concrete structures depends on the magnitude and distribution of imposed strain, the degree of restraint and the deformation capacity of the material. In the present paper these factors have been analyzed for a simple reference structure in the form of a wall with axial restraint. For the purpose of discussion, imposed strain may be idealized in two distinct cases, one where the imposed strain is *uniform* over the cross section and one where it is highly *non-uniform* with strong gradients.

For the case with uniformly distributed imposed strain applies the following:

-is mainly relevant for cooling processes in practice such as a temperature change from summer to winter

-even for full restraint, concrete can normally survive an imposed strain of 0.1-0.15 ‰ corresponding to a temperature change of 10-15°C without cracking

For the case with non-uniformly distributed imposed strain applies the following:

-is valid for situations with rapid changes in temperature as well as for imposed strain related to drying shrinkage

-a 30% reduction of the required minimum reinforcement is possible for cases where a through crack appears independently of the magnitude of external restraint

-for cases where the internal restraint is dominating and where the external restraint is limited, usually no through cracks will be created and thus the crack reinforcement may be limited, the distribution of cracks will take place anyway as in plain concrete without reinforcement

-the amount of reinforcement needed to distribute cracks is smaller for non-uniform strains such as drying shrinkage than for uniformly distributed strains characteristic for most of the cooling processes.

6. References

[1]   CEB, 'Design Manual on Cracking and Deformations', No 158, 1985.

[2]   Jaccoud J. P., 'Armature minimale pour le contrôle de la fissuration des structures en béton', École Polytechnique Fédérale de Lausanne, Thèse No 666, 1987.

[3]   Thelandersson S., Mårtensson A., Dahlblom O., 'Tension Softening and Cracking in Drying Concrete', Materials and Structures, (1988), 21, pp 416/424.

[4]   Nagy A., 'Thermally Induced Softening and Cracking in Concrete with Minimal Reinforcement', accepted for publication in RILEM Journal Materials and Structures. 1996.

[5]   Dahlblom O., 'HACON-T - A Program for Simulation of Temperature in Hardening Concrete', Vattenfall (Swedish State Power Board) R,D&D. U 1990/31. ISSN 1100-5130.

Numerical modelling of prefabricated segmental tunnels under embankments

Michel J. BASTICK
Development Manager,
Groupe TAI,
PARIS, FRANCE

Alain GUILLOUX,
General Manager
TERRASOL,
MONTREUIL, FRANCE

Christelle LONGUET,
Engineer,
TERRE ARMEE,
LE PECQ, FRANCE

Summary

Groupe TAI introduced the TechSpan arch system about a decade ago. Since then about 600 structures have been built. This article presents the possible design options and assesses their representativeness. The influence of various parameters on the arch behaviour is studied. A comparison with measurements on a real structures validates the specific approach selected for TechSpan.

1. TechSpan™ structures

TechSpan™ is a prefabricated arch system which is used to replace bridges, install tunnels under fill or in cut and cover situation. Shape is optimised so that the concrete is mainly in compression.

The concept of arch is quite ancient and has been successfully used for centuries for masonry arch bridges or for cast in situ culverts. Groupe TAI revisited the concept in 1986 and launched a three hinge prefabricated system consisting of two pieces [1]. Typical dimensions are 3 to 25 meters in span. Applications are for river crossings under fill, road and railway crossings, covering existing railway in order to save space and reduce noise, and for industrial applications. To date, about 600 TechSpan structures have been built around the world.

2. Shape optimisation

Whilst the arch concept is simple in itself, the actual load history a structure element will undergo while it is transported, erected and then backfilled is far from being simple. A safe structure will call for all the load cases to be designed for. The whole purpose of TechSpan is to optimise the shape in order to minimise the maximum tensile stresses to be resisted by steel reinforcement. This optimum shape obtained by a computer program leads to an economical design. In some instances TechSpan ability to be adapted in shape to the client's special requirement will prove useful in special cases when extending an existing structure for example.
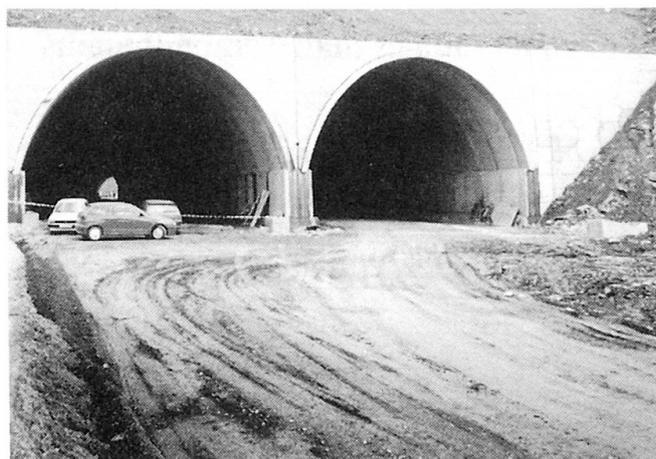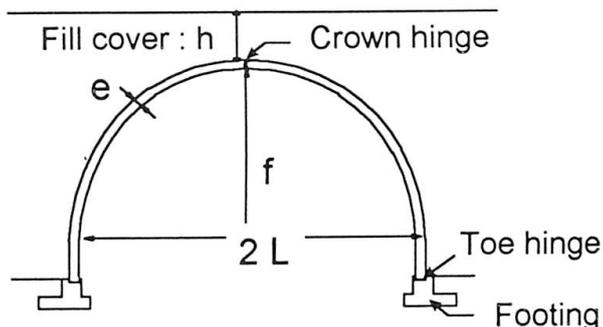
Fig. 1 : Example of a TechSpan

Fig.2 : Typical cross section and notations

In the end the system introduces the reliability and quality of an industrialised process in the geotechnical field, where the geometry, load and soil variability cause each structure to be unique. This uniqueness is accounted for by the shape optimisation, leading to a cost effective solution.

3. Various possible design methods

As for any underground structure, various calculation models can be used for the structural design. But it is well known that the behaviour of buried structures is a problem of soil-structure interaction, as the loads are dependant upon displacements.

The possible design methods can be classified in three categories, for which table 1 summarises the advantages and drawbacks :

- the static analysis, in which the backfill is modelized only by the loads imposed to the structure, without considering soil-structure interactions
- the beam and spring models, where the backfill is modelized both by the loads acting on the structure (assumed value) and by the reactions exerted by the soil on the structure. These reactions are dependant upon the calculated displacements, generally according to a linear elastic behaviour in compression (no tensile reactions), requiring the selection of adequate spring moduli characterizing the soil.

Feature Model → ↓	Static analysis	Beam & spring model	FEM with DUNCAN model
Soil-structure interaction	NO	Partly	YES
Staged loading	Possible*	Possible*	YES
Compaction effect	Possible*	Possible*	YES
Soil arching Marston effect	NO**	NO**	YES
Arching around the arch	NO	NO	YES
Soil-structure friction	NO	NO	YES
Foundation displacements	NO	Possible*	YES
Non linear soil behaviour	NO	Possible*	YES
Stress dependant modulus	NO	NO	YES
Soil parameters determination	N/A	Difficult (non intrinsic)	Easy (intrinsic)

*   Possible but usually not done   ** Marston effect not represented by the model, taken into account by a coefficient obtained from an independent computation

Table 1 : Representativeness of possible design methods

- the FEM (Finite Element Method) modelization, in which the soil is modelized as a whole, with its geomechanical parameters (elastic and elastoplastic) : such analysis does not require any additional assumption upon loads acting on the structure and reactions exerted on the structure. Of course, many constitutive laws can be used for soil modelization, but the most accurate for this kind of application appears to be the law presented by Duncan et al. [2].

4. Geomechanical parameters for FEM calculations

The previous table shows that the FEM is the only way to correctly represent all the features governing the soil-structure interaction, and a realistic behaviour of soils. For this reason and after a detailed investigation of the main parameters and their influence on the design, the FEM analysis was chosen as the usual design method for TechSpan.

4.1 Soil modelisation

The model presented by Duncan et Al. [2] was selected for the soil around the concrete arch in the FEM design because it takes into account all the important parameters that affect the behaviour of the structure :

- the stress strain curve is parabolic (Fig. 3)
- the initial modulus depends on the stress

$$E_i = K_i\, p_a\, (\sigma_3/p_a)^n$$

where p_a = atmospheric pressure

- the unload-reload modulus differs from E_i but also depends on σ_3
- the bulk modulus also varies with confining stress : $B = K_p\, p_a\, (\sigma_3/p_a)^m$
- Mohr-Coulomb criteria (c, φ) is used to define the deviatoric stress at failure
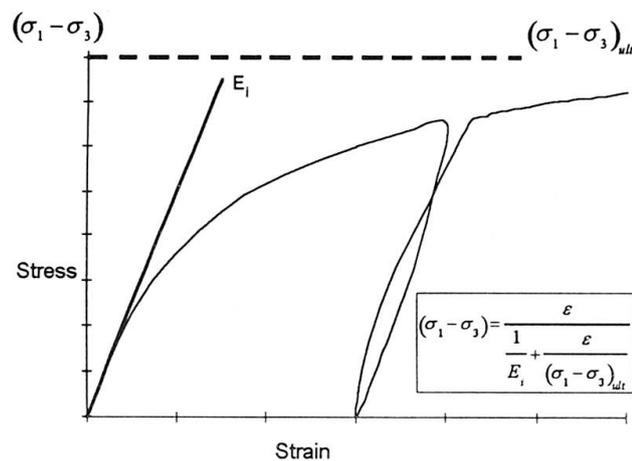

Fig. 3 : *Non linear stress-strain curve*

Realistic values for the main parameters may be found in the literature. Table 2 presents the recommended values which agree with the various soil and backfill types specified for TechSpan structures. Parametric analysis has shown that the model is numerically stable and that realistic variations around these values have a limited impact on the computed stresses in the elements.

Material	γ kN/m^3	ϕ (0)	c kPa	K_i (MPa)	n -	k_b (MPa)	m
Foundation soil	*	*	*	$10.E_1$	0	0.85.K_I (S) 0.55.K_i (R)	0
Dense backfill	21	33/36	0	600	0.35	300	0.2
Normal backfill	20	30/33	0	500	0.40	220	0.25
L . compacted	18/19	28/30	0	350	0.45	220	0.25
Non select fill	16/17	25/28	0/25	200	0.6	150	0.4

* : according to geotechnical data   S : soils   R : rocks

Table 2 : *Recommended parameters for TechSpan design*

4.2. Construction phase loadings

Final state is normally not the most severe design case. It is important to compute the model for each single construction step or fill layer and within each step to represent the compaction stress applied on the fill, with three sub-steps per layer : fill, compact, remove compaction load.

4.3. K coefficient

The $K = \sigma_h/\sigma_v$ coefficient around the tunnel is one of the main parameters governing the behaviour of the structure, as it characterises the supporting effect of the lateral backfill. While this parameter is an hypothesis in others models, it is a result of the FEM calculations.

It is of major interest to note that, during the different construction stages, K varies widely

- near the footings, K increases from 0.3-0.5 (between K_a and K_o) when backfill is erected up to the top of the vault, to 1.0 (much higher than K_o) for high backfill cover
- near the crown, K decreases from more than 1.5, to 0.6-0.8 (significantly higher than K_o) when backfilling reaches the crown, and then down to 0.4-0.5 (close to K_o) for high backfill cover

Such effect confirms that usual calculation methods cannot modelize the actual behaviour, as they generally consider constant K values (0.3 and 0.5) whatever the stage of backfilling
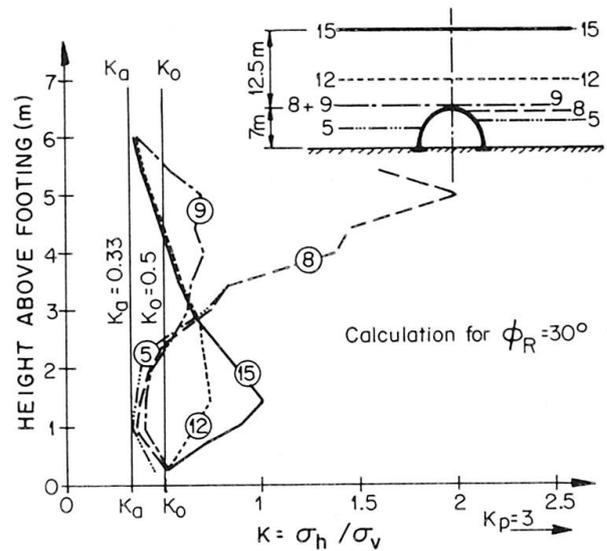

Fig. 4. Variation of K around the arch during backfilling stages

4.4. Marston effect

It is well known that rigid culverts under embankments are loaded by stress σ_v which can be much larger than the overburden pressure γh. This effect known as "Marston effect" [3] [4].is due to the differential settlements of embankment between the zone above culvert and the adjacent zones.

To account for this stress increase, Marston introduced a coefficient such that $\sigma_v = K_M \gamma h$. This coefficient is usually in the range 1.1 to 1.5 and may be as high as 2. Overlooking it in a design may lead to failure. Since this effect is not represented in either the static or the beam and spring model, the Marston coefficient is reintroduced in the system afterwards. Table 3 presents the ratio $\sigma_v/\gamma h$ obtained from the TechSpan FEM model for a given geometry. Flexible structures lead to lower values of K_M and the model is in good agreement with semi-empirical values when the hypothesis are made consistent with Marston's: rigid structure, constant modulus.

TechSpan 0.3. m thick	Rigid TechSpan 1 m thick	Rigid TechSpan Constant E	Semi-empirical Marston coefficient
1.10	1.22	1.30	1.35

Table 3 : Marston Coefficient

5. Comparison between predicted and monitored behaviour

5.1. The Oita TechSpan

Built in Japan in spring 1995, the Oita structure with 11.5 m span and 17.5 m of fill cover offered an interesting case for full scale experimentation. The monitoring was quite complete and included both stresses and displacement measurements in seven cross sections [5]. The measurements were quite consistent for the various section and in this short article we will only report average values.

5.2. Moments in the arch elements

Stress gauges were installed on the steel reinforcement cages in order to estimate the bending moment in the elements. From these steel strains the moment in the precast element may be derived assuming either a cracked or an un-cracked concrete section. Safety normally requires the designer to take the conservative assumption that the concrete will be cracked. This leads to a maximum bending moment of 30 kN.m which is much lower than the result of the analysis.

However the elements are designed and handled in a way that minimises bending moments and the hypothesis that the elements in the completed structure are un-cracked is more realistic. Under this assumption the measured moment in the element reaches 110 kN.m as a maximum. This is in very good agreement with the moment obtained from the Finite Element Method.

It must be noted that the shape and maximum value of the moment is not much affected by the E value selected for the concrete in the usual range (20 GPa to 36 GPa). Moment derived from other methods lead to unrealistic values (Table 4). Note that the asymmetric shape of the moment envelope corresponds to the asymmetric stress history during the backfilling stages.

Calculated maximum bending moment				Measuring bending moment	
Static analysis	Beam and spring	FEM $E_i = 36$ GPa	FEM $E_i = 20$ GPa	Un-cracked section	Cracked section
500 kN.m	150 kN.m	115 kN.m	105 Kn.m	110 kN.m	30 KN.m

Table 4 : Calculated and measured maximum bending moment in TechSpan

5.3. Deflection

Fig. 5 presents the measured vertical displacement at the crown (DY3) along with the value predicted with the finite element model. The FEM program was run with two sets of input : the standard properties with concrete stiffness of $E_c = 20$ GPa and no cohesion in the backfill and a second set with $E_c = 36$ GPa and C = 20 kPa. The second set leads to very representative results and should really be used when short term prediction is required. The standard set is more representative of long term. Both sets lead to deflection within a few millimetres of measurements and the impact of these parameters is small on the reinforcement design.

The shape of the curves is interesting as it shows that the elements will breath up and down during the backfilling to return close to an undeformed state for the completed structure. The corresponding moments (either from measurement or FEM) are much reduced. The fact that the permanent state of stress of the element is much smaller than the maximum for which it was designed leads to enhanced durability and long term safety.
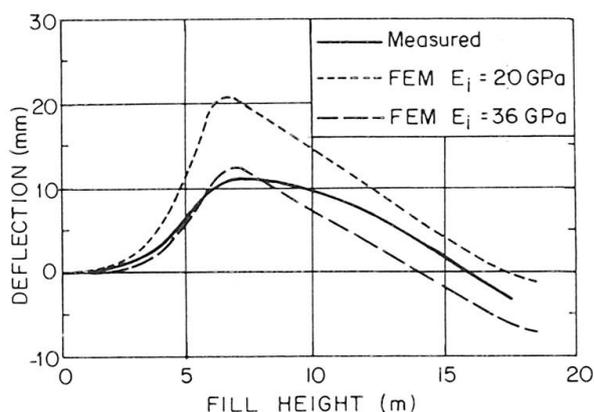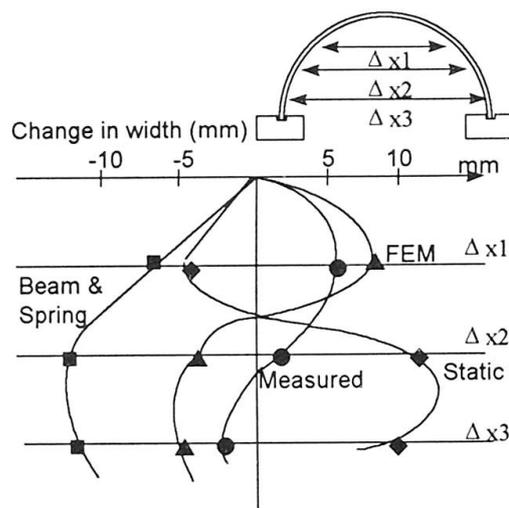
Fig. 5 : Computed and measured deflections

Fig. 6 : Measured and producted convergences for various design approaches

5.4. Lateral displacements

Fig. 6 presents the convergence or change in width of the structure at three elevations above footing for the final stage. Only the FEM study gives realistic values for these deformations while the beam and spring and the simple static model lead to results very different from measurements.

6. Conclusion

The soil interaction phenomenon's are taken into account in TechSpan up to the point that the shape of the structure is optimised accordingly. This specificity of TechSpan would be meaningless without its FEM design method. This method is the only one capable of representing the soil structure interaction phenomenon developing during the various phases of construction.

The parameters to be used in the method have been presented and the sensitivity of the results to variations of these parameters discussed. In the end the comparison with the monitoring of the Oita structure validates the method which was the only one to predict adequately the structure behaviour both in stresses and displacements, during construction phases and for its finished state.

Bibliography

1. SMITH R.J.H., "Development of a precast arch system" International Conference on Arch bridges - Bolton, UK. September 1995.
2. DUNCAN J.M., BYRNE P., WONG K., MARBY Ph., "Strength, stress-strain and bulk modulus parameters for FEM", Report UCB/GT/80-01, Univ. of Cal. Berkeley, 1980.
3. CLEMENT Michel, JEAN Pierre, "Ouvrages voûtés sous remblai - Pose en dépression", Rev. Ouvrages d'Art n° 21 SETRA-CTOA, France, Juillet 1995
4. LONG Nguyen Thanh, VEZOLE Pierre, "Ouvrages sous remblai - Pneusol et maîtrise des charges verticales", Annales ITBTP n° 515, Juille-Août 1993.
5. JENKINS D.A. "Analysis of Buried Arch Structures. Performance versus Prediction " CIA Conference, Adelaide, Australia, May 1997.

Development of Wing Segments

Toru Konda
Doctor of Engineering,
Professor, Engineering Department,
Tokyo Municipal University
Tokyo, Japan

Toshi Nomoto
Doctor of Engineering
Technological Laboratory,
Nishimatsu Construction Co., Ltd.
Kanagawa, Japan

Kenji Mito
Engineer, Civil Engineering
Civil Engineering Design Department,
Nishimatsu Construction Co., Ltd.
Tokyo, Japan

Hiroshi Yamazaki
M.E.
Technological Laboratory,
Nishimatsu Construction Co., Ltd.
Kanagawa, Japan

Abstract

Wing segments are developed aiming the efficient moment transfer at the joints of shield lining to maintain necessary lining stiffness in very soft ground where enough passive pressure is not mobilized, and to reduce the cost of joints. In developing wing segments full-scale loading tests have been conducted. The test results show that maintaining the shearing stiffness at the end of wing joint could attain sufficient moment transfer at joints. Unlike ordinary segments, the moment transfer by bolts is not significant and the number and size of bolts could be reduced in the segments.

1. Introduction

In Japan shield tunnels are often constructed in soft ground. Accordingly enough passive pressure is not mobilized and a large bending moment occurs in the lining. For ordinary rectangular segments, lining stiffness is covered by the longitudinal joint positions are not continuous for tunnel axis (hereafter referred to as staggered pattern). To maintain strength of the lining and prevent joint opening are needed, however, heavily reinforced and expensive joints are required.

The authors developed a wing segment that reduces the number of bolts used and decreases the bolt diameter by modifying the shape of the segment pieces. The longitudinal joints have extension part in circumferential direction that equal about half width of the segment, and tenons that we call shearing keys are placed in the joint surface. Wing segment can be attained efficient moment transfer caused by shearing stiffness, and sufficient ring strength and ring stiffness in very soft ground. This paper presents a basic construction of the wing segment and the results of the loading tests conducted with full-scale segments (5300mm external diameter, 1200mm width, 250mm thickness, six pieces).

2. Basic Construction of Wing Segments

2.1 Shape

Figure 1 shows the basic construction of wing segments. The segments are made up of the "main section" and "wing sections." The longitudinal joint surfaces of the segments have shearing keys, so that shear resistance force can be transmitted effectively.
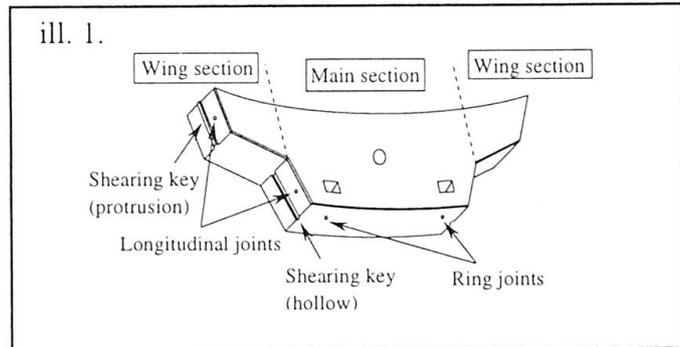
2.2 Mechanism of Bending Moment Transfer

Fig. 1 Basic Construction of Wing Segments

Figure 2 shows the structural transmission mechanism of bending moment in the wing segment joint. The bending moment that works on the joint (M) is divided into that which works on the bolts (Mb) and that which works on the base of the wing section (Mw). Mw is the sum of the bending moment that works on the shearing key (Ms = Sj x L) and Mb.

$$M = Mb + Mw$$
$$= Mb + (Ms + Mb) = 2Mb + Ms$$

M : Bending moment that works on the joint.
Mb : Bending moment that works on the bolts.
Mw : Bending moment that works on the base of the wing section.
Ms : Bending moment that works on the shearing key (= Sj x L).
Sj : Shearing force that works on the shearing key.
L : Wing length

Ms and Mb resist the bending moment M that works on the joint. Therefore, by placing a higher percentage of the bending moment on the shearing key the burden placed on the bolts can be reduced. In other words, the number of bolts or their diameter can be reduced.

Theoretical analysis was conducted by using a cantilever model as shown in Figure 3. A model was constructed in which both wing sections face each other and are joined by rotation springs and shearing springs.

The cross section of a single subway tunnel was used for the analysis. The relations between the wing length and the bending moment percentage on the bolt, the base of the wing section and the shearing key and between the wing length and equivalent rotation stiffness that converted ordinary joint were calculated. The results of the analysis are shown in Figure 4. The bending moment percentages on the each section are shown below.
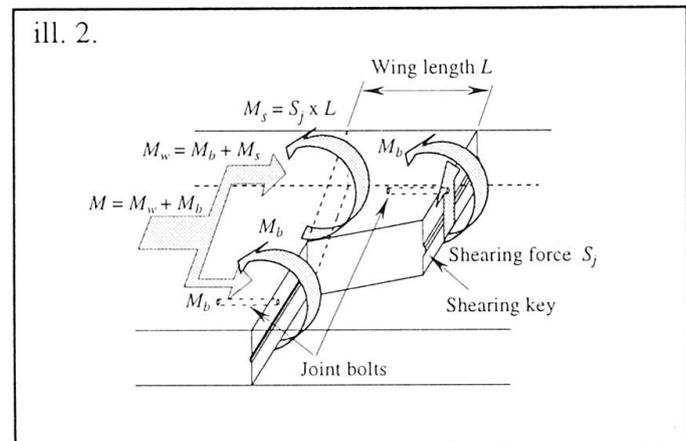

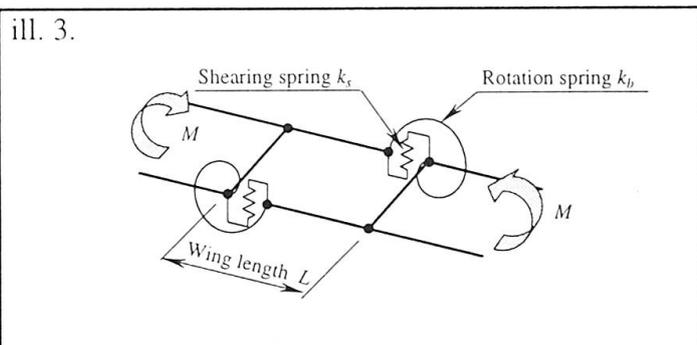Fig. 2 Mechanism of Bending Moment Transfer by Shearing Force
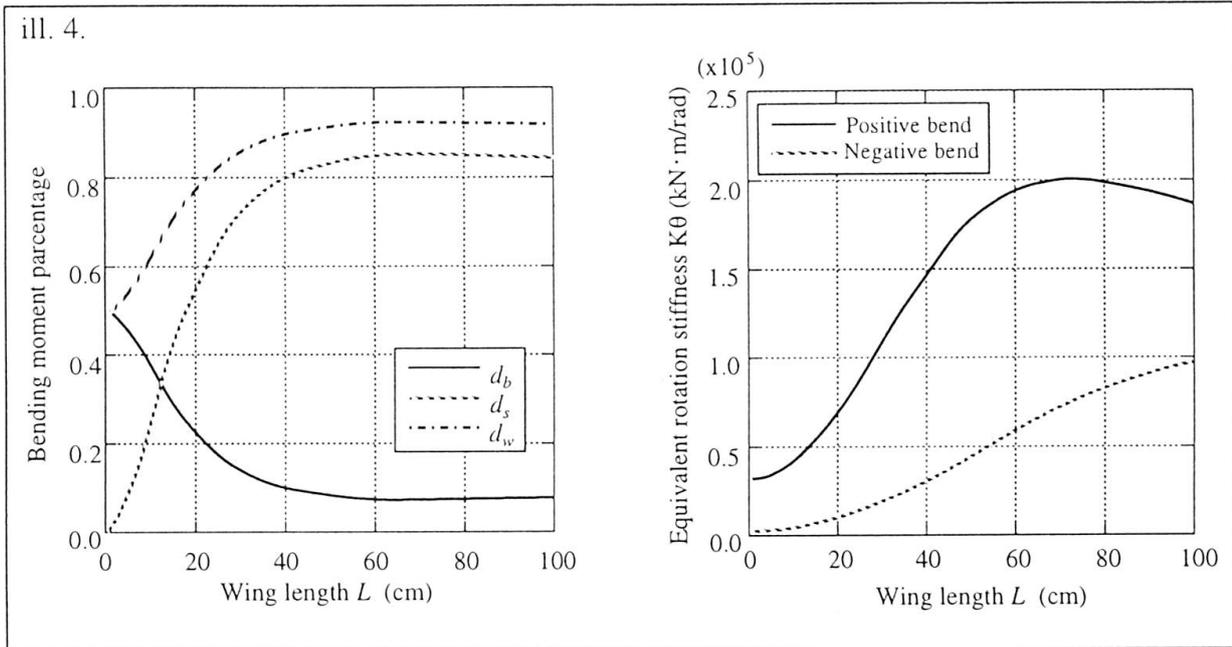

Fig. 3 Cantilever Model

ill. 4.

Fig. 4 Wing Length (L) Sensitivity Analysis

$$db = Mb/M$$
$$dw = Mw/M$$
$$ds = Ms/M$$

db : Bending moment percentage on the bolts.
dw : Bending moment percentage on wing section base.
ds : Bending moment percentage on the shearing key.

Longer wing sections are better to reduce the burden on the bolts. The analysis showed that the bending moment percentages and equivalent rotation stiffness became changeless when the wing length exceeded 60 centimeters. Therefore, the wing length in the full size segment load presence tests was set at 60 centimeters.

3. Loading Tests Using Full-Scale Segments

The aim of developing wing segments was to attain strength and stiffness equal to or higher than staggered pattern rectangular segments even if wing segments' longitudinal joint positions were continuous for tunnel axis (hereafter referred to as inline pattern). A series of the loading tests using full-scale segments was carried out in order to investigate this. Figure 5 shows the section items for the test piece. The materials used are shown in Table 1.
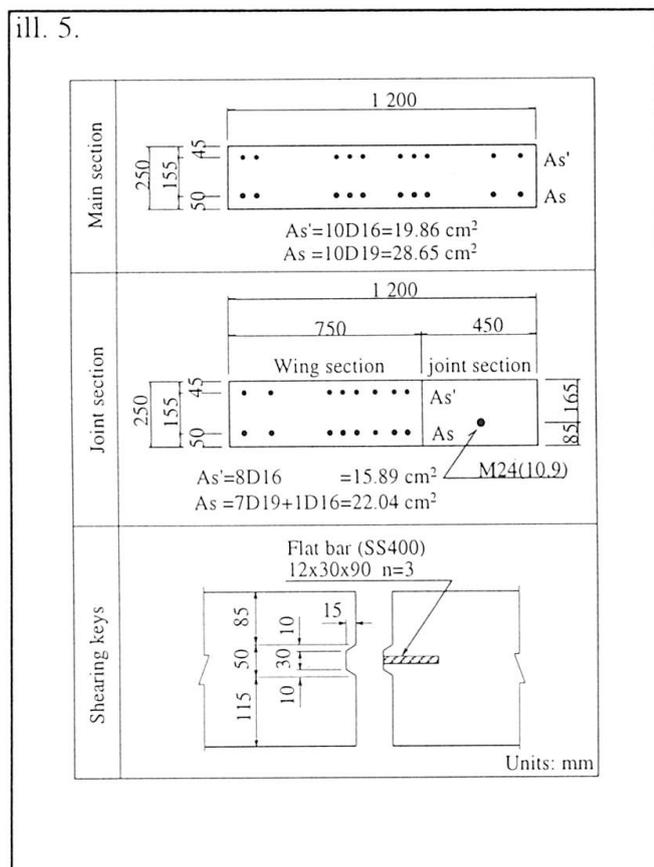
ill. 5.

Fig. 5 Cross Sections of the Test Piece

3.1 Shearing Key Shearing Test

3.1.1 Purpose of the test
To obtain the shearing spring constant and confirm shearing strength of the shearing key on the joint surface.

3.1.2 Testing Method
Figure 6 shows an outline of the testing method. Tests were conducted on the loading conditions that occurred positive bending moment (Case 1) and negative bending moment (Case 2) at the joint.. Axial force was set at 441 kN per segment width and 221 kN per longitudinal joint surface to comply with the joint bending test and ring loading test to be described later.

3.1.3 Test Results
1) Shearing strength
   Table 2 shows the test results. Because compression caused cracks early in Case 2, the collapse load was smaller than for Case 1. However, it was found that the shearing key had sufficient shearing strength because the collapse load is greater than the design ultimate load,.

2) Shearing stiffness
   Figure 7 shows the relations between presence load and shearing deformation. The design values in the figure do not take friction resistance caused by axial force into consideration. Although shearing cracks resulted after the allowable load was exceeded, it can be seen that there are no major changes in shearing stiffness even after the cracks appear. If the shearing stiffness of wing segments are overestimated, the bolts will be underestimated and safety problems will develop. The actual shearing stiffness measured was larger than shearing spring constant design values calculated after considering the stiffness of the concrete and the shear reinforcement. This showed that the design value of the shearing spring constant was safe value.

Table 1.

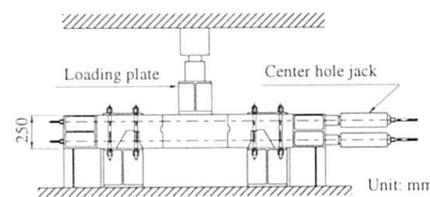| Material	Strength properties / Units: N/mm²	
Concrete	Standard design strength	$\sigma_{ck} = 48$
	Allowable compressive stress	$\sigma_{ca} = 17$
	Allowable shearing stress	$\tau_{ca} = 0.74$
Reinforcement	Yield stress	$\sigma_{sy} = 345$
	Allowable compressive stress	$\sigma_{ca} = 200$
	Allowable tensile stress	$\sigma_{sa} = 200$
Bolts	Yield stress	$\sigma_{sy} = 940$
	Allowable tensile stress	$\sigma_{sa} = 300$

Table 1 Materials

Fig. 6 Shearing Test Outline

Table 2.

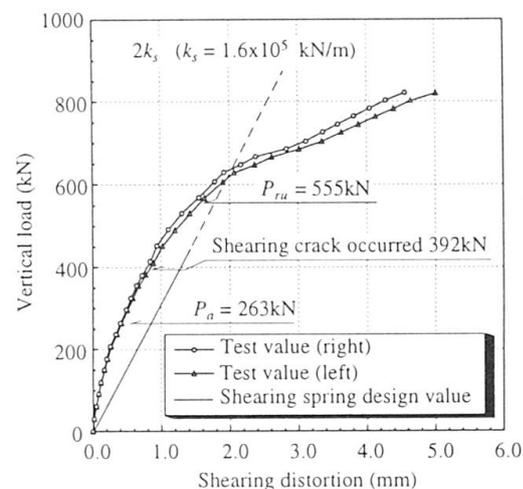|		Case 1	Case 2
Design values	Allowable load P_a (kN)	263	257
	Final load P_{ru} (kN)	555	512
Test values	Collapse load P_u (kN)	842	669
	Safety factor F_s (=P_u/P_a)	3.21	2.61

Table 2 Shearing Test Results

Fig. 7 Relations Between Load and Shearing Distortion

3.2 Joint Bending Test

3.2.1 Purpose of the test
To confirm the mechanism of bending moment transfer by the shearing key, and to verify the strength and stiffness of the joint.

3.2.2 Testing Method
Figure 8 shows an outline of the testing method. The load was applied so that the ratio of the bending moment and the axial force was constant until the allowable bending moment. After the allowable bending moment was exceeded, the load was applied so that the axial force remained constant and the bending moment increased. The section forces at the allowable bending moment were set at 368 kN/m for the axial force and 90.7 kNm/m for the bending moment to comply with the final proof stress confirmed through the ring load test.
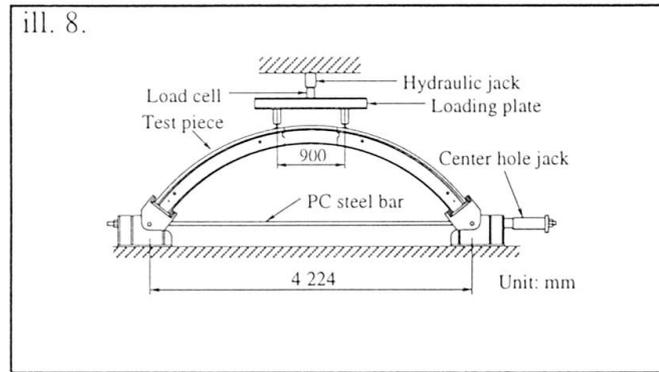
3.2.3 Test Results
Table 3 shows the test results. The bending moment at collapse was about the same as the design final bending moment. This is believed to be the result of sufficient transmission of the bending moment by the shearing key (shearing resistance (S) x Wing length (L)).

3.3 Ring Loading Test

3.3.1 Purpose of the test
To investigate the strength and deformation properties of the wing segment ring under the axial force.

3.3.2 Testing Method
Figure 9 shows an outline of the testing method. The load was applied so that the ratio of the bending moment and the axis force were constant until the allowable bending moment. Bending moment was applied by placing concentrated loads (P_V and P_H) on the vertical and horizontal directions of the segment. Part-1, 3 were placed on the ring so that the maximum positive bending moment worked on the main section and the maximum negative bending moment worked on the wing sections. Part-2 was placed opposite to Part-1, 3. In the test concentrated loads (P_V and P_H) were introduced proportionately until the design bending moment, but in the final load condition test P_H was set at 0.

Fig. 8 Joint Bending Test Outline

Design values	Allowable bending moment M_a	90.7
	Final bending moment M_{ru}	178
Test values	Bending moment at collapse M_u	180
	Safety factor F_s (=M_u/M_a)	1.99

(Units: kNm/m)

Note: An axis force of 368 kN was used for the joint bending test.
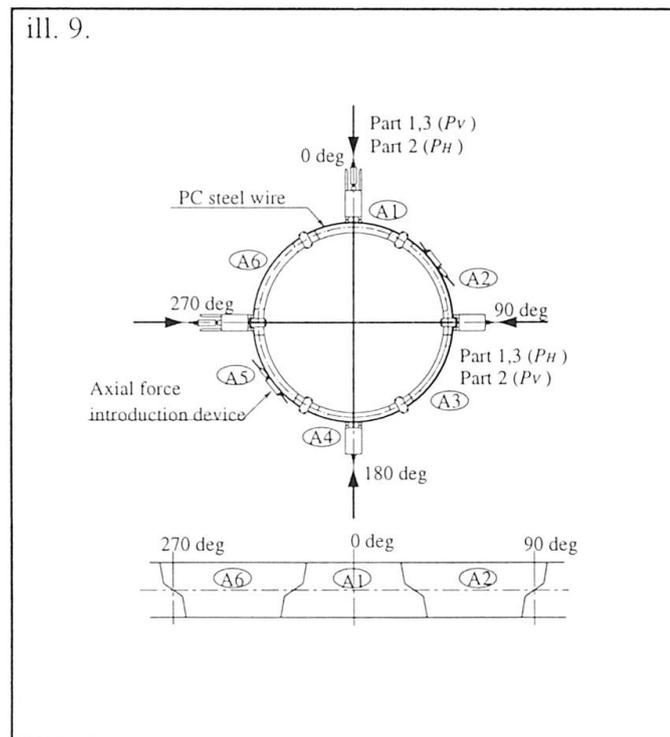
Table 3 Joint Bending Test Results

Fig. 9 Ring Loading Test Outline

3.3.3 Test Results

Figure 10 shows the relations between the load and convergence of the segment ring in Case 3. The specifications of the bolts in the wing segment were smaller than those for conventional bolts. At the allowable bending moment level the ring stiffness was equivalent to or greater than that of the rectangular segment staggered pattern ring calculations in the structural analysis. This shows that the bending moment is transmitted effectively by the shearing keys, and that stiffness has been improved. Also the bending moment distribution in the main section of the segment calculated from the strain measurements on the steel reinforcements is equivalent to the distribution in uniform stiffness rings. Therefore, it was confirmed that wing segments can be designed as uniform stiffness rings ignoring the joint.

Table 4 shows a summary of the final proof stress results. The bending moment at the end of tests was higher than the design final bending moment of rectangular segment staggered pattern rings. This confirms that wing segments can provide sufficient proof stress even inline pattern construction. In each test case bending collapse occurred at the position where the maximum positive bending moment was occurred.
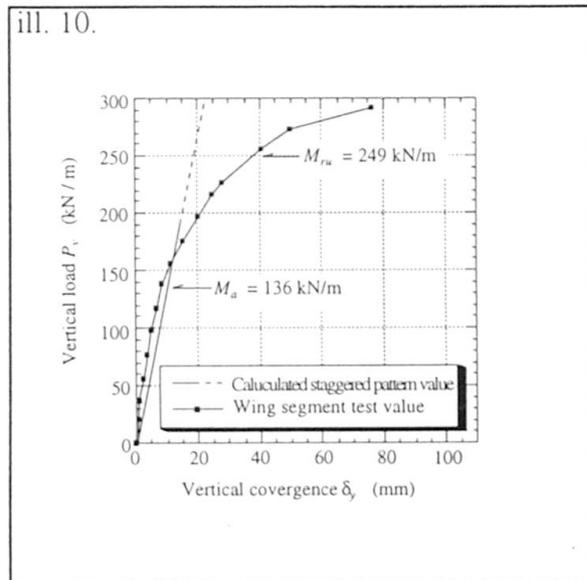
ill. 10.

Fig. 10 Relations Between Vertical Loads and Vertical Convergence

Table 4.

Maximum positive bend		Part 1 Main section	Part 2 Joint	Part 3 Main section
Design values	M_a (kNm/m)	110	90.7	110
	M_{ru} (kNm/m)	200	178	200
Test values	M_u (kNm/m)	209	212	243
	Safety factor F_s $(=M_u/M_a)$	1.90	2.34	2.22

Table 4 Ring Loading Test Results

4. Conclusions

The conclusions that resulted from the full size segment loading tests were as follows:

1) The wing segment feature of transmitting bending moment with shearing stiffness was confirmed, and it was verified that the number of bolts or their diameter can be reduced.

2) It was verified that ring proof stress and ring stiffness equal to or greater than that for rectangular segment staggered pattern rings could be achieved with inline pattern construction using fewer bolts or bolts with smaller specifications.

3) In joint bending tests where axial force was introduced, joint behavior similar to that in the ring loading test was confirmed. Therefore, it was confirmed that this simple test could sufficiently replace the ring loading tests.

Reference

1) Hiroshi Yamazaki, Toshi Nomoto and Kenji Mito; "Wing Segment Development"; "Tunnels and Underground," vol. 28, no. 5, pp. 387-395 (May 1997)

Full Scale Live Load Tests on a Corrugated Steel Culvert

Lars Pettersson
Head of Struct Eng Dept
Kjessler & Mannerstråle AB
Stockholm, Sweden

Lars Pettersson, born 1959, recieved his civil engineering degree in 1984. He has since then been active in the field of bridge design both as designing engineer as well as in research work.

Summary

As a part of a research project concerning the behaviour of large diameter corrugated steel culverts under shallow soil cover, full scale tests on a 6.0 m span pipe arch profile have been performed. The tests have included studies in the service limit state as well as failure load tests.

The loading tests have shown that the height of cover significantly influences steel strains, culvert deflections and soil pressures. The influence of moving vehicles almost equals that of static loading but it should be noted that the tests were conducted at low speed.

Failure load tests were performed at cover depth of 0.75 m (12.5 % of the culvert span). Although some influence on the bearing capacity of simulated defects of the culvert could be noted the degree of compaction dominated the behaviour of steel culverts and therefore the load bearing capacity. Measured failure loads were quite high and shows that design methods in current bridge codes are conservative for culverts with shallow cover influenced by live loads.

1. Introduction

Corrugated steel culverts have been used in Sweden since the mid 50's. The spans have been moderate and the minimum and maximum heights of cover have been chosen with great caution. The corrugated culverts have in many cases proved to be economical alternatives to conventional concrete bridges. Therefore the interest in such structures has increased. This is especially true today considering the intensive expansion of the infrastructure and an increase in load carrying capacity of older Swedish bridges in order to conform with European standards.

The culvert used in this study was a pipearch profile with a span of 6.04 m and a rise of 4.55 m. The corrugation was a 200×55 mm profile with thickness 3.25 mm. Main dimensions, excavation pit size etcetera are shown in Figure 1.

The structural steel plates forming the culvert was bolted together using 15 bolts/m. Th. number of bolts was intended to give a seam stronger than the structural plate itself based on the ring compression method combined with classical buckling criteria.

Gravely sand was used for culvert bedding and backfilling. The compaction effort conforms to Swedish standards (four passes with à 450 kg vibrating plate using 0.30 m lifts). Compaction
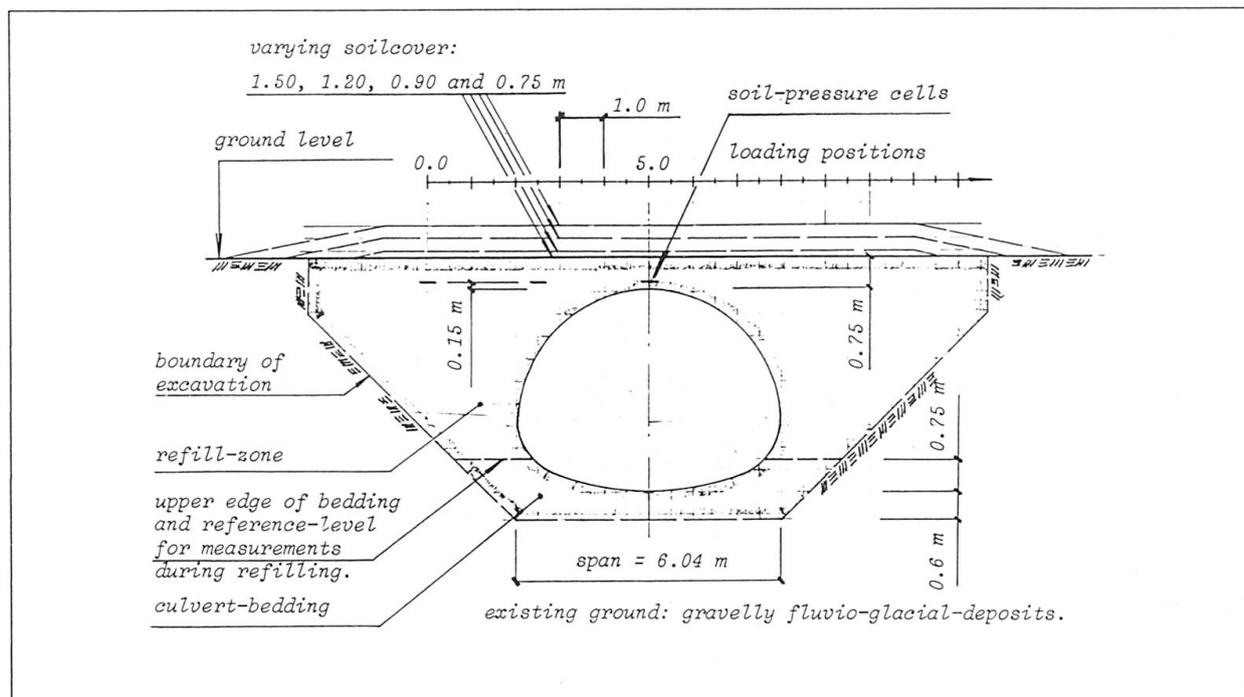

Fig. 1 Transverse section through test-culvert.

resulted in a mean dry density of 1.77 g/cm^3 giving a degree of compaction of 89% (modified Proctor). Also, plate pressure tests were performed at the level of the culvert crown. These tests, conducted according to the German DIN preliminary standard 18 134 gave an secant modulus (using pressures between 150 kPa and 350 kPa) of 56 MPa at the first load cycle and 107 MPa at a second load cycle.

2. Varying Height of Cover

The influence of the height of cover was the main objective of this study, since the soil cover is essential for the live load bearing capacity. Loading tests, statical as well as with a moving vehicle, were performed at successively reduced heights of cover of 1.50, 1.20, 0.90 and 0.75 m.

The loading tests were performed using a wheel loader with two axles and an ordinary lorry with three axles. The vehicles were moved over the culvert in 0.5 m steps. The configuration of the axles made it possible to study the influence of axle spacing, boggie loading compared to single axle loading, and the influence of increased load at given axle spacing. For each loading position soil pressures, steel strains and culvert deflections were recorded in three sections as shown in Figure 2. Note that the culvert is divided into three disconnected parts, reducing the end effects to a minimum. Some results from this investigation are shown in Figure 3.

Measured thrust of dead load only showed good agreement with the total weight of the super-imposed soil masses. However, there was a considerable redistribution of soil pressure measured directly under one wheel of the loading vehicle in loading positions 2.0, 3.5 and 5.0 (Figure 1) compared to free field measurements well away from the culvert.

It is well known that moving loads can cause increases in stresses compared to static load cases. Uneven surfaces and movements of the loading vehicle and the loaded structure can interact to
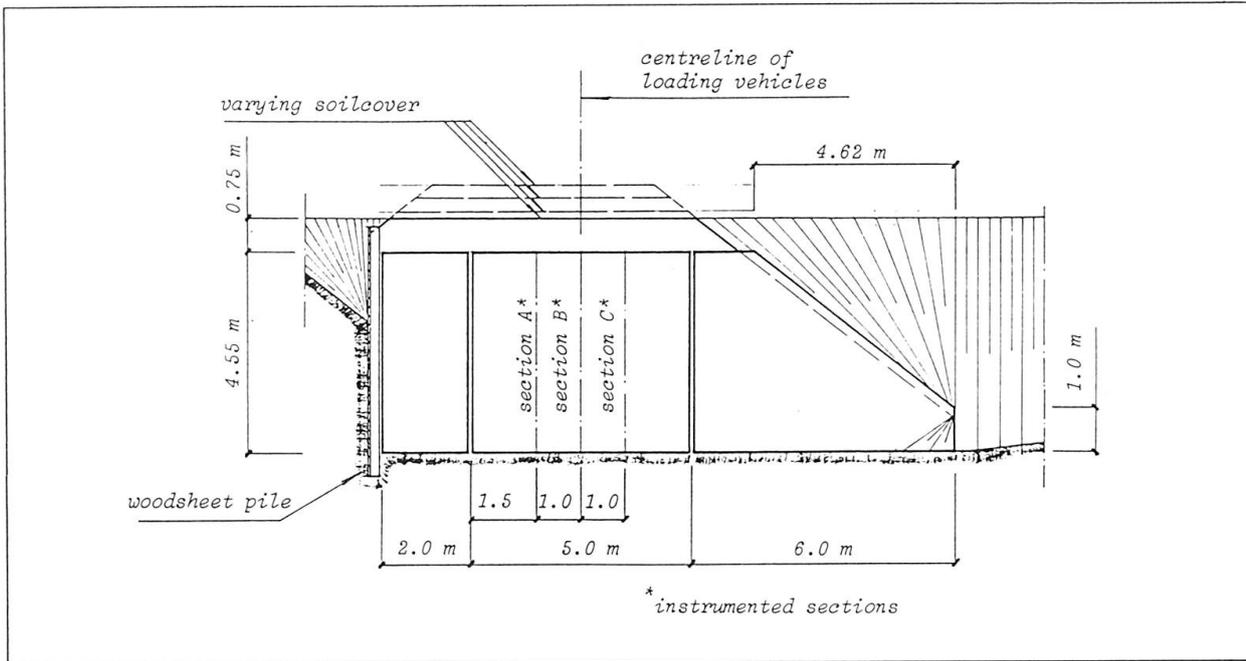

Fig. 2 Longitudinal section through test culvert showing instrumented sections.

cause considerable dynamic amplification of the stresses in the structure. It is believed that the impact factor is less for soil embedded structures than for conventional bridges. Some tests were therefore performed using a moving vehicle (wheel-loader at approximately 20 km/h) to compare the results with those from static loading tests. Some results are presented in Figure 4.
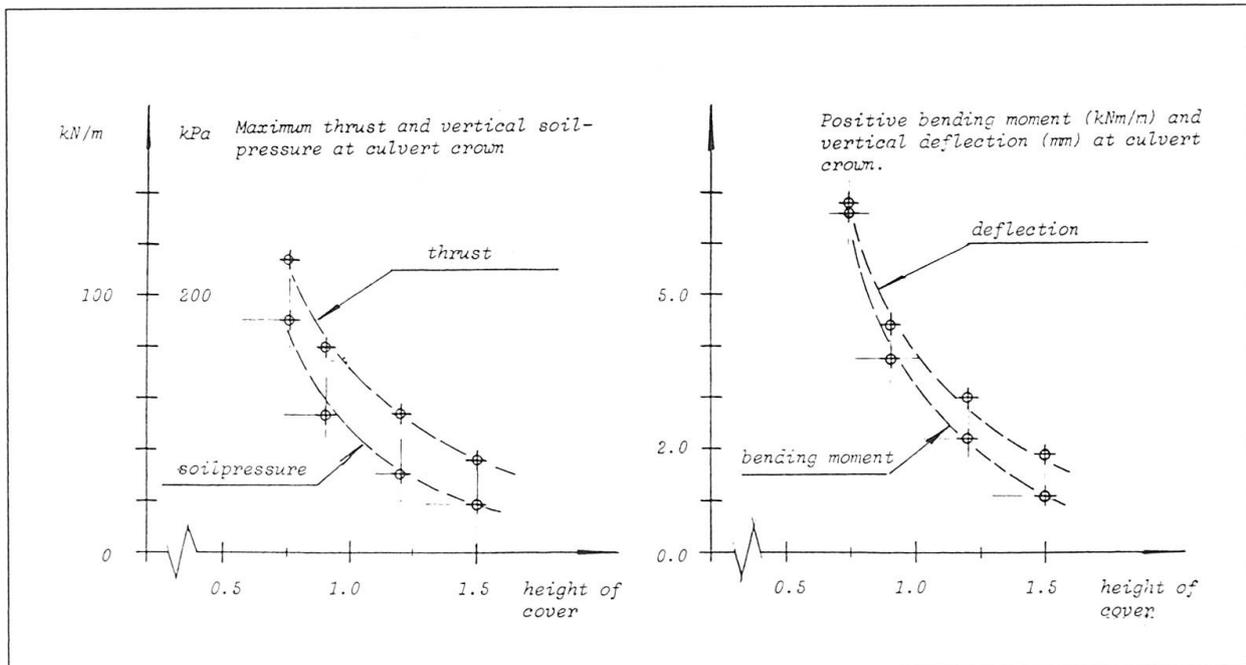

Fig 3. Thrust, bending moment, deflection and vertical soilpressure at culvert crown. Loading vehicle: 300 kN wheel loader with 225 kN on front axle.

3. Failure Load Tests

Knowledge of ultimate load behaviour is essential for the choice of safety factors for different kinds of structures. Because of the costs involved in full scale failure tests, there are very few such tests reported in literature. Due to the complex interaction between the culvert and the surrounding soil these tests are necessary in order to confirm theoretical studies. As a part of this full-scale test a series of five failure tests were performed all with a loading consisting of one axle. As failure tests lead to some parts of the structure being demolished (in this case the top plates) the culvert was uncovered and the top plates where exchanged after each test.
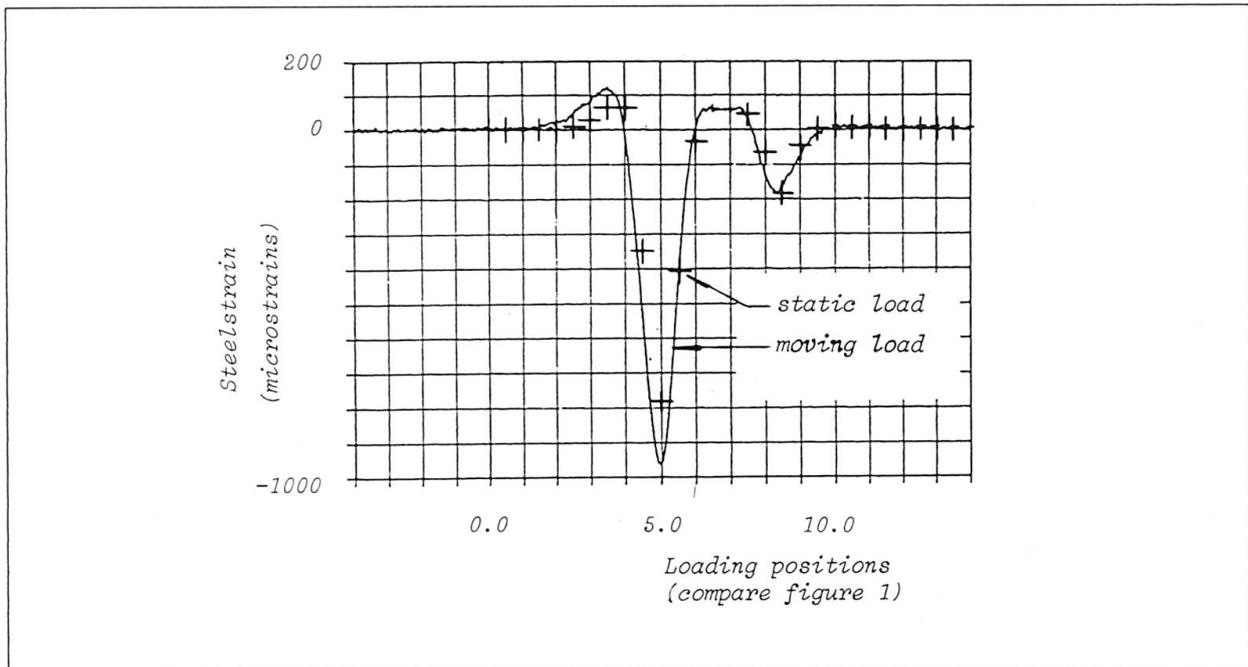

Fig. 4 Steel strains at culvert crown caused by a moving vehicle compared to steel strains caused by the same vehicle in static load positions.

The experimental program consisted of five independent failure load tests. The loading device is shown in Figure 5. It was designed to comply with the geometry of the live-load axle of the Swedish bridge code. The distance between the centre line of the two wheels is 2.0 m and the contact area of the wheels are 0.2 × 0.6 m. The load was applied using steel weights of 500 kg and 1000 kg respectively. All tests were performed at a height of cover of 0.75 m (12.5 % of culvert span).

At the first four tests, the load was applied directly over the crown of the culvert. In the last test the load was applied 1.0 m off the centre of the culvert (see Figure 5).

In the three first tests the degree of compaction (DOP) varied between very low values (approximately 80 % modified Proctor compaction) and high values (approximately 95 %).

Measurements showed that thrusts are almost independent of the DOP. However, moments and deflections increase with decreasing DOP which was expected. The vertical soil pressure over the crown of the culvert showed a linear increase with the load applied. When failure of the structure was encountered (a single wave buckle directly under one of the two "wheel loads") the soil failed in a manner similar to a punching failure.

At the last two tests, two rather usual defects on corrugated culverts were simulated in order to study their influences on the live load bearing capacity. A number of culverts have experienced slowly increasing deformations resulting in flattening of the culvert profile. The reasons being insufficient compaction of backfill material, poor quality of backfill material and poor quality of subground soils. These deformations also affect the moment distribution. Thrusts are probably not affected to any considerable extent.
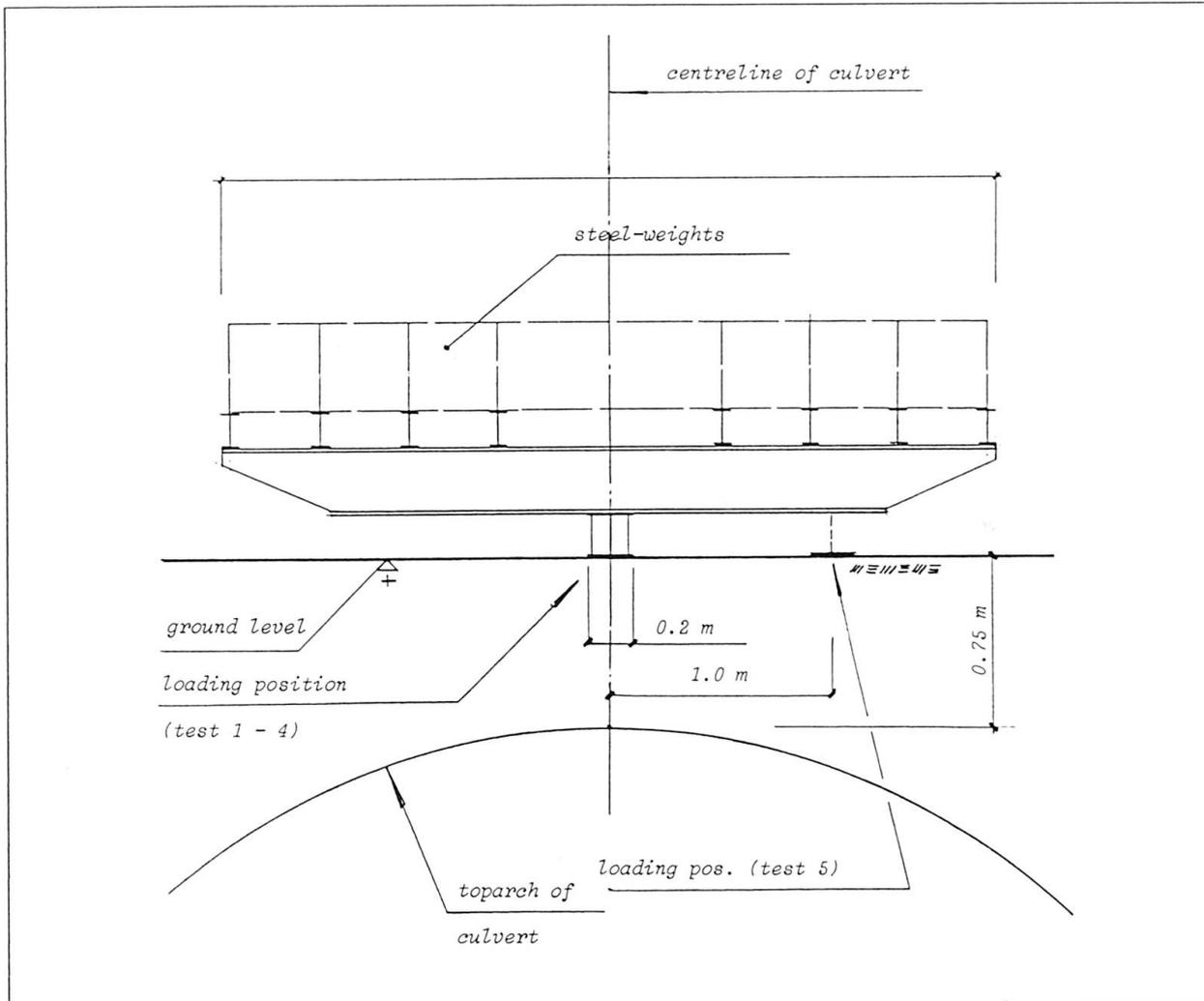

Fig. 5 Loading device for failure load tests.

The long term deformations were simulated by placing soil on top of the culvert before backfilling. The soil was kept in place by two "wings", in eleven and one o'clock positions as ca be seen in Figure 6. In this way a permanent vertical deformation of the profile of 0.18 m (3 % of culvert span) was achieved. After finished backfilling (the wings were removed during backfilling) the culvert was loaded to failure in the same manner as above. The failure load was reduced by approximately 15 % compared to the undeformed case. In this case yielding of the culvert wall started at the crown, initiated by positive bending moments.

Another encountered defect is local corrosion in the "splash zone" of water bearing culverts. This type of defect was simulated by cutting off small oval steel medallions, leaving a section approximately 2.3 m over the bottom of the culvert with only 10 % of the original steel area. Theoretical calculations showed that this reduction in wall section almost should cause yielding of the section from thrust only. The single axle was placed one meter away from the centreline
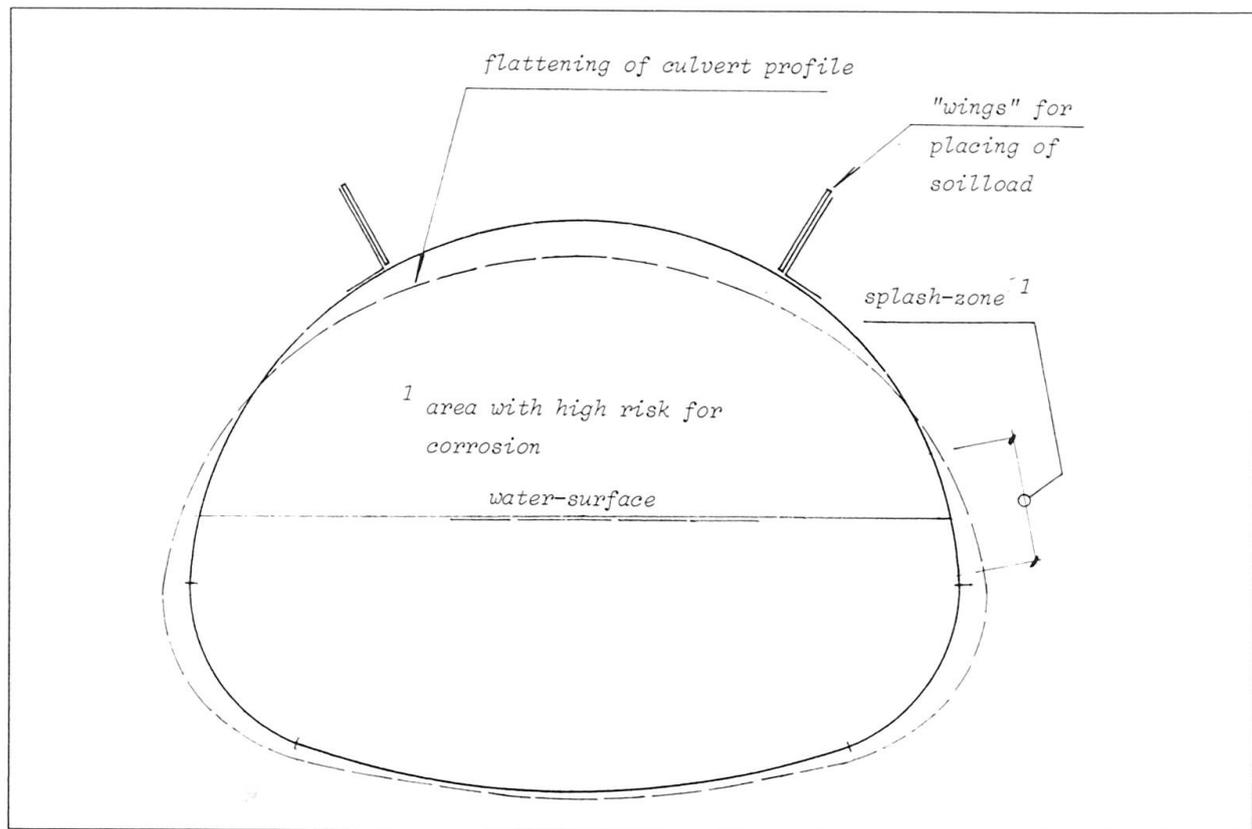
Figure 6: Typical defects of corrugated culverts (flattening of culvert profile and corroded splashzone).

of the culvert in order to attain maximum thrust in the weakened zone. The load was applied in the same manner as described above but the failure did not consist of a collapse of the "splash zone" but in a soilfailure with a sliding surface from the load towards the centre of the culvert (compare Figure 5). Checking of safety against soil failure must thus be included in an adequate culvert design.

Øresund Tunnel - Control of Early Age Cracking

Jonathan Baber
Senior Engineer
Symonds Travers Morgan Ltd
East Grinstead, UK

Theo A. M. Salet
Senior Consultant
Intron B.V.
Houten, Netherlands

Lars K. Lundberg
Concrete Production Manager
Øresund Tunnel Contractors I/S
Copenhagen, Denmark

Chartered Engineer working for Symonds Travers Morgan for over 8 years on immersed tunnel projects including the River Lee and Aktion Preveza Crossings. Worked on the tender design for the Øresund Tunnel and then in the design liaison team in Denmark, dealing with all aspects of the immersed tunnel, including co-ordination between STM, Intron and ØTC for the thermal analysis.

Materials Engineer for Intron for over 7 years. Advised ØTC in all matters related to early age crack control for tender design up to completion of the project and performed the necessary predictive numerical analyses. Previously involved as materials consultant in amongst others West Bridge, Great Belt Link in Denmark and Northumberland Strait Crossing in Canada.

Responsible for concrete production on the Øresund Tunnel project for both the tunnel and approach structures. Also in charge of testing and development of concrete mixes. Previously was materials and concrete manager for the East Bridge, Great Belt Link Project, Denmark for E.Phil & Son A.S. in joint venture with Great Belt Contractors.

Summary

The concrete segments for the Øresund Immersed Tunnel are poured in one continuous operation. This permits early age cracking to be controlled without the use of embedded cooling pipes. The feasibility of this was established at the project tender stage and was the principle around which the construction method was developed. The thermal analysis formed an integral part of both the tender and detailed design process and the work carried out by the two consultants involved is described in this paper. The project shows the benefits of dealing with early age cracking on the design table and not treating it as a problem to be overcome by implementation of measures on site. The construction method has been successful in eliminating early age cracking.

1.   The Øresund Tunnel Casting Technique

The Øresund tunnel has a total length of 3.5km and comprises 20 immersed tunnel elements. Each element is formed by 8 segments. Watertightness of the structure is achieved by high quality concrete which is designed to be free of early age cracking. The 22m long, 8.5m high and 41.7m wide segments are each cast in a single concrete pour. Casting is carried out in a tightly controlled environment - factory conditions have been created in a purpose built casting facility. A highly complex formwork system, foundation and support jack system was developed to allow segments to be cast in the shed and then jacked forwards, making room for the next segment to be cast.

The construction method provides a watertight, durable structure without the use of embedded cooling pipes to control early age cracking. Similar construction methods have been used before for much smaller scale immersed tube service tunnels and outfalls. The Øresund Tunnel has extended the principle to a large, five bore tunnel cross section where 2700m³ of concrete is placed continuously. The construction method was developed at the tender stage when the control of early age cracking was considered as an integral part of the design. Key constraints on the concrete properties and construction techniques were identified at this time. This early integration has lead to a high quality of construction and provides a lower risk construction method compared to the traditional cooling pipe solution.

2. Contract Requirements

The Contract specifications required the tunnel concrete to be free of early age cracks. The risk of cracking was limited to 70% of the available tensile strength of the concrete. Additionally, D_{int}, the difference between surface and core temperatures, was limited to 15°C and D_{ext}, the difference between new and old concrete, was limited to 15°C. The Contract assumed a traditional staged construction so the latter criteria was therefore not appropriate. A maximum temperature of 70°C was permitted in the base and 65°C in the walls and roof during the hydration period, in order to avoid expansion within the concrete matrix due to delayed ettringite formation (though this was later found not to be a problem for the type of cement used). Temperature and stress simulations were required, using a finite element method of analysis which took account of the liberation of heat of hydration, heat loss by convection and radiation, autogeneous shrinkage, the evolution of Young's modulus and ageing creep phenomenon of concrete loaded at early ages.

3. Design Method

3.1 Organisation

Thermal analysis was undertaken by specialist materials consultant Intron B.V. It was combined with the structural analysis performed by Symonds Travers Morgan to obtain a full understanding of the stress evolution at early ages. Whilst this type of approach is relatively uncommon it was necessary because of the unusual nature of the construction method. It required close co-operation between the main designer and the specialist materials consultant. Close liaison was also necessary with the production staff of the Contractor, Øresund Tunnel Contractors (ØTC), to accurately model the concrete behaviour and the conditions in the controlled factory environment.

3.2 Modelling Technique

The thermal analysis was performed with the module HEAT/2.5D of the finite element analysis software Femmasse. This type of software was necessary for modelling both the concrete temperatures and stresses and the changing support conditions of the tunnel segment at early ages. The analysis was time based, extending from the start of concrete placing through to the point when thermal equilibrium was reached. As well as time based events the analysis took full account of the time dependant properties of the concrete materials.
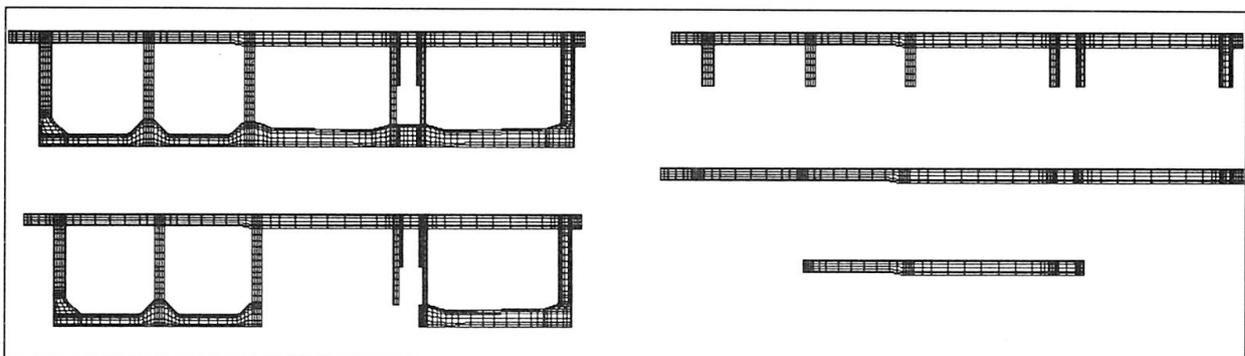

Figure 1. Finite element model for stress and temperature analysis, built up in stages corresponding to the casting sequence.

The FE model that was created for the analysis is shown in Figure 1. Because of the asymmetry the full cross section was modelled. The element geometry was selected to give accurate output in surface zones where the greatest stress gradient is present. Constant shear elements were used to minimise the amount of elements and thus save on computation time.

3.3   Input Parameters

There are many variable parameters which were input into the thermal analysis. To avoid analysing a large number of permutations of these parameters a benchmark condition was established and sensitivity analyses performed. The risk of cracking was computed for a variation in a single input parameter and compared back to the benchmark condition. The influence of each parameter on the risk of cracking was therefore evaluated in terms of whether it had a significant effect. Variations were considered for both winter and summer conditions for the following:

- Temperatures within the casting shed and inside the tunnel bores;
- Outdoor temperatures including daily fluctuations, thunder storms and wind velocities;
- Initial concrete temperatures at the time of placing;
- Total pour duration and casting sequence;
- External loading from formwork and second stage construction within the tunnel;
- Degree of retardation in the outer wall concrete;
- Early age shrinkage behaviour;
- Variations in cross section geometry e.g. ventilation fan niches in roof slabs.

Support conditions were modelled as rigid when the segment was supported by formwork and as soft springs when the weight was released onto the piston jacks. Cross-checks were made with the Lusas 3D finite element structural analysis model for a variety of load conditions to ensure the support conditions in the thermal analysis accurately represented the real behaviour. One of the sensitivity studies considered distortions arising from the piston jack supports of the segments. These were determined from the 3D structural model and were translated into the 2.5D thermal analysis model as imposed deformations at the supports.

The concrete mix used was an OPC mix. At the project tender stage a low w/c ratio blast furnace slag cement was thought to be necessary because of the beneficial slow heat development and high strain capability this would have at early ages. Pre-testing was carried out on two OPC and two BFSC mixes, in combination with two aggregate types. One aggregate enabled a lower elastic modulus to be achieved at early ages and test results for a mix with these aggregates and OPC were input into a thermal analysis and found to be satisfactory. The OPC mix also enabled higher early strengths to be achieved which allowed segments to be jacked earlier. This was crucial in enabling ØTC to meet the cycle time for segment production required by the construction programme. The main mix characteristics are summarised in Table 1.

Material/Characteristic	Quantity/Property
Aalborg Portland Cement	340 kg/m^3
Fly Ash	55 kg/m^3
Aggregate, Nordstone Granite	Maximum Size 25mm
W/C Ratio	0.39
Strength	40 MPa

Table 1. Summary of concrete mix characteristics.

4.   Analysis Results

4.1   Segment Behaviour

The maximum temperatures computed were 48°C after 93 hours in the winter scenario and 65°C after 72 hours in the summer scenario. These peaks occurred locally in the thickest section in the roof slab above the service gallery. Because of the time required to complete the concrete pour (up to 48 hours) the peaks in temperature in the base, walls and roof occur several hours apart.

The delay in the temperature peaks in different parts of the structure causes distortions in the plane of the cross section. The roof slab expands relative to the base slab causing bending in the walls and the stresses caused by the bending combine with those due to thermal gradients across the sections. This aspect of the design was of particular concern because of the large width of the tunnel. However the single pour method is of significant benefit in minimising this problem as there is still some expansion occurring in the base when the roof is at its peak temperature. The effect of the heat development on structure distortions can be seen in Figure 2. This shows the bending effects generated in the outer walls at an exaggerated scale for the temperature distribution at 80 hours after pouring, when the top of wall temperatures are at a maximum.
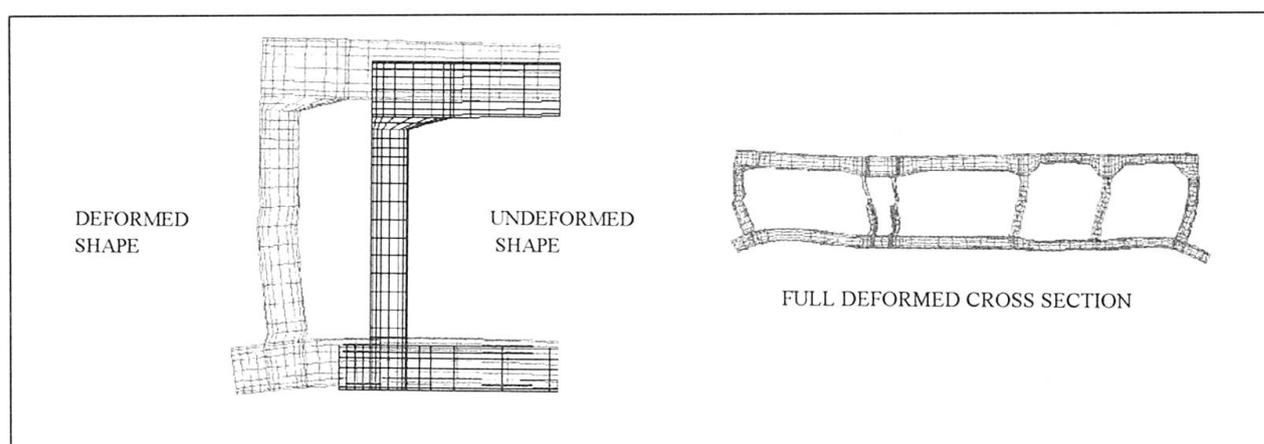

DEFORMED SHAPE   UNDEFORMED SHAPE   FULL DEFORMED CROSS SECTION

Figure 2. Distorted shape of tunnel cross-section due to temperature evolution.

In the longitudinal direction the length of the segment was not specifically modelled. Stresses were computed in the longitudinal direction assuming an infinitely long structure. Separate investigations were made for the actual segment length to determine the time permitted to complete the roof slab after finishing the outer walls. The delay in the temperature peaks in different parts of the structure also causes distortions in the longitudinal axis of the tunnel. The relative rate of expansion is important in this instance and a retarder was specified for the wall concrete to minimise the stresses caused by the roof slab expanding and pulling on the walls. The retarder caused the hydration process in the walls and roof to occur more simultaneously and also reduced the stiffness of the wall concrete at the point when the roof slab was expanding, so that stresses remained within the acceptable limits.

With traditional staged construction the tendency would be for the free ends of the segment to curl upwards longitudinally because of the shrinkage occurring in the last poured concrete. This phenomena is avoided with the continuous pour as the base slab, walls and roof slab all expand and shrink more closely together.

The full section casting minimises stresses arising from differential shrinkage between elements of the structure. No construction joints are present and the supporting jacks and shear key detailing allows the segments freedom to move relative to its adjacent segment. Stresses are therefore primarily the result of thermal gradients, the pour duration and the member thicknesses. The risk of cracking was found to be greatest in the top of the outer walls and at the section cores above the walls. Figure 3 shows a typical longitudinal stress distribution in outer wall of the motorway tube and the transverse stress distribution at the same point. Note that the tensile stress limit shown on the graphs corresponds to the P=0.70 limit imposed by the Contract.
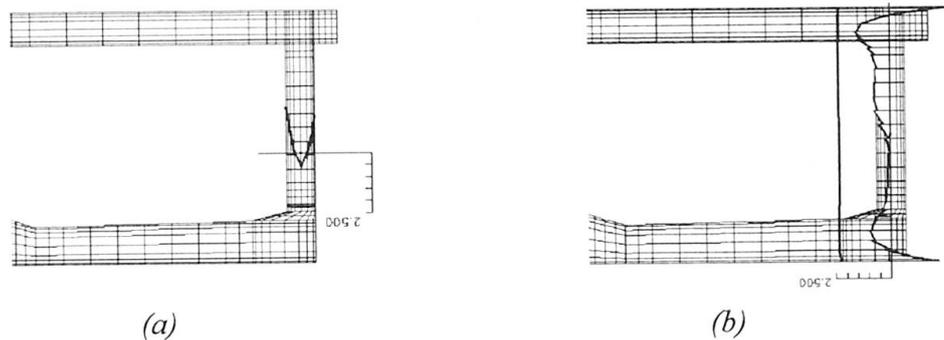

(a)   *(b)*

Figure 3.   a) Longitudinal stress profile in outer wall at the concrete core after 504 hours.
*   b) Stress profile in plane of cross section in the outer wall after 504 hours.*

When assessing the risk of cracking thermal stresses were considered in combination with stresses arising from static loads and the transfer of self weight from the formwork onto the piston jack supports. It was important to consider the superposition of these stresses as the thermal behaviour and formwork striking operations both cause bending stresses which combine with local thermal stresses. The combination of the stress profiles could result in through section cracking and present a risk to the watertightness and long term durability of the concrete. The combined effects were therefore checked to ensure the risk of cracking was not exceeded. This study was crucial in determining the earliest time when formwork could be stripped, when the weight of the segment could be transferred onto the piston jacks and when jacking operations could commence. Concrete strength criteria and specific points in the temperature evolution were specified as trigger points for each activity to commence on site.

4.2   Benchmark and Sensitivity Analyses

The benchmark and sensitivity analyses showed that the risk of cracking was acceptable and that early thermal cracking would not occur if the following measures were taken during construction:

a) Retarding of the concrete in the outer walls by up to a maximum of 6 hours;
b) Insulation of the final segment was required if it was to be jacked out of the factory immediately after striking the shutters;
c) Insulation of thin sections was required, for example at ventilation fan niches in the roof slab;
d) Completion of the roof after the outer walls was required within a specific time period;
e) Temperatures in factory had to be kept up at 10°C throughout the winter period;
f) Temperatures within the bores had to be kept close to those outside of the segment;
g) Formwork stripping was limited by concrete strength and temperature peaks;
h) The maximum concrete temperature at placing was limited to 23°C.

5.   Comparison to Traditional Construction Methods

To show the benefit of controlling the thermal stresses in the design phase it is useful to compare the risk of cracking for the full section casting with a 3 stage construction. This is done using the cut and cover approach structures of the tunnel. Figure 4 shows the risk of cracking in the outer wall for the 3 stage construction before and after cooling pipes are incorporated and compares this to the same point in the structure for the full section casting. Note that the 100% risk of cracking relates to the P=0.70 contract requirement. The risk of cracking is 160% in the uncooled 3 stage construction compared to 35% for the immersed tunnel segment. Cooling pipes reduce the risk of cracking in the approach structures to an acceptable level but the tunnel will have a greater margin of safety in the design. The economic benefits can be seen also as approximately 24 cooling pipes and the work associated with installing and operating a cooling system are saved for 160 tunnel segments. Construction risk is also reduced because variations in fresh concrete temperatures are accounted for in the design - for a cooling pipe solution a temperature variation could lead to cracking because the method is largely pre-determined and inflexible once set up.
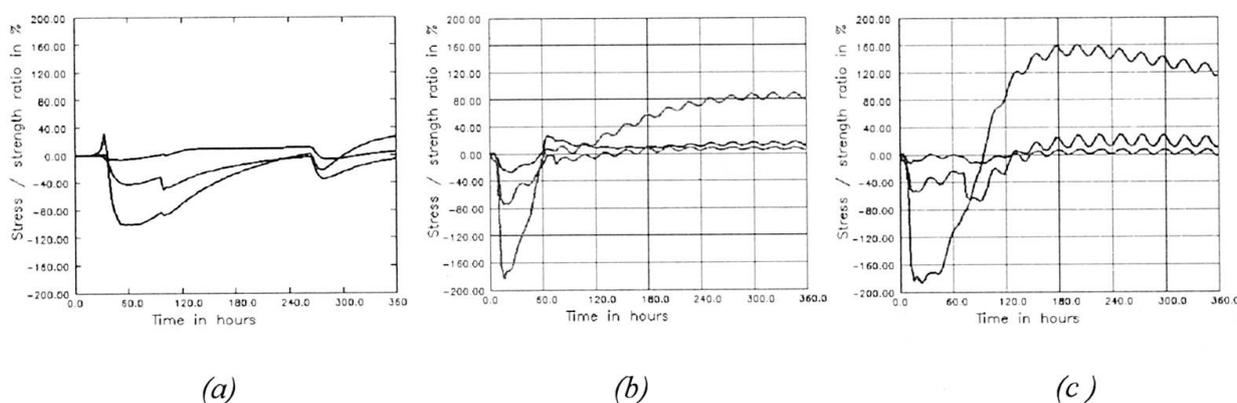

(a)   *(b)*   *(c)*

Figure 4. a)   Risk of cracking for full section casting 1.0m above base slab in outer wall.
*   b)   Risk of cracking for 3 stage construction 1.0m above base slab in outer wall.*
*   c)   Risk of cracking for 3 stage construction with no cooling pipes.*

6.   Conclusions

The project demonstrates the benefits of viewing early age cracking not as a problem to be overcome after design (i.e. with cooling pipes), but as a problem that can be avoided by incorporating construction methods into the design. No early age cracking has been observed in the tunnel segments and temperature curves from the monitoring system used on site have been cross checked successfully with the design to show that the concrete is behaving as expected.

The use of cooling to control early age cracking will always be a viable method for many projects, particularly where the structures are simple and the technology is tried and tested. However the approach taken for the Øresund tunnel suits slightly more unusual projects and is particularly viable when a large number of repetitive concreting operations are required, such that the expenditure on the complex temporary works facilities remains economic.

The approach taken in the design is one which is most suited to design and build projects, but it should be recommended regardless of whether traditional or more creative methods are used to control early age cracking.

Cut-and-Cover Tunnels at the Arlanda Link

Magnus Mörnstad
Chief Engineer
NCC AB
Malmö, Sweden

Magnus Mörnstad, born 1944,
received his civil engineering
degree at Lund Institute of
Technology in 1969

Summary

The Arlanda Link is a new high-speed train connection between the centre of Stockholm and
Arlanda Airport. A railway of about 20 km will be designed and constructed in the project. In the
airport area the railway runs below ground surface. The underground sections have a total length
of about 5 100 metres and include four cut-and-cover tunnels. Due to different loading and
geotechnical conditions the cut-and-cover tunnels are designed in different shapes. This report
covers the predominating design considerations.

1. Introduction

The Arlanda Link is a new high-speed train connection between the centre of Stockholm and
Arlanda Airport. The project commenced in June 1995 and is scheduled to be completed for
commercial use in the end of 1999. It is estimated that the project will cost about 4 700 million
SEK (=650 million USD) including construction works, tracks, signal systems and shuttle trains.
With this new connection the travelling time from the centre of Stockholm to the airport will be
reduced from 45-50 minutes to only 20 minutes.

This BOT-project (Build-Operate-Transfer) is directed by a joint-venture company esablished by
GEC ALSTHOM, NCC AB, and John Mowlem Construction AB. The joint-venture company
has in turn established A-Train AB, a company which will operate the traffic on the Arlanda Link
until 2040.

The project includes the design and construction work of a railway of approximately 20 km
length, running from the main line at Rosersberg via Arlanda Airport and reconnecting with the
main line at Odensala. In the airport area, the railway will run below ground surface. The
underground section has a total length of about 5 100 metres and includes rock and concrete
tunnels as well as three train stations integrated in the airport terminals. In this part, four sections
of cut-and-cover tunnels will be constructed :
Section 1: The Märsta River Tunnels; Inter-city Tunnel (L=318 m) and Shuttle Tunnel (L=437m)
Section 2: The Åsa Tunnel (L=175 m)
Section 3: The Brunnby Tunnel (L=232 m)
Section 4: The E4/65 Tunnel (L=150m), (equal to the Inter-city Tunnel as mentioned in section 1
and not to be described in this report).

All cut-and-cover tunnels in sections 1-3 are connected to rock tunnels at both ends. Due to different loading and geotechnical conditions the tunnels are designed in different shapes. This report covers the predominating design considerations.

2. General

2.1 Tunnels below the Märsta River

The tunnels below the Märsta River are the longest and most complicated. This section involves two tunnels crossing each other at a very sharp angle. The double-track tunnel for inter-city trains is located at the lowest level and has a total length of 318 m between the connections to the rock tunnels. The single-track shuttle-train tunnel is designed as a fly-over and has a length of 437 m. Depending on a very low available height between the tracks at the fly-over point, the two tunnels had to be integrated for a length of 75 metres, which means that the roof slab in the lower tunnel serves as bottom slab in the upper one, Fig 1.
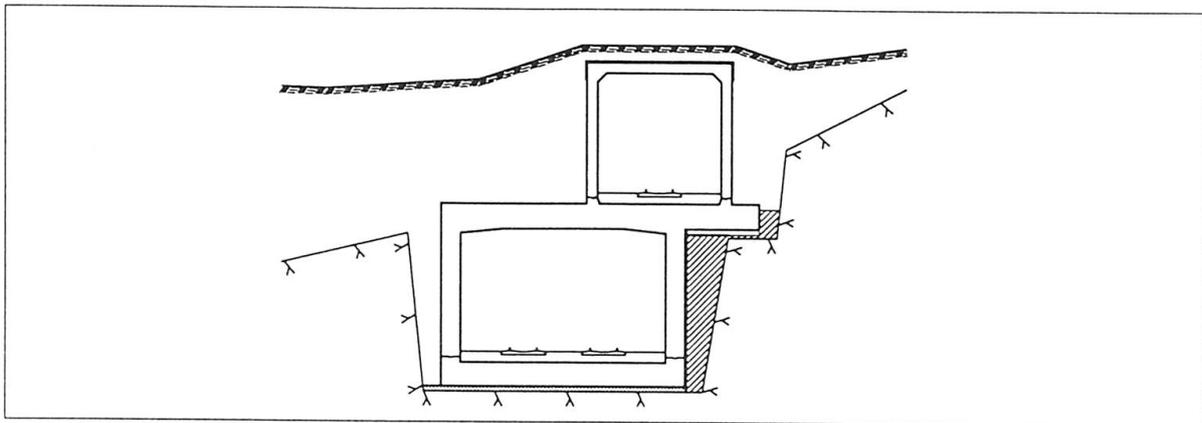

Fig 1 : Fly-over tunnels below the Märsta River

The double-track tunnel has an internal width of 11.50 m and a total internal height of 7.50 m. The wall thickness is 1.10 m, the bottom slab 1.35 m and the thickness of the roof slab varies from 1.05 to 1.35 m. The internal width of the shuttle-train tunnel is 7.00 m and the height is 7.30 m. The roof slab and the walls are 0.65 m thick. The bottom slab has cantilevers to prevent water uplift, Fig 2.
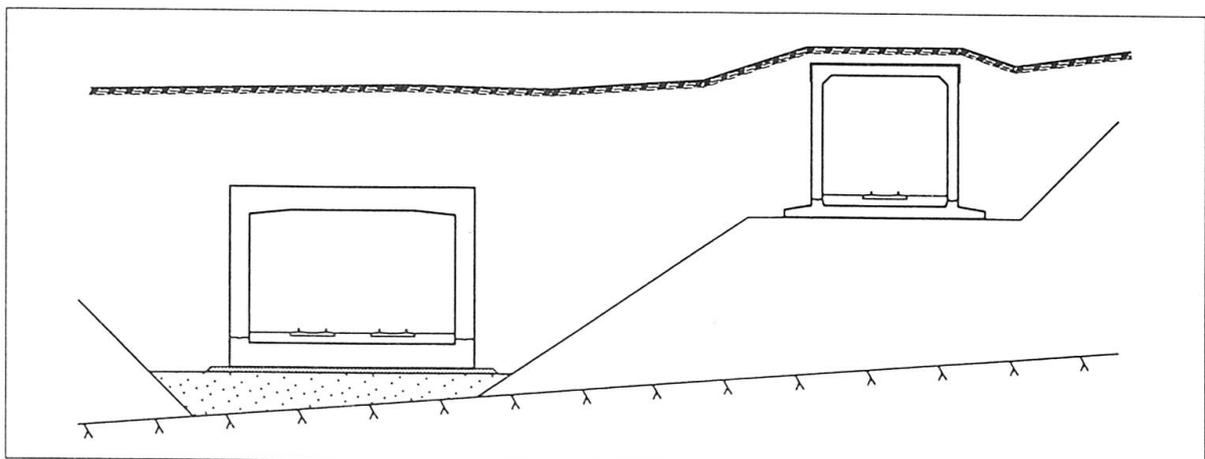

Fig 2 : Tunnels below the Märsta River

2.2 The Åsa Tunnel

The cover of the Åsa tunnel, which is 175 m long, is arch shaped with a radius of 7.50 m as seen in Fig 3. This is the lowest point of the tunnel and the tickness of the covering filling masses is up to 20 m from the top of the arch to the ground surface. The arch has a fixed thickness of 0.65 m and rests on rock shelves about 2.50 m above the track level.

At an early stage it was considered to build this section in accordance with the so called "Spiling-method", which is adviceable when very deep earth excavation work is required and there are ground surface accessibility restrictions. However, due to bad geotechnical conditions in the area, these plans had to be changed to cut-and-cover tunnel.
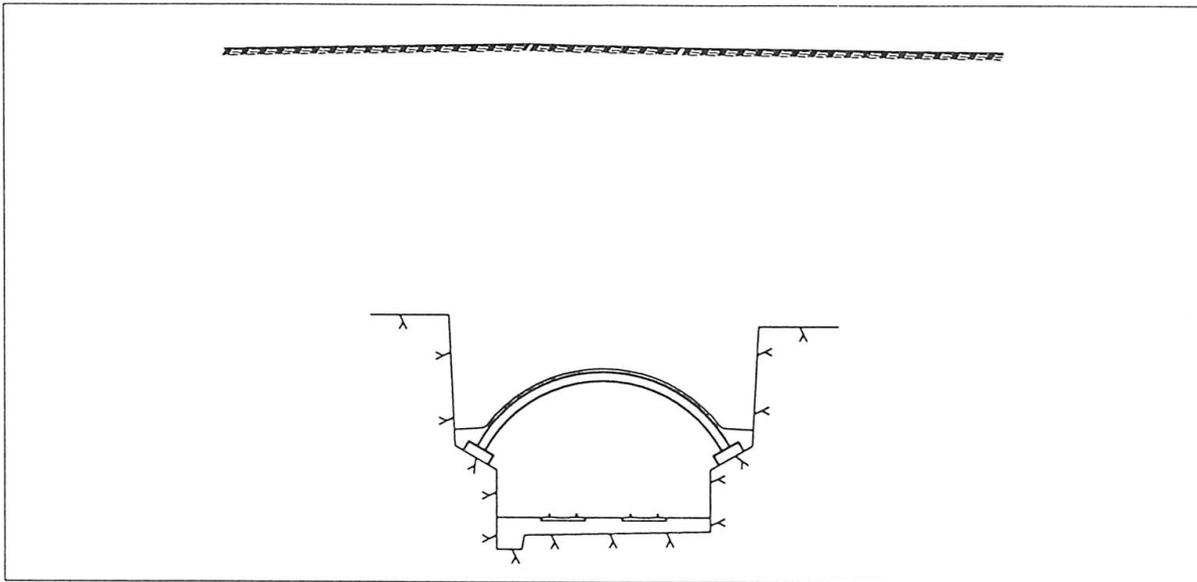

Fig 3 : The Åsa Tunnel

2.3 The Brunnby Tunnel

The Brunnby tunnel is 232 metres long and located in the northern area of the airport just before the railway reaches ground level, Fig 4. Due to low filling thickness, the loading on this tunnel is less heavy and it was possible to minimize the dimensions of the superstructure. Different analyses indicated that a shape with leaning walls close to the roof slab was the most advantageous construction. Wall and roof slabs are 0.70 m thick. Whilst the internal width is the same, the height had to be increased to 7.75 m to accommodate train inclination.
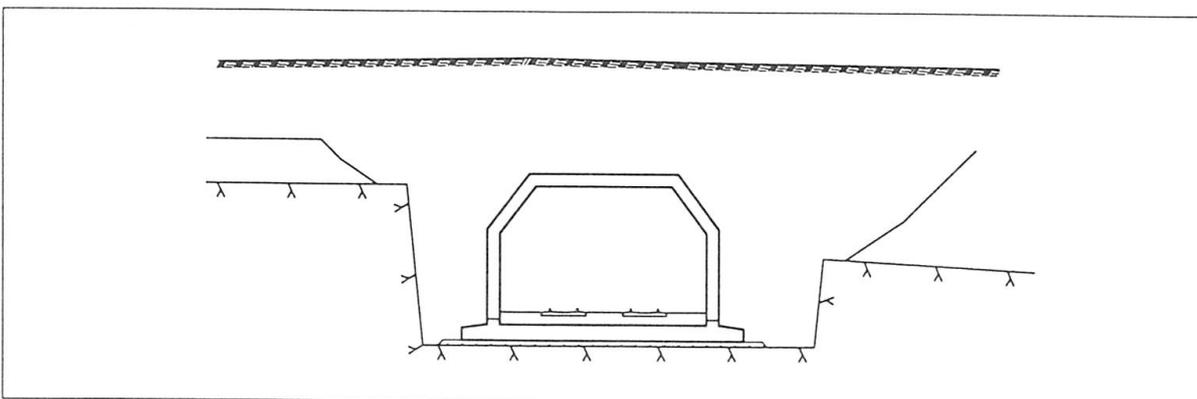

Fig 4 : The Brunnby Tunnel

3. Geotechnical Conditions

3.1 Tunnels below the Märsta River

In this area the railway is passing underneath the Märsta river. The river valley runs in an east-westerly direction and is about 500-600 meters wide. The northern and southern areas of the valley consist of steep mountain sides and the thickness of rock is sufficient to allow construction of rock tunnels.

In the mid section of the valley, the soil consists of 3-7 m clay. The clay has a dry solid top layer and underneath it is very soft with a shearing strength between 11 and 14 kPa. The clay layers are resting on moraine with varying thickness between a few metres and almost 20 m. In some areas the moraine top layer is comparatively soft but lower layers are very hard. Rock surface has been discovered about 21 m below the ground surface at the lowest point. The mean ground water level is 16 m above the foundation level.

The foundation of the lower inter-city tunnel is mostly built on a layer of compacted blast stones on the rock. In the middle of the valley, the foundations of some sections of the tunnel had to be built on moraine, which is at most 3-4 m thick. In the southern section, the foundation of the shuttle tunnel is integrated in the roof slab of the inter-city tunnel and in the northern section built on a 10-12 m thick moraine layer. In the surroundings of the fly-over point, the backfill is made of concrete in order to avoid vertical settlements. In the northern section the foundation is built on compacted blast stones on the rock.

The excavation work started with preventive reinforcements of the clay layer. About 20 percent of the clay volume had to be reinforced with lime-cement pillars. As a result of this, the shearing strength increased by approximately 100 percent. Afterwards the excavation work could be carried out at a mean inclination of the slope by 1:1. Lowering of the ground water level is effected by pumping in wells. Because of difficulties in lowering the ground water level in the impermeable moraine layer, some problems occurred during the excavation work. When the excavation work reached about one metre above the final depth of the foundation level, it was temporaraily stopped to make it possible to verify the solidity of the moraine layer with ram penetration tests.

3.2 The Åsa Tunnel

In this section the railway will pass through a very low depression in the rock and sufficient rock cover does not exist for a distance of 175 m although the surface of the rock is located at a higher level than the foundation level. The top soil consists of an eight metres thick layer of soft clay with a shearing strength between 12 and 16 kPa. The clay is resting on moraine with thickness varying between 8 and 10 metres. The upper moraine layer is moderately soft while lower layers are very hard. The ground water level is normally at the same level as the ground surface.

The excavation work to great depth could not be accomplished without supporting the ground. This was carried out by steel sheet piling through the clay, five metres of soil-nailing and below that "Berliner-piling" through the moraine. Due to the risks of getting settlements in the area close to the airport runways it was not possible to lower the ground water level. Therefore, water had to be recharged for infiltration around the excavation area.

To achieve accurate size and shape of the rock shelving, the blasting operation had to be performed very carefully and reinforcement bolting was necessary for stabilization. The joint between the foundation of the arch and the rock surface will be tightened with cement grout.

3.3 The Brunnby Tunnel

Also in this section the railway is passing through a minor valley. Due to a depression in the rock, a rock tunnel was not possible. In the middle of the valley, the top soil consists of a 3-4 m thick layer of peat and mud resting on an 8 m thick layer of soft clay. Underneath, there is a 1-6 m thick layer of gravelly moraine. The lowest rock surface level is located 12-14 m below the ground level. The mean ground water level is at the same level as the ground surface.

Before the excavation work started, layers of blast stones had been forced down through the soft top soil layers serving as embankments. It was then possible to carry out the excavation work through the moraine with a slope by 1:1 between the embankments.

The basis of the foundation of this tunnel section is a layer of compacted blast stones on the rock.

4. Design of and Actions on Structures

The structural design of the tunnels is based on actions, combinations of actions and safety factors according to Swedish codes BRO 94 (general rules for road bridges) and BV BRO (general rules for railway bridges).

Permanent actions are specified as:
- self-weight of concrete structures and ballast
- earth pressure from backfill of compacted moraine
- future filling to a higher level in the airport area
- water pressure
- loads from future buildings, 40 kN/m2
- imperfections
- shrinkage

Variable actions are specified as:
- railway loads in the tunnels
- traffic loads on the ground level
- aircraft loads, 80 kN/m2
- variation of ground water level
- temperature variations
- temporary crane loads during erection

Accidental actions are specified as:
- impact from derailed vehicles
- explosion, 70 kN/m2
- fire

5. Material properties and durability

The tunnels are designed to meet the requirements of an adequately durable structure with respect to its service life of 120 years. The concrete mixes are based on ordinary Portland cement with low temperature development and added with 5% silica fume. The water-binder-ratio of the concrete is maximum 0.50, corresponding to strength classes K40/45. To achieve a sufficient salt-frost resistance, the air volume is determined to at least 5%.

The reinforcing steel applies to grade K500 with characteristic yield stress fyk=500 MPa. The minimum concrete cover is determined to 45 mm. Cracking is limited to 0.2 mm under service actions in structures exposed to water pressure. With respect to reinforcement corrosion the crack width may not exceed 0.3 mm.

6. Detail Arrangements

The structures are arranged in 15 m sections separated with expansion joints. However, in the fly-over area, the section is determined to be 75 m long to avoid oblique-angled slab elements. The expansion joints are provided with two separate PVC-waterstops and an extra volclay sealing. The construction joints between the bottom slab and the walls are provided with a single waterstop and an injection hose for epoxy injection, if necessary. In cases where the tunnels are based on moraine layers, the expansion joints are designed to withstand even perpendicular movements.

7. Construction Methods

The 15 m tunnel sections are cast in two stages. The bottom slab is cast in the first stage and the wall and roof slabs are cast simultaneously in the second stage. To avoid cracking in the walls due to temperature differences between the previously cast bottom slab and the walls, special arrangements were required:
1. appropriate concrete mixes with a minimum content of cement/binder
2. cast-in heating cables in the bottom slab
3. insulation
4. cast-in cooling tubes in the walls

The temperature progress is measured continuously by cast-in temperature gauges and the data is transmitted by radio to a computer in the site office to enable immediate actions in case of undesireable temperature differences.

The steel reinforcement has been prefabricated in large cages and is placed in the formwork by crane.

****

Evaluation of Steel-concrete Composite Structures Applied for Multi-micro Shield Tunnel

Yoshihiro Tanaka
Research Manager
Taisei Corporation
Yokohama, Japan

Osamu Mochizuki
Construction Manager
Taisei Corporation
Yokohama, Japan

Tuyoshi Hirono
Design Manager
Taisei Corporation
Tokyo, Japan

Kouichi Kanou
Research Engineer
Taisei Corporation
Yokohama, Japan

Summary

Metropolitan Expressway Public Corporation is now developing the technically challenging multi-micro shield tunneling (MMST) method to construct huge span tunnels without use of the cut-and-cover method in urban areas minimizing environmental affects as well as the total construction cost. The experimental and analytical investigations of the flexural, shear and tensile resistant behaviors of the sandwich structure, the segment connector and the composite joint have been conducted to develop the reliable and cost effective joint structures as well as the design method for the MMST. A finite element approximation applying the concrete constitutive model based on fracture energy can well simulate the flexural and shear nonlinear behavior of the sandwich beam.

1. Introduction

It becomes difficult to construct the cut-and-cover tunnel for highway in urban areas because of the restrictions to obtain the private estate in the planned construction area, and to keep the traffic flow capacity as well as to control the environmental aspects. The MMST method is proposed for those demands to construct the huge span tunnel providing the multiple traffic lanes without disturbing the ground traffic flow. Underground air ventilation ducts equipped for the multi-lane expressway junction tunnels are now under construction by this method in advance of the huge multi-lane junction tunnels to confirm the construction process especially how to control well the shield machine with rectangular cross section and to verify the design method of the sandwich structure as well as the composite joint. Several technical developments have been and still being carried out for this project ; i.e., the development of both lateral and vertical sided shield machines, the cost effective reinforcement of the composite joint and the sandwich structure, and the design method for the composite structures including the structural checking for each construction stage. This paper is focused on the structural design verification for the underground air ventilation ducts being under construction as well as new proposals for cost effective composite joint and reinforcing the sandwich for future long span tunnel construction.

2. Construction Process of MMST

The general construction process illustrated in Fig. 2.1 are made up by the following stages ; 1) excavation shield tunnels and erection the segment alternatively using both lateral and vertical sided shield machines, 2) excavation inside the junction space among the shield tunnels and set up the joint reinforcement, 3) casting concrete into both shield tunnels made of steel segments and junction spaces reinforced by joint beams to build outer steel-concrete composite wall and slab for the final tunnel, 4) at a stretch excavation the inside of the final outer wall and slab without using any supporting members, 5) building the inner reinforced concrete walls and slabs for the traffic lanes. The structural requirements for the members are different for each construction stage and important to confirm the structural safety and to reduce the construction cost. There are three major structural requirements to solve as illustrated in Fig. 2.2. The first point is how to conduct the shear reinforcement for the sandwich structure as well as how to evaluate the shear and flexural behavior of the sandwich structure as an outer slab. The second requirement is how the segment

connector can have better bending performance than the general steel segment at the shield tunnel construction stage as well as it can have better tensile performance than the general one as a sandwich slab at the construction stage of excavation the inside of the final outer slab. The last requirement is how the composite joint among the shield tunnels can conduct better shearing and bending performance than the general sandwich structure.
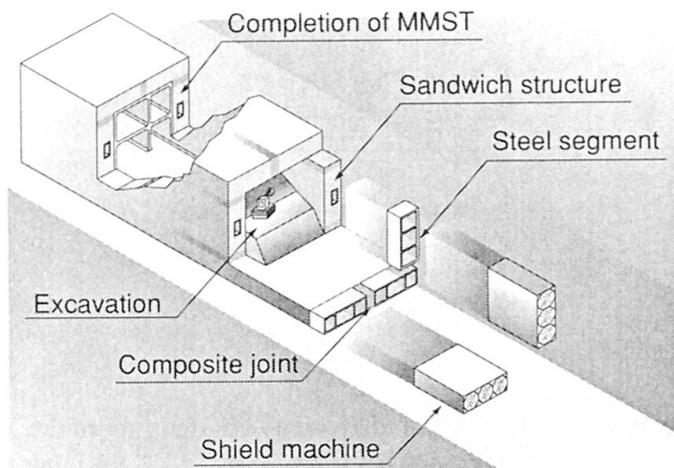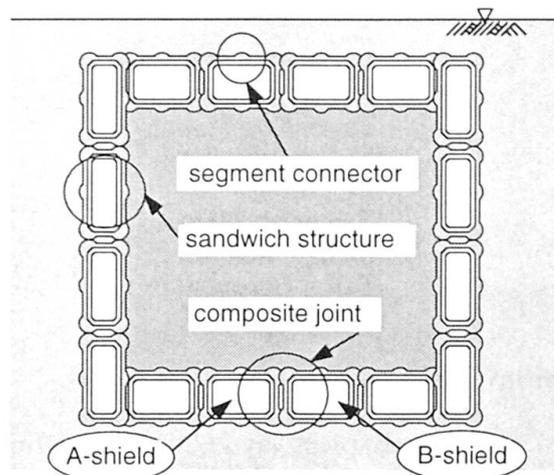

Fig. 2.1 Construction process of MMST　　　　Fig. 2.2 Structural requirements for MMST

The dimensions of the steel segment frame for the underground air ventilation duct tunnel being under construction are 2.5m in height and 7.0m in width for the lateral sided shield machine as illustrated in Fig. 2.3. One ring of segment frame whose length is 1.2m, is composed of six pieces of segment and each segment is jointed by the segment connectors. The main segment frame is made of H-beam or channel-beam whose height is 30cm and it is covered with skin plate whose thickness is 6mm. It is also supported by four mid-columns per one segment ring. The shear connector set up perpendicular to the main frame is originally designed to transmit the reaction force caused by several jacks promoting the shield machine to the main frame without buckling. Both lateral and vertical sided shield machines manufactured for the construction of the underground air ventilation duct is illustrated in Photo. 2.1. Four corner circles equipped in the shield machine are designed to make up reinforced soil roofs around the main frame corners.
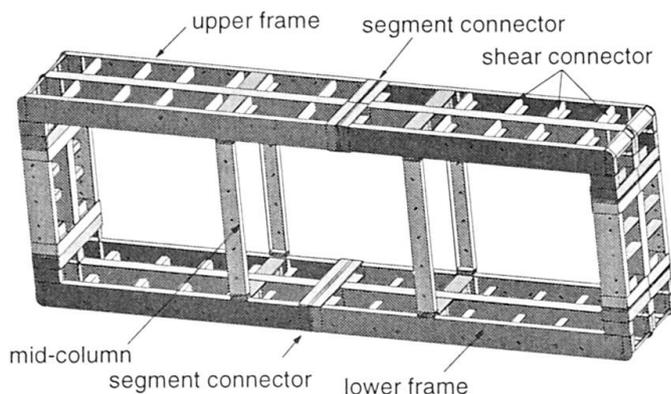

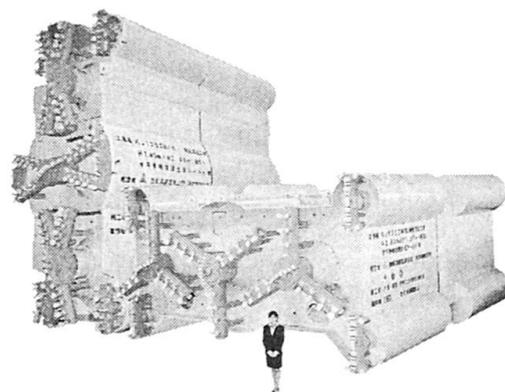Fig. 2.3 A ring of steel segment frame　　　　Photo. 2.1 Shield machines for MMST

3. Structural Concept and Experimental Program

3.1 Sandwich Structure

After casting concrete into the shield tunnel, the shield tunnel itself turns to be the sandwich structure. Two major questions come out in the process of the structural design for this structure ; 1) the shear connectors which are originally set for the reinforcement of the jacking system in

shield machine, are good enough to transfer the shearing force, 2) the mid-columns as shown in Fig. 2.3 which are originally employed as supporting members, work sufficiently well for shear reinforcement. Three flexural and shear loading tests as shown in Fig. 3.1 have been carried out using 1/2 scale specimens. Case-1 is just same as the segment frame as shown in Fig. 2.3. The interval of four mid-columns is approximately same as the sandwich beam depth, therefore the diagonal abrupt cracks may be easily caused by the shear force. In addition, the mid-column is fixed to the upper and lower frames by high tension bolts which have smaller yielding capacity than the mid-column, so the shear reinforcement ratio is only 0.074%. Case-2 is reinforced for shearing force by fixing the deformed bars to the shear connectors as illustrated in Fig. 3.1. Hence the pitch of shear reinforcement reduces to about 22cm and the shear reinforcement ratio due to rebar becomes 0.153%. Case-3 is planned to evaluate the reinforcing effect by rebars on the shear capacity through the shear loading test. The concrete compressive strength are designed to be 24Mpa and the maximum aggregate size is to be 10mm considering size effect.
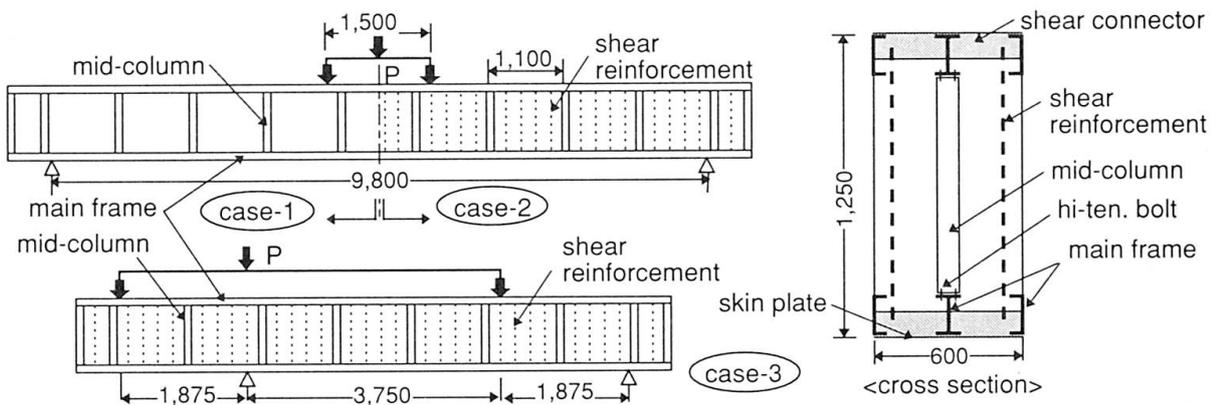

Fig. 3.1 Flexural and shearing tests arrangement for sandwich structure

3.2 Segment Connector

The segment connector used for the usual shield tunnel is designed to resist only for the bending moment due to the hydrostatic and earth pressure and it is required to tightly fit together each segment to prevent from leaking, while the segment connector for MMST is further required to resist for the tensile force as reinforcement of the final tunnel's outer wall . Therefore it is important from the design point of view how to separate the stress in joint bolts due to the first stage bending moment from the stress in these due to the second one. Flexural and tensile loading tests have been conducted for three specimens of segment connector as illustrated in Fig. 3.2. Case-A whose scale is 1/1, is the simplest connector to assemble quickly the segments each other and it is planned to investigate the tensile behavior of the lower joint bolts for the first stage bending moment as well as the three dimensional zig-zag effects on the bending resistance. Case-B whose scale is also 1/1, is an advanced connector modified from case-A. It is known from the analyses that case-A can not sustain the comparable tensile force to the main frame, because the end plates facing each other might deform easily by tensile force and it results in that the tension in
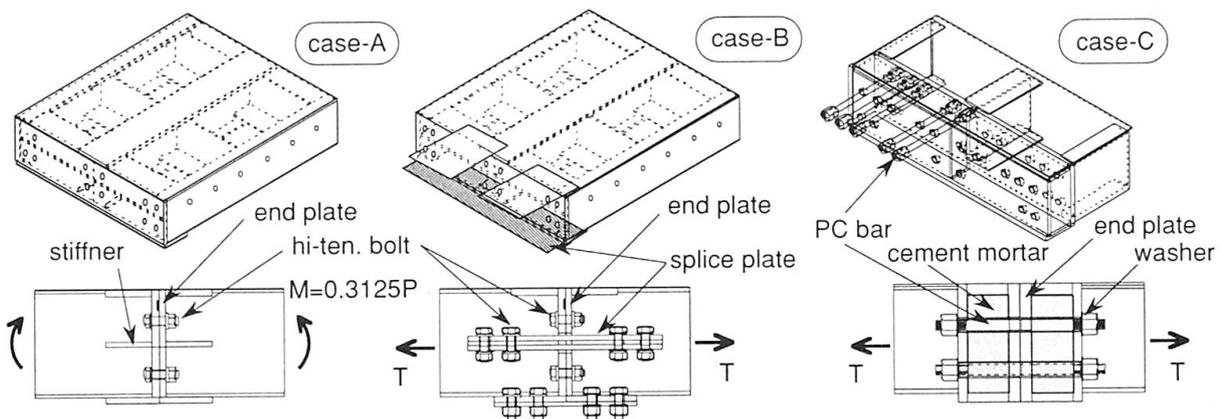

Fig. 3.2 Flexural and tensile tests arrangement for segment connector

each joint bolt does not distribute with even shares. The design concept of case-B is that the facing short bolts work only for the first stage moment while the splice plates resist only for the second stage moment. The specimen case-C whose scale is 1/2, is a further advanced connector combined from both case-A and case-B. Case-B needs to tie a lot of hi-tension bolts with the splice plate under controlling torque, hence this would take a long cycle time to assemble the segments. Case-C is composed of the steel plate box instead of the end plate and PC long joint bars. Shrinkage compensating cement mortar is injected in advance into the steel plate box because it might increase the rigidity which must smoothly transfer the tensile reaction force in joint bars to the main frame. It is noted that the lower PC long joint bars work for the first stage bending moment while the upper PC long joint bars sustain for the second one.
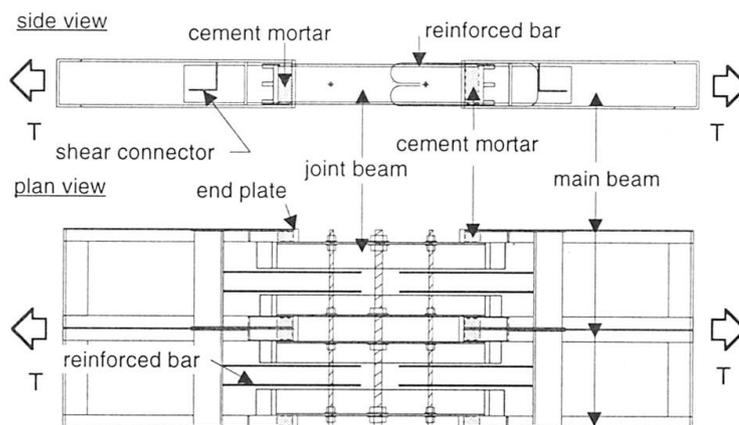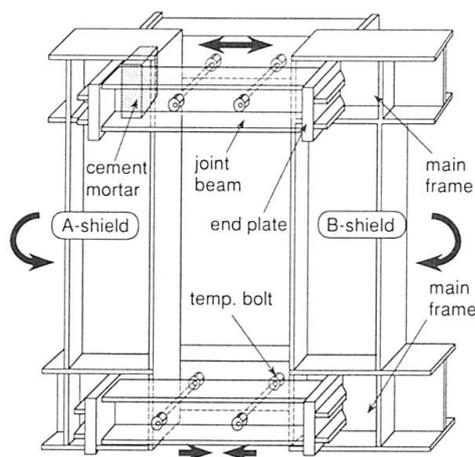

Fig. 3.3 Concept sketch of composite joint   Fig. 3.4 Tensile test arrangement of composite joint

3.3 Composite Joint among Shield Tunnels

The joint structure assembled inside the junction space among the shield tunnels, need satisfy at least two requirement ; 1) it should keep the comparable flexural and shear resistance compared with the sandwich structure, 2) it needs to be adjustable for the dislocation of the segment frame due to the construction error without reduction of structural performance. A typical joint method may be to set the longitudinal joint rebars and stirrups to transmit the tensile force due to bending moment in main frame via bond stress on joint rebars and shear stress in concrete. This type of joint however, can not usually possess the full flexural capacity same as the sandwich structure because of the limitation of joint rebar's location and space. The concept sketch of proposed composite joint is illustrated in Fig. 3.3. The structural concept for this joint is that 1) joint beams located in the center of the main frame are employed to directly transmit the tension to the main frame, 2) the cement mortar injected into the spaces which are located in both ends of joint beam, acts to transmit the tension from the main frame to the joint beam via compressive stress and it can adjust the dislocation of the segment frame. In advance of the flexural and shear loading test of this composite joint, the fundamental tensile loading test for the assembled joint member has been carried out to confirm force transmission mechanism and tensile capacity. The test arrangement for one ring segment frame scaling 1/2, is shown in Fig. 3.4. Concrete is cast inside the joint space to consider the lateral confinement effect of concrete on the lateral deformation of joint beams.

4. Experimental Results and Evaluation

4.1 Flexural and Shear Behavior of Sandwich Structure

The comparisons of the experimental results and the numerical analyses for the sandwich structure are demonstrated in Fig. 4.1. The crack pattern of case-1 to -3 are compared with the principle strain distribution calculated by the FE analysis in Fig. 4.2. The load and deflection curves for case-1 and -2 seem to be similar each other, but the failure modes are different ; case-1 indicates shear failure while case-2 shows flexural failure. The failure modes difference is demonstrated in the crack pattern ; 1) crack-A and B were open just before the final load but diagonal crack-C
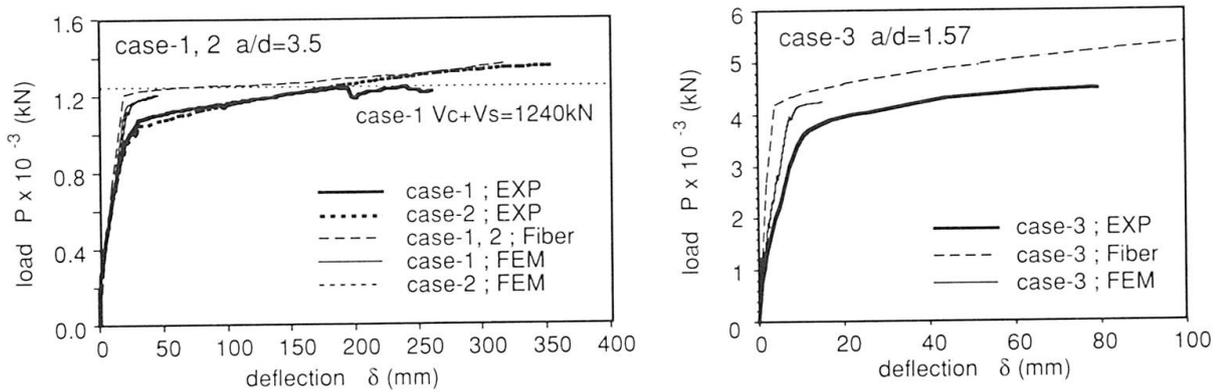
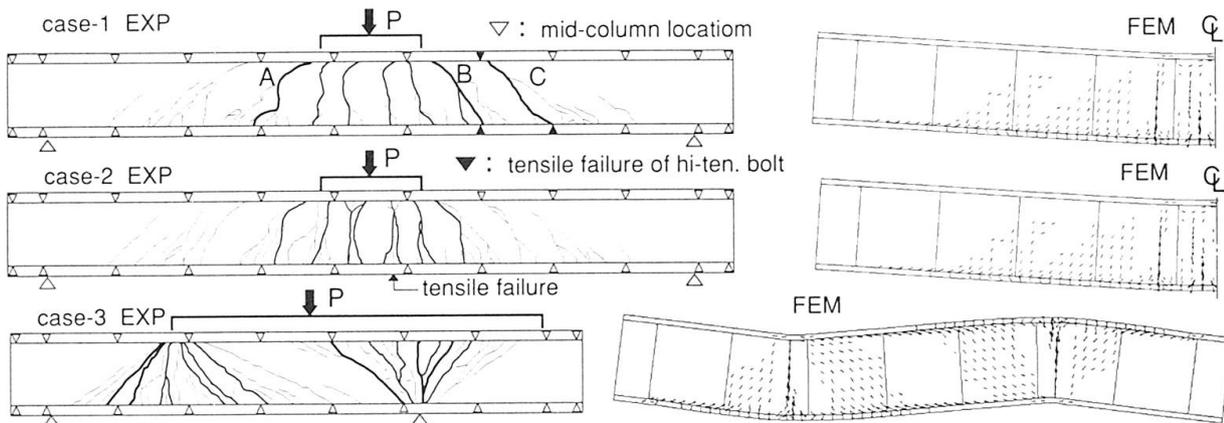Fig. 4.1 Load and deflection of sandwich structure

Fig. 4.2 Crack pattern of tests and FE analyses

which does not cross the mid-column, opened abruptly at the final load where the hi-tension bolts both ends of mid-column were failed, 2) crack pattern of case-2 is scattered wider than case-1 and the typical flexural cracks increased uniformly in width to result in the tensile failure in the main frame at the final load. These difference can be also explained by simple hand calculation ; 1) the flexural capacity by RC formula is $P_{flx}=1100kN$, 2) the shear capacity by Okamura's formula results in $P_{s1}=1220kN$ for case-1 and $P_{s2}=2170kN$ for case-2, respectively. Case-3 indicates shear failure mode and its crack pattern demonstrates scattering uniformly compared with case-2 because of difference of shear-bending ratio. It is observed in all cases that all cracks begin to grow from the shear connectors in the main frame. The capacity predictions for case-2 and 3 by the FE model demonstrate good agreement, but estimation for case-1 by the FE model does not result in the shear failure. The FE model can not estimate the proper deflection; the reason may be that the model does not include the confinement effect due to skin plate. The crack pattern results demonstrate nice agreement with test results. The capacity and deflection prediction for case-2 by fiber model agrees well with test results; this means RC theory can follow the flexural behavior of the sandwich structure.

4.2 Flexural and Tensile Behavior of Segment Connector

The load and deformation results are illustrated in Fig. 4.3. Most deflection in case-A after yielding is caused by the deformation of the end plate and the lower tension bolts. Segment connector case-A lost the bending resistance at the final load 3140kN by fracturing one lower bolt located near the main frame. This observation can be simulated even by the linear FE model. The web splice plate in segment connector case-B indicates yield at around the tension force 1200kN under which the elasto-plastic FE model can simulate accurately. The reason why the FE model underestimates the tension force for over the rage of yield point is that modeling of splice plate does not include the reduction of frictional force due to web's yielding. The final failure mode of case-B was a slip of the splice plate. It should be noted that all tension joint bolts for case-B and the lower PC joint bars for case-C were not set in the loading tests to separate a prior stress in bolts. The elongation of case-C indicates smaller than case-B and its yield point is not so clear

because the end plate box injected cement mortar is so rigid that the stress from PC joint bar can spread over the main frame. The elasto-plastic FE model can predict quite accurately the final resistant capacity which was determined in test by the abrupt failure of all of the PC joint bars. In addition this model might predict precisely the elongation if the deformation of washer for the PC joint bars were considered into the modeling.
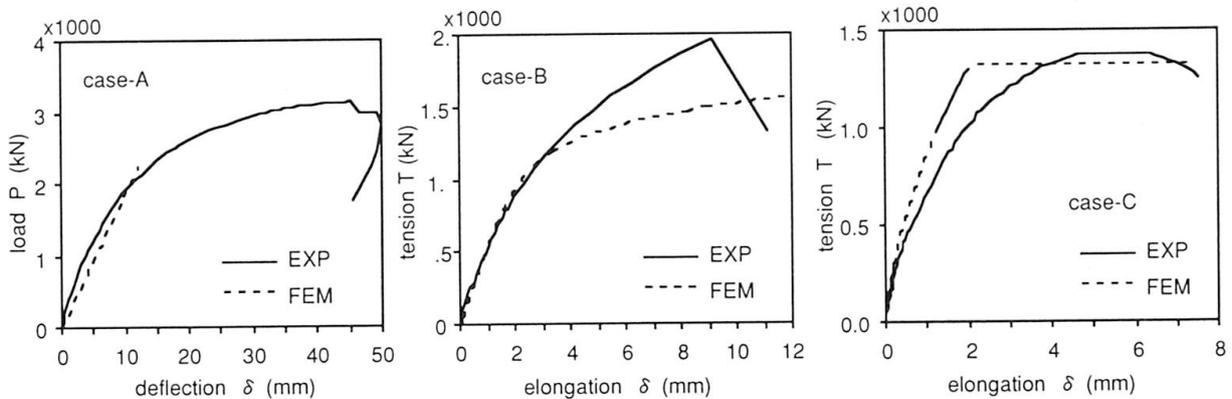

Fig. 4.3 Load and deformation of segment connector

4.3 Tensile Behavior of Composite Joint

The comparison of the test results and the FE model for the composite joint are illustrated in Fig. 4.4 and the deformation sketch by elasto-plastic FE model at yielding point is also illustrated. The first slope of rigidity at around 300kN in the test result comes from 'tension stiffness' caused by surrounding concrete. The yielding point at around 1100kN is mainly caused by yielding at the web plate of which thickness becomes normal in the main frame as illustrated in the deformation sketch. The yielding load predicted by the FE model is higher than the test result but the final load agrees quite well with the experiment. It should be noted that proposed composite joint can sustain the tensile capacity of the main frame without a serious damage in joint part.
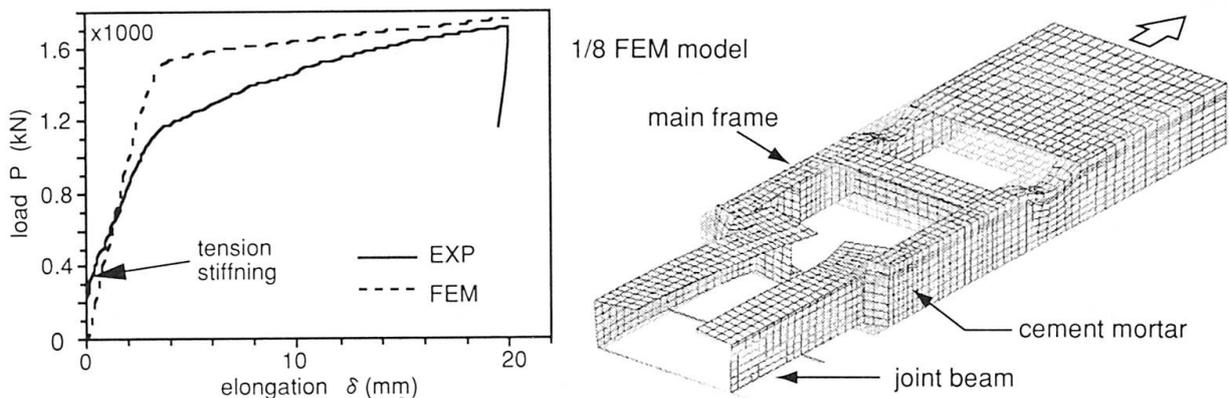

Fig. 4.4 Load and elongation of composite joint

5. Concluding Remarks

1) The sandwich structure for MMST is a multi-purposed useful structure for a huge span of tunnel and its flexural performance is similar to the reinforced concrete. 2) The mid-columns employed as supporting members are not good enough to keep the shear resistance hence the shear reinforcement by rebars with small pitch is useful for scattering the cracks and cost effective. 3) The design of the segment connector for MMST needs to be taken a careful consideration because of dual purposed usage. The segment connector of long PC bars with the cement mortar injected plate box indicates good performance for those requirement. 4) So far the tensile test result of proposed composite joint, the sandwich structure applying this composite joint must demonstrate good flexural and shear performance and also cost effective performance.

# Design of Tunnel Structures and linings for ice pressure

Jesper Krus
PhD
Tyréns Consultants,
Stockholm, Sweden

Jesper Krus, born 1961,
received his MSc in 1987
and his PhD in 1995. He
is now working as a
Bridge engineer at Tyréns
Consultants.

Håkan Sundquist
Professor,
Royal inst. of
Technology,
Stockholm, Sweden

Håkan Sundquist, born
1944, received his MSc in
1967 and his PhD in
1979. After working first
as a consultant structural
engineer he worked as
technical director at one
of the major Swedish
Construction companies.
He was appointed
professor in Structural
Design and Bridges 1992.
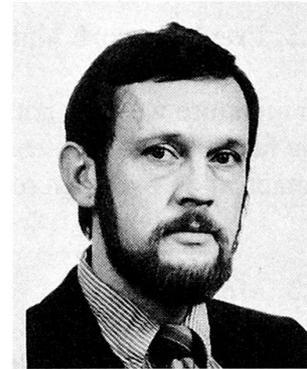
Summary

The normal procedure for design of tunnels in soil or rock is to drain out water that flow into the tunnel. In geotechnically sensitive areas were lowering of the ground water table will result in settlement of the soil, it is not allowed to drain out the water. An interesting question is then, if there is a risk for the formation of ice between the tunnel lining and the rock or soil.

A computer program has been developed for the non-linear calculation of temperature variation in tunnel linings on soil and rock. Special emphasis was laid on the proper modelling of the non-linear ice forming energy loss and gain during the freeze and thaw process. It is believed that this problem has been solved by the program and the results are in close agreement with measurements and other applied tests.

The calculation shows that the temperatures behind the linings could become below –2°C during cold winters. The frost depth and the amount of water that could freeze is normally though not enough to form pressures greater than the load carrying capacity of the actual tunnel linings.

1. Definition of the problem

This paper is concentrated on problems actual for studying the risk for forming of ice pressures around concrete linings of the type that projected for the Ring Road in Stockholm.

1.1 Questions

For many of the planned tunnels in Stockholm there are some very special design parameters. The tunnels have to be tight not to lower the ground water table. Lowering of the ground water could result in settlements in the soft soils adjacent to the tunnels, which in turn could cause great damage to many old buildings. The concrete tunnels are thus constructed water tight and in rock the rock is tightened using injection.

The above-mentioned design restrictions results in that full water load and load from the soils should be considered in the design. In countries with cold winter climate and for tunnels with good ventilation the temperature will for long time during the winter have temperatures below zero. A special question is then if there is a risk for the formation of ice pressure behind the linings.

1.2 Previous work and external references

In literature we have not found any information regarding this problem. This is probably due to the fact that this problem have not been met before, because few tunnels are constructed with this combination of design restrictions.

1.3 Measurements

In one older tunnel in Stockholm measurements have been made for measuring the temperature variation from the openings and on different stations in the tunnel. The temperature variation on different depths in the linings have also been measured for a couple of years. Of course such a short period will not show extreme and interesting results. Some verifying comparisons with the theoretical calculations have though been carried out.

2. Ice pressure

2.1 Interaction between temperature and pressure for water and ice

There is a relation between pressure and temperature that decides whether the water transforms into ice or not, see *Figure 1*. The figure shows that in a totally closed, non-expandable volume, very large pressures arises. Since the water expands approx. 9 % when transformed into ordinary ice, one can see that extra volume is needed to cope with the expansion. Most materials are porous and contains volumes in which the ice can expand.

There is also a relation between the size of the volumes in which freezing occur and the freezing temperature, see *Figure 2*. The figure shows the relation between equivalent radius of pores and the freezing temperature.
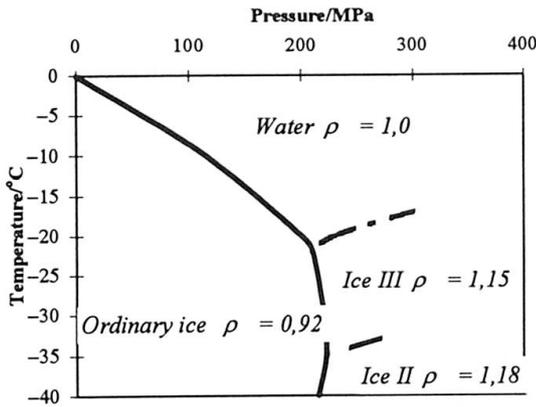
2

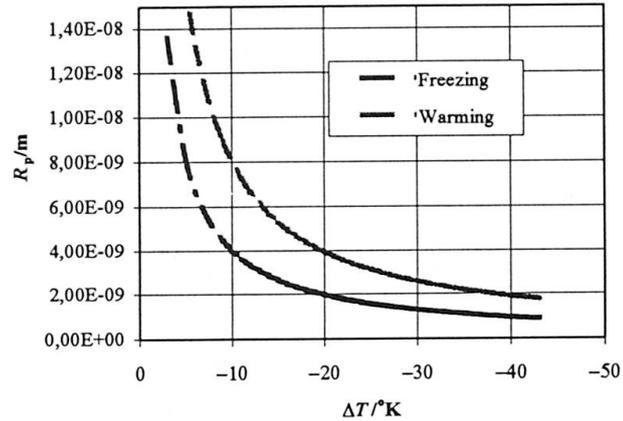Figure 1 Relation between temperature and pressure and ice formation.

Figure 2 Relation between equivalent size of volume and the lowering of freezing temperature.

The problems discussed in this paper are closely related to the problem of frost in ground. For frost heaving in ground there has been set up relations between frost and ground heaving. The pressures actual in those cases are however much smaller than the ones discussed in this paper. Extrapolation of values for frost in ground shows that the risk for large pressures should be small even in the case of tunnels in soil. For the rock case no information could be found in the literature.

2.2 Reduction of pressures due to deformable structure

A pressure could not be built up if there is no structure to resist the volume change. As an example we assume we have a circular pipe formed tunnel structure acted on by a pressure from the outside. The resistance the pipe makes against this pressure could be evaluated by the formula

$$p = 0{,}1E \frac{w_h t_j t_k}{R^2} \qquad\qquad\text{(a)}$$

where

p pressure, MPa
E Young's modulus of elasticity, MPa
w_h water content in the surrounding material, %
t_j thickness of the frozen soil or rock, m
t_k concrete thickness, m
R radius of the tunnel, m

Equation (a) is shown in *Figure 3*. The figure is based on a tunnel with 10 m radius and the pressure is plotted against 'effective ice thickness', t_{eff}. t_{eff} is defined by equation (b).

$$t_{\text{eff}} = (w_h - w_p) \cdot t_k \qquad\qquad\text{(b)}$$

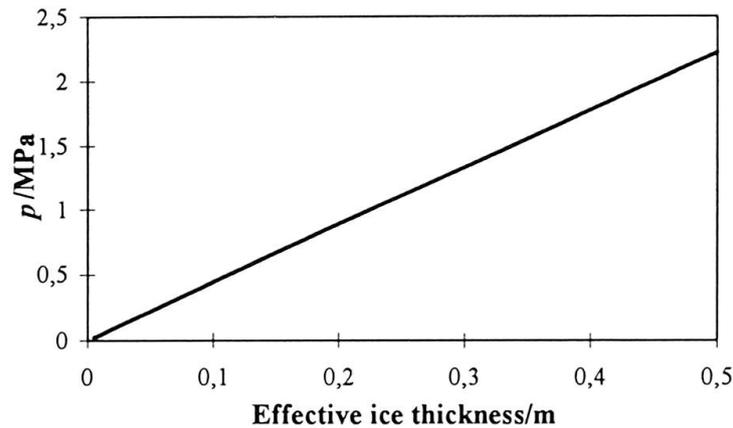where w_p is the air content of the soil in %.

Figure 3   Example of relation between 'effective ice thickness' and pressure against a tunnel structure. Effective ice thickness is equivivalent to the amount of water that could freeze.

3. Analysis

3.1 General

A computer program has been developed for the linear and non-linear calculation of temperature variation in tunnel linings in soil and rock. Special emphasis was laid on the proper modelling of the non-linear behaviour of the process.

The computer program has the capability to take different parameters into account such as:

- Temperature variation in the tunnel
- Different material layers such as concrete, rock, soils with different water content, insulation, air voids and water filled pores
- Ice forming energy gain and loss during the freeze and thaw cycles.

3.2 Results without consideration of the ice forming energy

A problem not so complicated to analyse is the case when the temperature varies outside a infinite half-space. *Figure 4* and *Figure 5* show how the temperature varies at various depths inside a structure when the outside temperature varies sinusoidal with the amplitude T_{max}. In *Figure 4* the wavelength is 1 day and night and in *Figure 5* the wavelength is one week. 4 different lining structures are considered, a thin 50 mm concrete lining (i.e. shotcrete on rock), 400 mm concrete on rock and finally 1000 mm concrete without and with insulation. The calculations are based on the following material properties:

Concrete, thermal conductivity 1,8 W/(m·K) and specific heat capacity $2,5·10^6$ J/(m^3·K) = 0,7 kWh/(m^3·K).

Insulation, thermal conductivity 0,05 W/(m·K) and specific heat capacity $0,1·10^6$ J/(m^3·K).

Rock, thermal conductivity 4,0 W/(m·K) and specific heat capacity $2,0·10^6$ J/(m^3·K).

Soil, thermal conductivity 2,1 W/(m·K) and specific heat capacity $2,5·10^6$ J/(m^3·K).
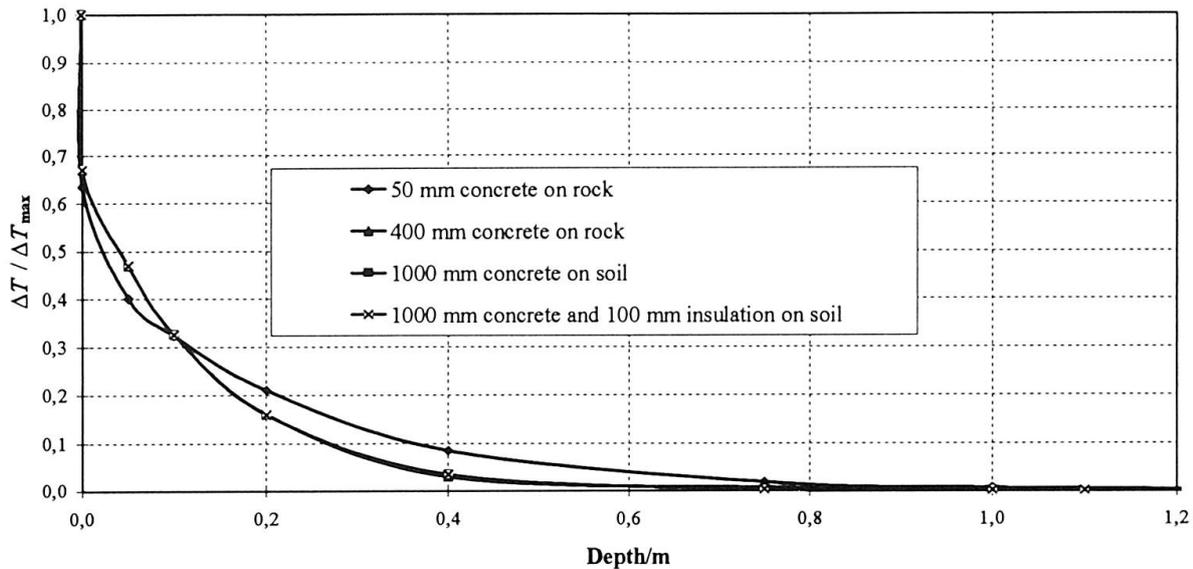
Figure 4   *Temperature variation ΔT at different depths in a lining when the temperature is varied with a period of one day and night with the amplitude ΔT_{max}.*
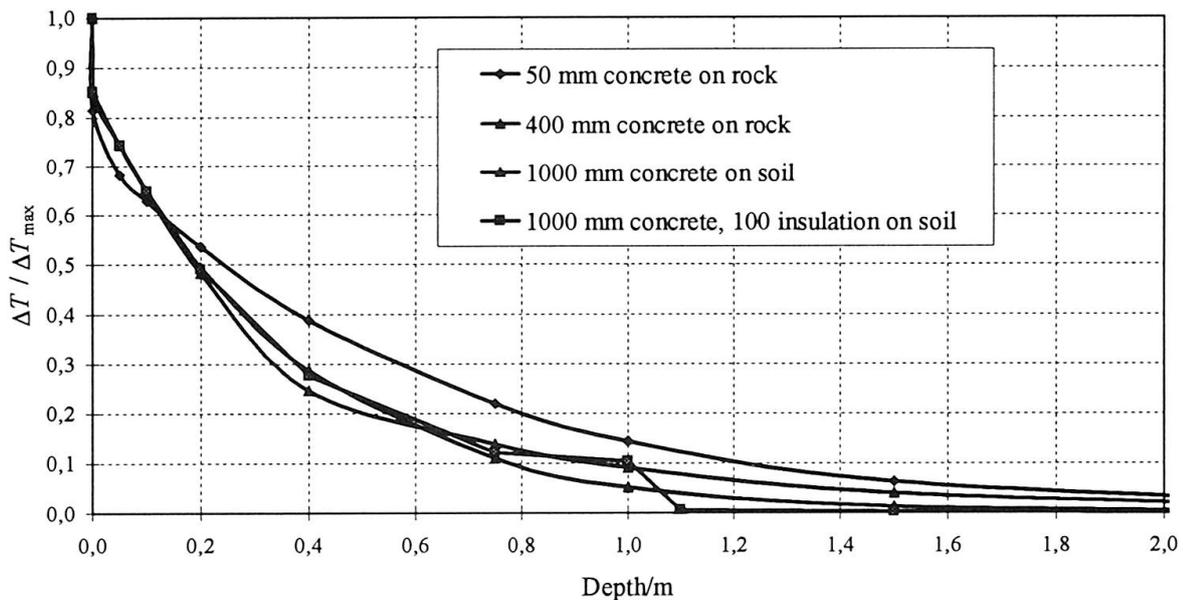

Figure 5   *Temperature variation ΔT at different depths in a lining when the temperature is varied with a period of one week with the amplitude ΔT_{max}.*

3.3 Results with consideration of the ice forming energy

Water might cause problems when cyclic freezing and thawing of the boundary between lining and rock occur. The reason to this is the possibility for the water to rearrange. It is therefore interesting to investigate by which frequency there is a temperature amplitude of 2K, 400 mm from the concrete surface in the case when we have a 400 mm concrete lining on rock. −2 °C is the temperature when we assume that water in concrete is transformed into ice.

In this study the heat transfer resistance in the air/concrete interface was given the value 0,033 $m^3 \cdot K/W$. The same values for material properties as before has been used.

Temperature cycles longer than one day has to be some kind of change of the weather. In *Krus* the best value, for the amplitude of this kind of temperature cycles in Stockholm was found to be around 10 K.

In order to investigate the most dangerous wavelengths, amplitudes between +4°C and −6°C were applied. For 6 day long cycles and 400 mm concrete on rock, results according to *Figure 6* were obtained. The water content in concrete was assumed to bee 1 % in concrete and 0,1 % in rock.
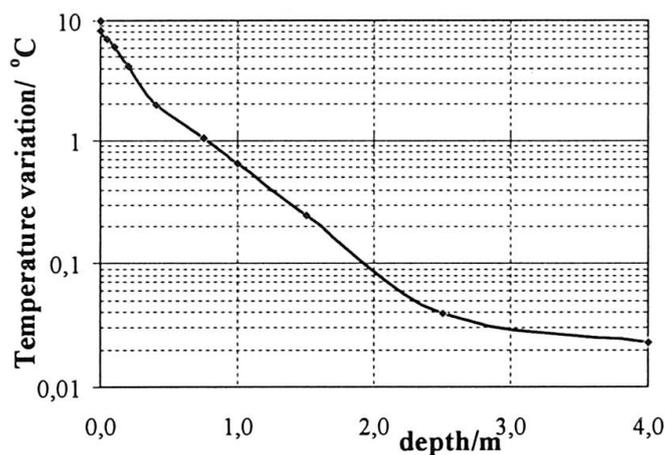

Figure 6   *Temperature penetration when the outer temperature varies in 6 day cycles (+4°C to −6°C) for a 400 mm concrete lining on rock.*

As can been seen in *Figure 6* temperature amplitudes with magnitude 2 K penetrated 400 mm into the structure. For other frequencies for the wavelengths, results according to *Figure 7* were obtained.
As can be seen from Figure 7 the penetration to an amplitude ΔT of 2 K is:

1 day and night	0,15 m
3 days	0,28 m
6 days	0,4 m
2 weeks	0,8 m

Since the calculations are close to 0 °C the energy loss and gain when the ice melts and freezes moderate the amplitudes at each cycle.
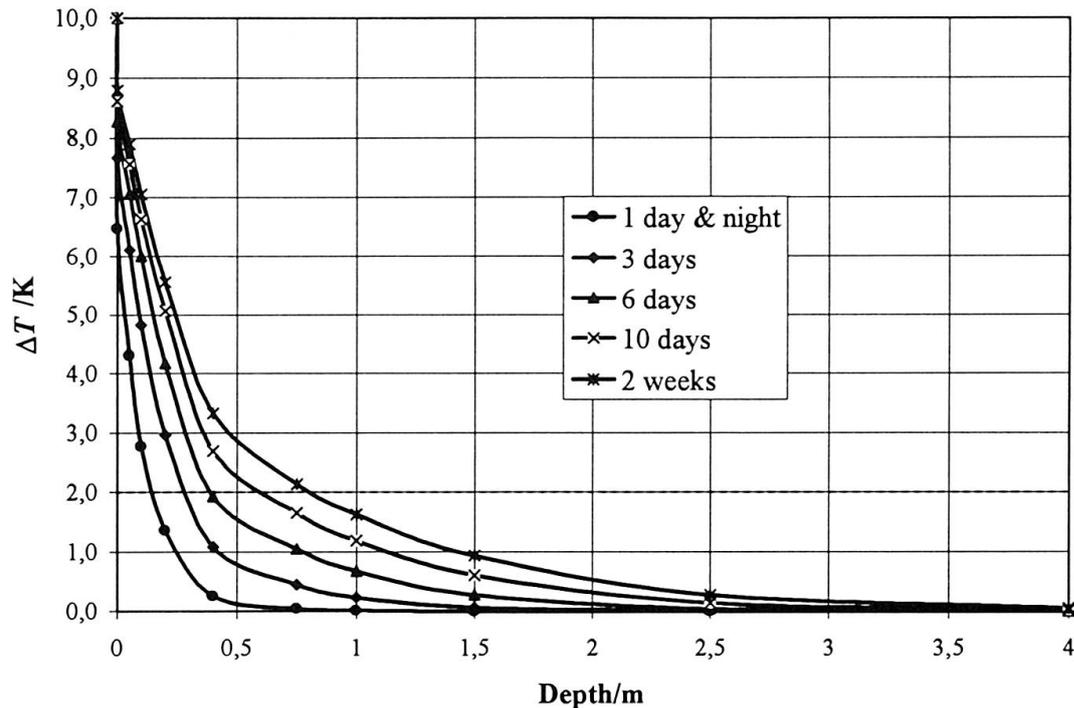
6

Figure 7   *Temperature penetration at different depths when the outer temperature varies in 6*
              day cycles for a 400 mm concrete lining on rock.

In the special Swedish design code for tunnels there is a special design curve, see *Figure 8*, for
the lowest design temperature, that should be considered regarding the risk for formation of ice
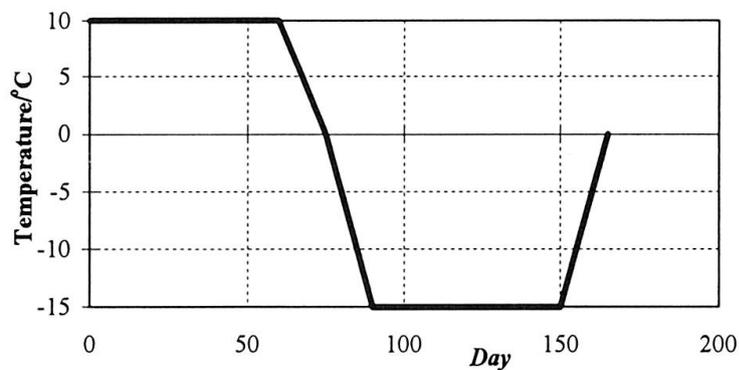in tunnels.

Figure 8   *Variation of dimensioning winter temperature according to the Tunnel Code of the*
              Swedish Road Administration.

Applying the temperature curve according to *Figure 8* calculations of the penetration have been
made for two cases, namely 400 mm concrete on rock, *Figure 9*, and 1000 mm concrete on soil,
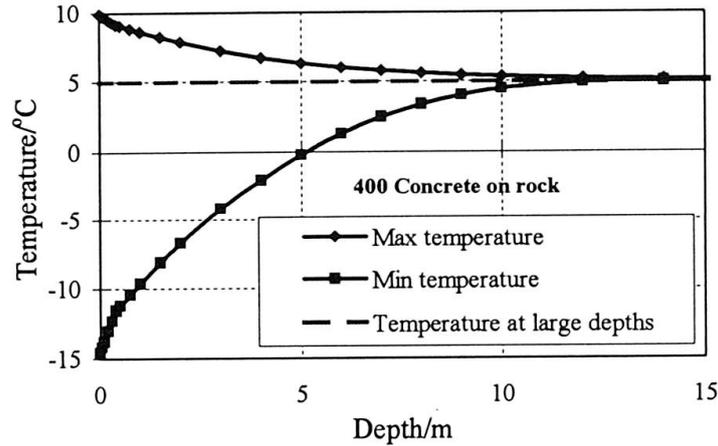*Figure 10*.

7

Figure 9   *Temperature penetration for the winter according to Figure 8 into a lining with a thickness of 400 mm on rock.*

As can be seen in *Figure 9* the variation in amplitude reached 12 - 13 m into the rock. 0 °C penetrated 5 m and −2 °C penetrated 4 m.
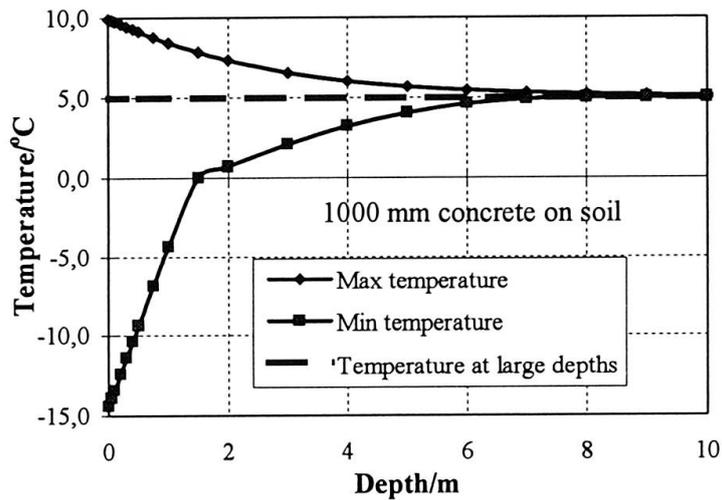
Figure 10   *Temperature penetration for the winter according to Figure 8 into a lining with a thickness of 1000 mm on soil.*

As can be seen in *Figure 10* the variation in amplitude reached 8 - 9 m into the rock. 0 °C penetrated 1,8 m and −2 °C penetrated 1,5 m.

An other question of importance is the influence of the moisture content in the concrete. Results of calculations showing this variation are shown in *Figure 11*. In *Figure 11* the amplitude at the air/concrete interface is 5,7 K in winter. As can be seen in *Figure 11* the variation in moisture content makes very little difference in the penetration depths.

8

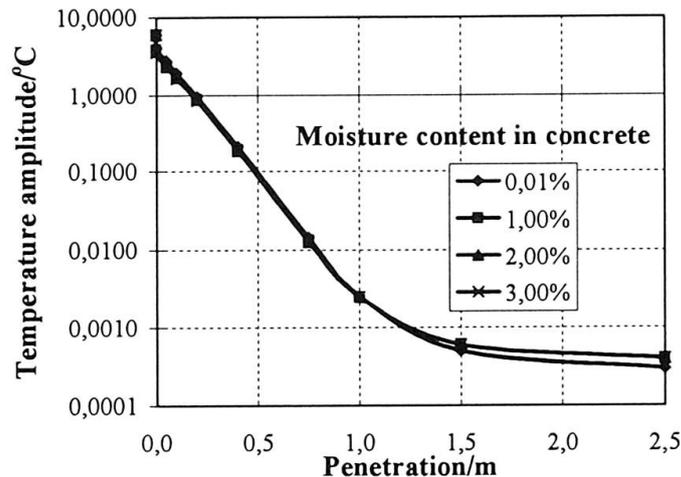*Figure 11*   *Temperature penetration for an amplitude of 6 K from +2 °C to −4 °C for different moisture contents in the concrete.*

4. Conclusion and proposal for interpretation of results

A computer model has been set up for analysing the risk for hazardous formation of ice behind concrete linings in rock or soil. The non-linear computer model has the ability to calculate the penetration of frost into the materials around the tunnel for different material combinations an with varying temperatures. The calculations alone does however not solve the problem. There must also be a model for the pressures formed by the ice. The crucial parameter is then the amount of free water that is present in the rock or soil and that could freeze.

The combination of analysing the theoretical results and the engineering judgement of the possible amount of water present leads to the conclusion that the risk for ice pressures higher than the water pressure is very small. If a larger cavity between the lining and rock could be formed there could exist a risk. With god workmanship this risk seems to be small and thus the ice pressure could be neglected.

This paper is based on a small investigation, initially as a by-product from investigations regarding the risk for degradation of concrete bridges due to freeze-thaw cycling. Problems of this kind are very complicated if one tries to find what really happens inside the materials. The aim of the current investigation has consequently been to find an engineers on-the-safe-side solution to the stated problem.

5. References

Beskow G., "Scandinavian Soil Frost Research of the past decades", Proc. 27th Annual Meeting, Highway research Board, USA 1947.

Harnik A.B., Meier U., Rösli A., "Combined Influence of Freezing and De-icing Salt - Physical Aspects", ASTM Special Technical publication, STP-691, Philadelphia 1980.

Krus J.,   "Geografiskt betingade fryscykler i svenska betongkonstruktioner", TRITA-BKN, Rapport 39. Brobyggnad 1996. (in Swedish)

Marchand J., Pleau R., Gagne R., "Deterioration of Concrete Due to Freezing and Thawing", Materials Science of Concrete IV.

Vägverket RYT, "Beräkning av temperaturer bakom isolerat innertak i bergtunnel", Stockholm 1994. (in Swedish)

Wehmhörner G., "PM Platsgjutna förstärkningsvalv och betonginklädnader", PM 1996. (in Swedish)

The Design of the Western Harbour Crossing, Hong Kong

Martin W Morris
Technical Director
Hyder Consulting Limited
Guildford, United Kingdom

Martin Morris is a Fellow of the Institution of Civil Engineers and a Technical Director of Hyder Consulting Limited in UK. He was resident in South East Asia for nearly 20 years where he was responsible for the company's immersed tube tunnel work in Hong Kong and Australia. He was Project Design Manager for the Sydney Harbour Tunnel in Australia and Project Director for the Western Immersed Tube rail tunnel in Hong Kong as well as for the Western Harbour Crossing road tunnel which is the subject of this Paper.

Summary

The Western Harbour Crossing is the fifth Hong Kong harbour crossing, the third road tunnel and the first dual 3-lane tunnel, all constructed by the immersed tube technique. It was implemented using a build-operate-transfer strategy and constructed under a fast-track design and build contract in just 44 months. This Paper reports on key areas of the immersed tube tunnel design.

1.   Introduction

A tunnel crossing of the western end of Hong Kong Harbour was identified in 1981 in a report prepared internally by Hong Kong Government[1]. In 1983, the Study of Harbour Reclamations and Urban Growth (SHRUG)[2] identified a suitable Kowloon landfall on the proposed Western Reclamation. In 1989, the Second Comprehensive Transport Study (CTS2)[3] formally proposed a third harbour crossing as a means of meeting increased cross harbour traffic demand.

In 1989, Hyder Consulting as leader of a joint venture, Western Harbour Crossing Consultants, was appointed to undertake a feasibility study of the Crossing. Their report, presented in early 1991, determined that a dual 3-lane tunnel would meet traffic needs into the 21st Century, and would provide a satisfactory return as a BOT project.

The franchise was subsequently offered to competitive bidding and was won by the Western Harbour Tunnel Company Ltd (WHTC) in 1993. WHTC awarded a construction contract to Nishimatsu Kumagai Joint Venture (NKJV), who in turn appointed Hyder Consulting, as part of a joint venture, to undertake the design of all tunnel works, including the immersed tube, approach tunnels and ramps, and traffic surveillance and toll systems. Within the confines of this Paper it is only possible to concentrate on the immersed tube tunnel section.

2.   Alignment

The tunnel alignment (Figure 1) was defined by exhaustive studies at the feasibility stage and constrained by existing and committed development. The alignment extends from an interface with the West Kowloon Expressway (WKE) on the West Kowloon Reclamation (WKR) to a major interchange and connection to Route 7 at Sai Ying Pun on Hong Kong Island.

The West Kowloon Approach and the immersed tube tunnel were maintained on a straight alignment to simplify construction and maintain, as far as possible, a constant cross section. The need to connect the north-south tunnel with the east-west Route 7 within a limited coastal fringe at Sai Ying Pun necessitated curving the Sai Ying Pun approach to a horizontal radius of approximately 400m.
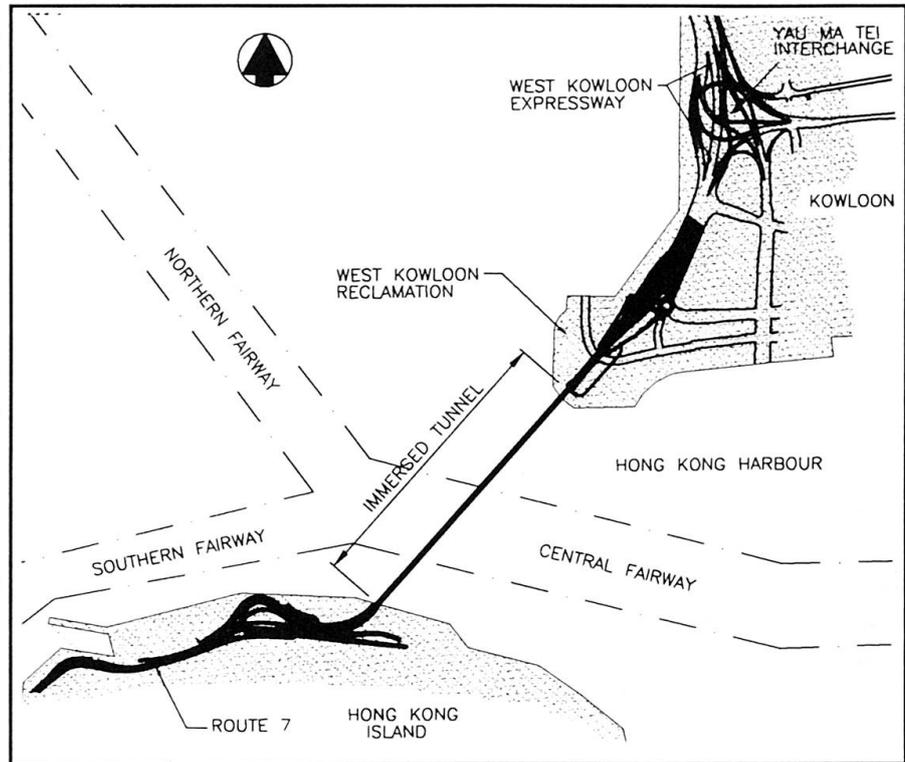

Fig 1 Tunnel Alignment

This enabled the interchange to be fitted between the existing seawall cope line and the existing and planned building developments immediately to the south of Connaught Road West, whilst maintaining a design speed of 70km/h.

The tunnel is 2.2km long from portal to portal. The immersed tube section is 1360m long and was constructed as 12 units, each 113.5m long, 33.4m wide and 10m high. They were constructed in three batches of four in a casting basin at a quarry site at Shek O on the southeast coast of Hong Kong Island. The quarry floor was excavated to a sufficient depth to enable the units to float when the basin was flooded to sea level. The rock working platform relieved the necessity for any consideration of settlement effects during construction.

The vertical alignment of the tunnel was governed by the required navigational clearance of 14m in the Central Fairway over a width of 700m. The vertical alignment was otherwise maintained as shallow as possible to limit gradients to 5%, to minimise the length of the approach tunnels and to minimise the depth of excavation at the Ventilation Buildings. On the Sai Ying Pun side, this means that the tunnel units project above existing seabed level, necessitating additional marine protection.

3. Cross Section

The two primary factors in determining the immersed tube cross section were the traffic gauge and the ventilation duct requirements. The traffic gauge for a dual 3-lane tunnel was defined within the Project Brief. Walkways were provided adjacent to the centre wall, connected by fire doors at 50m intervals. The ventilation duct area was designed to meet the airflow requirements for an acceptable user environment and for emergency ventilation and smoke extraction requirements.

The desire to minimise the depth of the cross section and to minimise dredging and the necessary depth of the casting basin, led to the decision to locate the ventilation ducts outboard of the traffic ducts to achieve the cross section shown in Figure 2.

4. Design

4.1 Buoyancy

The structural cross section was determined from buoyancy considerations such that the unit would float with a factor of safety against sinking of at least 1.02, representing a freeboard of approximately 200mm. Provided that water plane area is maintained, metacentric height and therefore stability, is not a problem with rectangular units of this width. After sinking, the units were required to have factors of safety against flotation of 1.04 without backfill and 1.20 with 1.5m of backfill.

Within the limitations set by the buoyancy criteria, top and bottom slab and outer wall thicknesses (and local haunching) were determined by bending capacity of reinforced concrete sections. Internal wall thicknesses were determined on the basis of vertical shear capacity. Despite the long spans of the dual 3-lane traffic ducts, transverse prestressing proved not to be required. Longitudinal prestress was considered but rejected on cost grounds.

4.2 Analysis and Design

Transverse structural analysis was based on a standard pc-based plane frame software. Plane grid models were used to determine local load concentrations and distribution in the vicinity of joints. Longitudinal analysis was based on line elements on an elastic foundation, using spring constants or moduli of subgrade reaction derived from settlement analysis.

Design loads were identified in four groups.
- Dead load, the long term loads on the structure including water pressure from the mean sea level case.
- Live loads, traffic, earth pressure including that from the surrounding backfill as well as variable hydrostatic loads (tidal variation, storm surge etc) and siltation of the harbour bed.
- Exceptional and extreme loads, including the effects of variation in foundation stiffness, loss of foundation support through erosion or other causes, effects of applied load from a sunken ship, anchor impact, flooding of the tunnel, explosion, fire, design earthquake and the resulting soil displacements.

- Construction stage loads, including wind and wave forces on the unit during towing and sinking.

These load groups were considered in a number of combinations at the serviceability and ultimate limit states using load factors defined in the Project Brief and developed as part of the Feasibility Study.
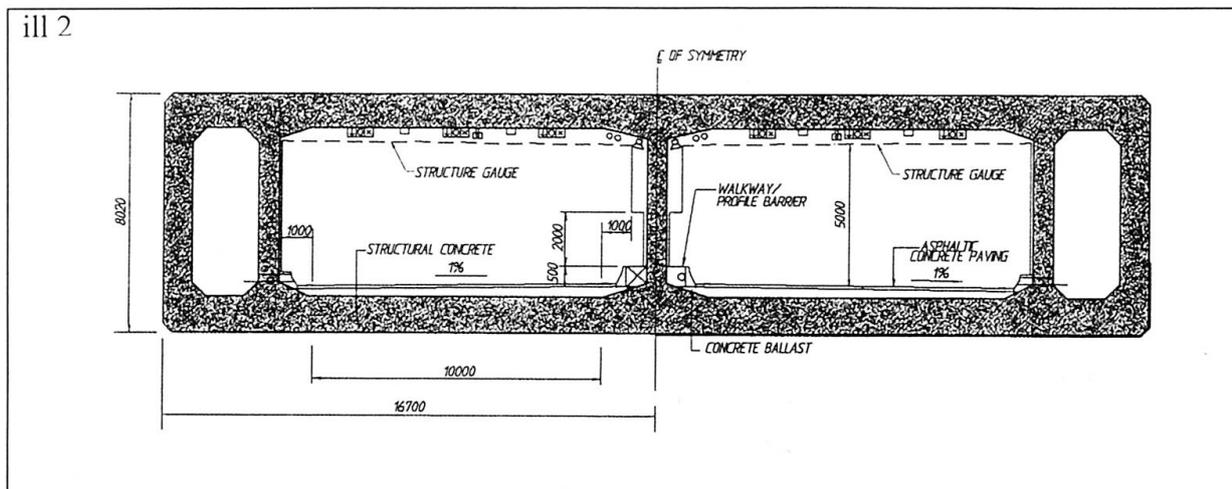

Fig 2 Typical Cross Section

Design of the concrete structure was based on BS8110[4] and BS8007[5] with flexural crack widths limited to 0.2mm. Thermal reinforcement was designed to BS8007[5] and CIRIA Report 91[6]. Each unit was cast in separate base, wall and roof pours with a bay length of 15m. Thermal restraint was modelled using finite element analysis based on a defined sequence of construction. Thermal crack widths were limited to 0.1mm with an overall limitation on combined thermal and flexural crack width of 0.2mm. Leading quantities were: concrete (characteristic strength 40N/mm^2 at 28 days) 149,000m^3 and reinforcement (Grade 460) 30,000 tonnes, representing a reinforcement provision of approximately 200kg/m^3.

4.3 Durability Analysis

The tunnel structure was subject to a special durability analyis. The two major components were the structural concrete and the waterproof membrane.

Experience gained from the Sydney Harbour Tunnel, Australia was used to develop a mix which simulated low heat cement whilst maintaining high resistance to chloride ion penetration. Pulverised fuel ash (pfa), which is readily available in Hong Kong to high quality, was used in preference to ground granulated blast furnace slag (ggbfs) which would have had to be imported. The final mix used 450kg/m^3 cementitious content (300kg/m^3 opc, 150kg/m^3 pfa) with a water cement ratio of 0.4. Superplasticiser was used to add workability. Laboratory chloride penetration tests were used to demonstrate a 120 year design life.

The waterproof membrane on the roof and walls of the tunnel was a 2-part methylacrylic membrane, spray-applied in 2 layers, and originally developed for use in waterproofing bridge decks. The roof membrane was protected from abrasion by a 75mm thick (minimum) mesh

reinforced concrete layer. This layer was also used to provide trimming ballast to ensure that the correct freeboard was obtained. Precast cover units cast into the edge of the external protection concrete provided a measure of protection to the side walls.

For the base of the unit, following the precedent of the Sydney Harbour Tunnel, the usual steel bottom plate was replaced by a high density polyethylene (HDPE) sheet 1.5mm thick. This was anchored to the concrete by extruded ribs.

5.   Foundations and Joints

The units were sunk, supported from pontoons, onto temporary foundations (Figure 3). The void below the foundation was filled with a sand/water mixture placed via pipes cast into the units. Typical unit to unit joints must provide rotational capacity, whilst maintaining vertical shear capacity and preventing significant vertical displacement.
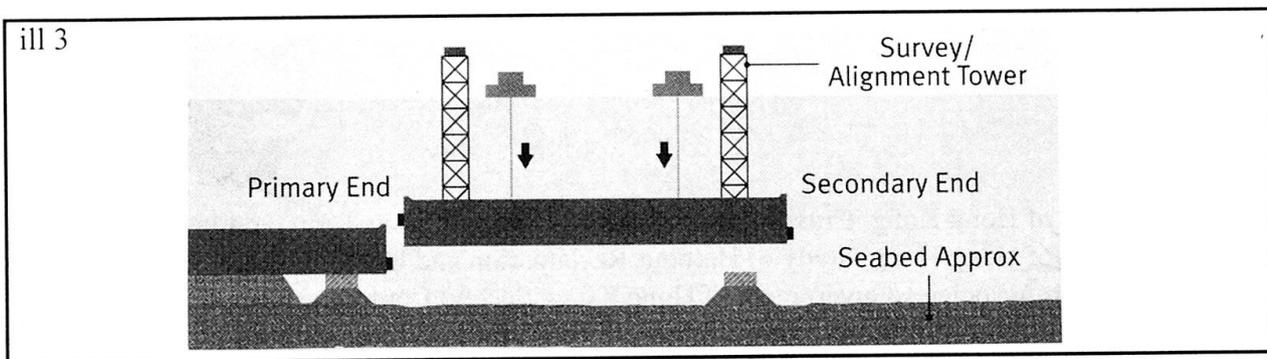
Fig 3 Sinking Arrangement

The units are jointed with conventional gina profile primary seals and omega section secondary seals. Vertical shear is transmitted by large interlocking steel shear keys, attached to the concrete section using stressbars. Laminated rubber bearings between the keys allow slight rotational movement and enable the very high peak shear forces which would be generated by a rigid vertical connection to be reduced. The bearings are inserted as late as possible after sinking and backfilling and shimmed to fit, thereby minimising the initial 'locked-in' load in the key system. At the landfalls, the potential for long term differential settlement between the landfall units (1 and 12) and the Ventilation Buildings had to be addressed. The units are supported on a sill beam and barrettes. No shear key is fitted and the gap between the underside of the unit and the sill beam has been grouted as late as possible after primary settlement has been completed.

6.   Backfill and Armour Protection

The tunnel units are generally set below existing seabed level and are backfilled using suitable granular material. Protection against marine hazards is provided by 0.6m backfill, overlain by 0.9m of rockfill with particle size 25-250mm. Further protection against dragging anchors is provided by bands of rock armour (100-500kg), 5m wide, set either side of the tunnel. This

material is designed to cause anchors to release from the backfill before penetrating deeply enough to damage the tunnel structure.

In the area of the Sai Ying Pun landfall, where the units project above seabed level, the backfill and armour is extended laterally to a minimum of 15m from the tunnel structure. This is intended to provide sufficient space and resistance for a grounding ship, having left the fairway for whatever reason, to be arrested before impinging on the tunnel structure.

7.   Programme

The franchise was awarded in August 1993. Design commenced immediately and was substantially completed in the following 12 months, some 1400 working drawings having been provided by the design consortium. The tunnel was opened to traffic in April 1997, some 3 months ahead of schedule.

References

1. Government of Hong Kong, Cross Harbour Traffic - Study of Long Term Options, 1981.
2. Government of Hong Kong, Study of Harbour Reclamation and Urban Growth, 1983.
3. Wilbur Smith Associates/Government of Hong Kong, Second Comprehensive Transport Study, 1989.
4. British Standards Institution, BS8110, The Structural Use of Concrete, London, 1985.
5. British Standards Institution, BS8007, The Design of Concrete Structures for Retaining Aqueous Liquids, London, 1987.
6. Harrison TA, CIRIA Report 91, Early Age Thermal Crack Control in Concrete, Construction Industry Research and Information Association, 1992.

Acknowledgements

The Design of the Western Immersed Tube Tunnel, Hong Kong

Martin W Morris
Technical Director
Hyder Consulting Limited
Guildford, United Kingdom

Martin Morris is a chartered engineer and a Technical Director of Hyder Consulting Limited. He was resident in South East Asia for nearly 20 years where he was responsible for the company's immersed tube tunnel work in Hong Kong and Australia. He was Project Design Manager for the Sydney Harbour Tunnel in Australia and Project Director for the Western Harbour Crossing road tunnel in Hong Kong as well as for the Western Immersed Tube rail tunnel which is the subject of this Paper.

Summary

The Western Immersed Tube Tunnel carries Hong Kong's new Airport Railway under Victoria Harbour. It comprises a twin track immersed tube tunnel, constructed of ten tunnel units. The tunnel was constructed for the Mass Transit Railway Corporation under a design and build contract strategy and completed in only 30 months. The Paper briefly describes key aspects of the design of the immersed tube structure.

1. Introduction

The Western Immersed Tube (WIT) carries the new Airport Railway under Hong Kong Harbour. The Airport Railway comprises the Airport Express Line (AEL) from the new Hong Kong Airport at Chek Lap Kok and a new mass transit railway, the Lantau Line (LAL) from Tung Chung New Town adjacent to the airport, both to the Central Business District on Hong Kong Island. WIT connects AEL and LAL on common tracks between the West Kowloon Reclamation, via Victoria Harbour to Central Station on Hong Kong Island. At the Hong Kong landfall, turnouts are located so that separate tracks can diverge to the AEL and LAL platforms at different levels.

Contract C502, for the Western Immersed Tube, was awarded to Kumagai - Tarmac Joint Venture (KTJV), a joint venture of Kumagai Gumi of Japan and Tarmac Construction of the United Kingdom. KTJV employed Hyder Consulting Limited to prepare the tender design on their behalf and subsequently awarded a design contract to Hyder Consulting for all permanent works design and for independent checking of KTJV's own temporary works designs. A key feature of the Contract was the need for close cooperation between Employer, Contractor and Designer to achieve the programme.

2.   Alignment

The alignment of the tunnel is dictated by the railway alignment on both sides of the Harbour. Airport Railway Feasibility Studies determined that the most appropriate location for the Central Station was on an east-west alignment on the new Central and Wanchai Reclamation (Figure 1).   It is conveniently placed for connections to the existing Tsuen Wan and Island Lines as well as to the Central Business District itself.
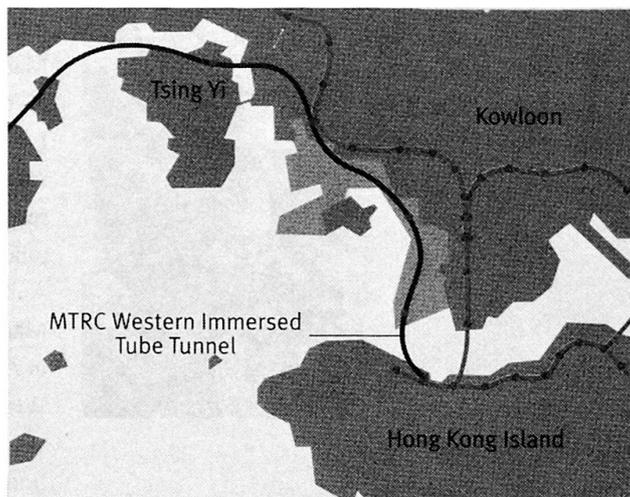

Fig 1 Key Plan

On the Kowloon side, the most convenient access was a north-south route via the new West Kowloon Reclamation rather than attempting to install a further line through the congested Kowloon hinterland. These two landfalls necessitated a variably curved alignment, turning some 60° in total with a minimum radius of 850m (Figure 2). WIT has a total length of 1260m between landfalls and comprises 10 immersed tube tunnel units, each 126m long.

The Hong Kong landfall is at a special tapered unit which accommodates turnouts to enable tracks to diverge to serve separate AEL and LAL platforms. This unit was installed under the Reclamation contract to meet programme constraints but was also designed by Hyder under a direct commission to MTRC. At the Kowloon landfall, the last tunnel unit connects directly to a stub end projecting from the Kowloon Ventilation Building and constructed under Contract C502.

Options for combining the tunnel with the Western Harbour Crossing vehicular tunnel were considered at feasibility stage of both projects but the alignment constraints eventually dictated the need for two separate tunnels. Both immersed tubes were however designed by Hyder and cconstructed by Kumagai so that a common approach to design and construction was adopted.

The vertical alignment is governed by required track levels and gradients at the landfalls and by the fairway width and depth in Hong Kong Harbour set by Marine Department. The resulting alignment takes the track level to about -25m PD and keeps the majority of the units and their backfill at or below existing seabed level. However, the track level constraints at the Hong Kong end were such that Units 1, 2 and part of 3 rise above seabed level, whilst maintaining the necessary depth requirements in the onshore traffic zone between the fairway and the Reclamation limit.

The cross section is a rectangular box 12.42m wide and 7.65m high containing twin ducts for the twin rail tracks. Internal spatial requirements were set primarily by compliance with the structure and kinematic gauges within the MTRC Design Standards Manual (DSM)[1]. The

horizontal curvature within the tunnel alignment is not constant, some units being straight, some incorporating transitions and some curved to the minimum 850m radius.

3. Geotechnical Conditions and Settlement

The seabed consists of extremely soft marine muds underlain by sandy/clayey alluvium, underlain by completely decomposed granite (cdg). The vertical alignment resulted in most units (except 1, 2 and 3) being founded in the alluvium.

Low foundation pressures from the units lead to small settlements which are predominantly elastic (i.e. short term). For typical units, predicted total elastic settlements were in the range 10-60mm with 10-40mm occurring within the construction period. Residual non-elastic settlements were of the order of 25-65mm. The Kowloon landfall unit (Unit 10) exhibited higher levels (up to 120mm elastic and 50mm residual) because of the higher loading from the Reclamation. By delaying lock off of the shear keys between tunnel units, long term differential settlements between units could be minimized. Elastic settlement in the construction period was accommodated by setting up the units by that amount when placing them. Post construction settlement was accommodated by oversizing the unit.
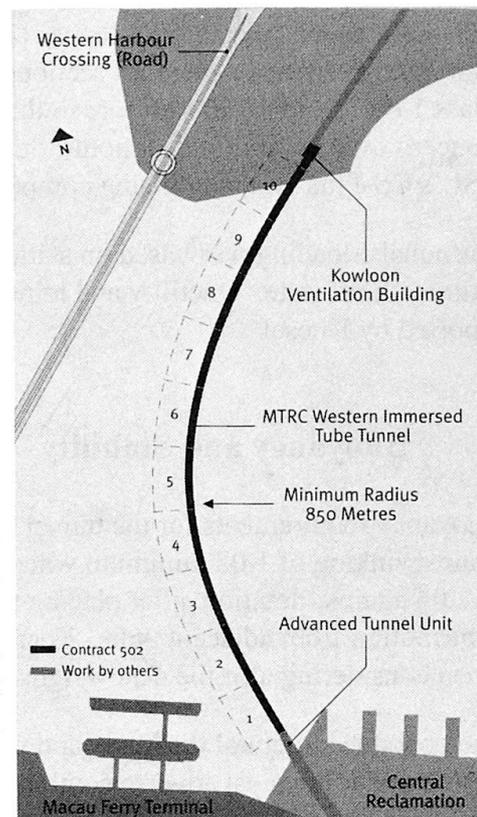

Fig 2 Tunnel Alignment

4. Structural Analysis and Design

Loading cases included self weight, services (including track and trackslab), backfill (and development surcharge allowances on reclamation), hydrostatic pressure, extraordinary loads such as marine hazards, earthquake, flooded tunnel) and temporary loads during construction. Load factors were defined in principle by the MTRC DSM[1] and agreed in detail between the Designer and MTRC following established practice on other IMT's in Hong Kong.

Loadings were applied to a plane frame for transverse analysis, a shear flexible plane grillage to assess load distribution from shear keys and other assymmetric loads and a longitudinal plane frame to assess longitudinal bending and shear in the tunnel units.

Transverse reinforcement was designed in accordance with BS8110[2] to limit flexural and thermal/drying shrinkage crack widths to 0.2mm total based on a notional (rather than actual) cover of 40mm to the outermost bar. Actual cover to both faces of external walls and slabs was 70mm and to the internal walls 40mm. Typical transverse reinforcement was T20 @ 150mm in both faces of base and roof slabs and T25@150mm in outer faces and T20@150mm in inner

faces of walls. Longitudinal reinforcement was T16@150mm. Overall reinforcement density excluding prestress was about 160 kg/m^3.

Thermal and drying shrinkage reinforcement was designed in accordance with BS8007[3] and CIRIA Report 91[4].

Longitudinal prestress was provided by 26 no. VSL 31K13 tendons (i.e. 31 strands of 13mm low relaxation strand per tendon) stressed to approximately 75% UTS. These provided a uniform compressive stress in the cross section of about 2.3N/mm². This was sufficient to provide a Class 1 (i.e. no tension) structure in the serviceability limit state, eliminating flexural cracking. Concern over durability and monitoring of the prestress led to the first use in Hong Kong of VSL's CS-Plus system utilising composite material ducting and anchorages.

Earthquake loading was based on static load enhancement utilising an acceleration of 0.07g at ultimate limit state. Ductility and joint opening/closing were checked using the BART criteria reported by Kuesel[5]

5.   Buoyancy and Stability

Buoyancy requirements for the tunnel units were conventional and required a factor of safety against sinking of 1.02 minimum when floating fully outfitted for sinking and a factor of safety of 1.04 against flotation after placing to include all permanent ballast but not backfill or any contribution from adjacent units. There was a further requirement of a factor of safety of 1.20 when considering also the deadweight only of backfill on the plan area of the tunnel unit.

The concrete structural thickness and the ballast area was determined to enable these criteria to be met under the most adverse combination of concrete density and seawater density. The range considered was 22.5 to 23.3 kN/m3 for concrete and 9.96 to 10.06 kN/m3 for seawater. Tunnel units of this slenderness and curvature are almost unique and there was concern about floating stability and dynamic effects during towing and mooring. The issue was further exacerbated by the need to use the sinking pontoons from the adjacent Western Harbour Crossing (WHC) Project. These were sized for the much larger WHC units and weighed some 245 tonnes each.

The units were subject to severe wave conditions during towing and when stored on single point moorings (significant wave height up to 3.5m). Analysis of stability and towing/mooring force variations was confirmed by model testing at Kumagai Gumi's Institute of Construction Technology in Tsukuba City , Japan. Peak mooring force was 70t and maximum roll with all temporary fittings was 3°. Figure 3 shows the tunnel units under construction in the casting basin.
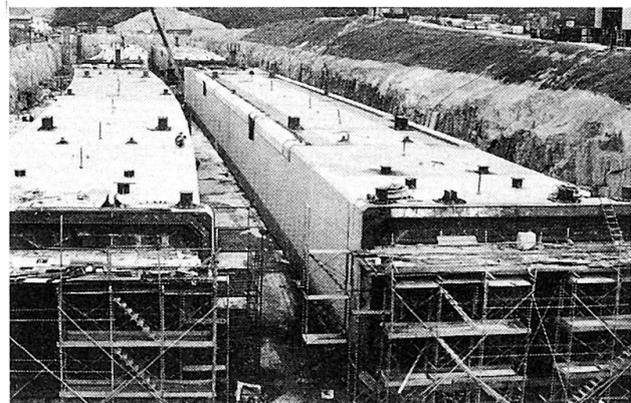

Fig 3 Tunnel Units under Construction

6.   Joints

The joints between typical units are conventional hydrostatic joints incorporating two independent seals, the primary gina-profile seal and a secondary omega seal. The detailing was complicated by the need to incorporate the prestress tendon anchorages.

Programming constraints at each landfall dictated that the tunnel units could not be laid in a simple end-to-end sequence. Units 1-8 were laid in sequence from the Hong Kong landfall at the ATU and Unit 10 at the Kowloon (KVB) landfall. Unit 9 was laid last and the final joint formed in-situ between Units 8 and 9.

The final joint was formed by pre -compressing the Unit 8/Unit 9 hydrostatic joint onto the end of Unit 8 during construction in the casting basin, utilising prestressing bars across the joint. This left only a 2.5m section to be constructed in situ between Units 8 and 9. The section was enclosed in steel formwork placed underwater and sealed to the unit, after which the joint was dewatered and concreted in situ.

7.   Shear Keys

The combination of extra-ordinary loading conditions with loss of foundation support under the units generates high vertical shear forces at unit/unit joints. These forces need to be carried across the joint to prevent any vertical displacement (particularly important with a rail tunnel) whilst still providing rotational flexibility.

The keys are steel fabrications on heavy steel backplates. Rotational capacity is maintained by laminated rubber bearings. A high stiffness is necessary (1000 kN/m) to limit vertical deflection in the service condition to 0.5mm. Fireproofing of the whole system is achieved with Durasteel (a proprietary steel/fibre sandwich plate) cover plates.

8.   Durability

Concrete mix design was optimised to achieve the best balance of high density, low permeability, low water/cement ratio, high cementitious content, low heat of hydration and maximum chemical resistance. Characteristic strength was 40 Mpa using a cementitious content of 425 kg/m^3 (280 kg/m^3 opc and 145 kg/m^3 pulverised fuel ash(pfa)). Pfa was incorporated to reduce permeability and to minimise heat of hydration. The temperature rise (65°C above ambient) and, particularly, thermal gradient criteria (15°C to an adjacent surface within the pour and 20°C between the current pour and th previous adjacent pour) set by the DSM[1] were stringent and could not be achieved without the use of cooling. Cooling pipes were incorporated into critical sections (i.e. in areas of high restraint adjacent to construction joints).

An acrylic resin based waterproof membrane, 2mm thick, was applied to the walls and roof of the tunnel unit. The base was protected by a 9mm thick steel plate attached by headed studs. Neither was taken into account in assessing exposure criteria for concrete durability.

A corrosion monitoring system was installed in selected units to identify corrosion or earth leakage currents from the 1500v DC traction supply system. In the event that corrosion was identified, provision has been made for the retrofitting of a cathodic protection system.

9.   Foundation and Backfill

The units were sunk into place, supported from pontoons, onto temporary foundations. The void between the units was then filled a sand layer, nominally 800mm thick, with a tolerance of -10mm/+500mm. The layer is placed after sinking the unit by pumping a sand/water mixture via pipes cast into the centre walls of the unit at 8.7m centres.

The typical backfilling arrangement incorporated locking fill at the lower sides of the units to hold it in place laterally, general fill for the rest of the trench and 1.0m rock armour as protection on top of the unit. The armour extends to a minimum of 25m each side of the tunnel centre line. The armour and general fill was designed to provide protection against scour, falling anchor (design anchor 7.8 tonne) and a falling dredger bucket (design bucket 23 tonnes).

10.   Programme

The design and construct contract was awarded in June 1994. Design commenced in July 1994 and was substantially complete by January 1995.   Fabrication of units commenced in late 1994. The final joint was completed in October 1996 and the complete tunnel was handed over to MTRC for track laying in December 1996.

References

1.   Design Standards Manual, Mass Transit Railway Corporation, Hong Kong.
2.   BS 8110, The Structural Use of Concrete, British Standards Institution, London.
3.   BS 8007, The Structural Use of Concrete for Retaining Aqueous Liquids, British Standards Institution, London.
4.   CIRIA Report 91, Early age thermal crack control in concrete, TA Harrison, Construction Industry Research and Information Association 1992.
5.   Kuesel TR, Earthquake Design Criteria for Subways, American Society of Civil Engineers, Journal of the Structural Division, Vol. 95, No. ST6, June 1969.

Acknowledgements